

**MODELING OF HEAVY VEHICLE BRAKING RELATED
TO ACCIDENT RECONSTRUCTION FOR A RANGE OF
VEHICLE AND ROAD CHARACTERISTICS**

MAHDIEH ZAMZAMZADEH

**FACULTY OF ENGINEERING
UNIVERSITY OF MALAYA
KUALA LUMPUR**

2020

**MODELING OF HEAVY VEHICLE BRAKING
RELATED TO ACCIDENT RECONSTRUCTION FOR A
RANGE OF VEHICLE AND ROAD CHARACTERISTICS**

MAHDIEH ZAMZAMZADEH

**THESIS SUBMITTED IN FULFILLMENT OF THE
REQUIREMENTS FOR THE DEGREE OF DOCTOR OF
PHILOSOPHY**

**FACULTY OF ENGINEERING
UNIVERSITY OF MALAYA
KUALA LUMPUR**

2020

UNIVERSITY OF MALAYA

ORIGINAL LITERARY WORK DECLARATION

Name of Candidate: Mahdieh Zamzamzadeh

Registration/Matric No: KHA120037

Name of Degree: DOCTOR OF PHILOSOPHY

Title of Project Paper/Research Report/Dissertation/Thesis ("this Work"):
MODELING OF HEAVY VEHICLE BRAKING RELATED TO ACCIDENT
RECONSTRUCTION FOR A RANGE OF VEHICLE AND ROAD
CHARACTERISTICS

Field of Study:

I do solemnly and sincerely declare that:

- (1) I am the sole author/writer of this Work;
- (2) This Work is original;
- (3) Any use of any work in which copyright exists was done by way of fair dealing and for permitted purposes and any excerpt or extract from, or reference to or reproduction of any copyright work has been disclosed expressly and sufficiently and the title of the Work and its authorship have been acknowledged in this Work;
- (4) I do not have any actual knowledge nor do I ought reasonably to know that the making of this work constitutes an infringement of any copyright work;
- (5) I hereby assign all and every rights in the copyright to this Work to the University of Malaya ("UM"), who henceforth shall be owner of the copyright in this Work and that any reproduction or use in any form or by any means whatsoever is prohibited without the written consent of UM having been first had and obtained;
- (6) I am fully aware that if in the course of making this Work I have infringed any copyright whether intentionally or otherwise, I may be subject to legal action or any other action as may be determined by UM.

Candidate's Signature

Date: 21 July 2020

Subscribed and solemnly declared

before, Witness's Signature Date:

Name:

Designation:

UNIVERSITI MALAYA
PERAKUAN KEASLIAN PENULISAN

Nama: Mahdieh Zamzamzadeh

No. Pendaftaran/Matrik: KHA120037

Nama Ijazah: DOCTOR OF PHILOSOPHY

Tajuk Kertas Projek/Laporan Penyelidikan/Disertasi/Tesis ("Hasil Kerja ini"):

MODELING OF HEAVY VEHICLE BRAKING RELATED TO ACCIDENT
RECONSTRUCTION FOR A RANGE OF VEHICLE AND ROAD
CHARACTERISTICS

Bidang Penyelidikan:

Saya dengan sesungguhnya dan sebenarnya mengaku bahawa:

- (1) Saya adalah satu-satunya pengarang/penulis Hasil Kerja ini;
- (2) Hasil Kerja ini adalah asli;
- (3) Apa-apa penggunaan mana-mana hasil kerja yang mengandungi hakcipta telah dilakukan secara urusan yang wajar dan bagi maksud yang dibenarkan dan apa-apa petikan, ekstrak, rujukan atau pengeluaran semula daripada atau kepada mana-mana hasil kerja yang mengandungi hakcipta telah dinyatakan dengan sejelasnya dan secukupnya dan satu pengiktirafan tajuk hasil kerja tersebut dan pengarang/penulisnya telah dilakukan di dalam Hasil Kerja ini;
- (4) Saya tidak mempunyai apa-apa pengetahuan sebenar atau patut semunasabahnya tahu bahawa penghasilan Hasil Kerja ini melanggar suatu hakcipta hasil kerja yang lain;
- (5) Saya dengan ini menyerahkan kesemua dan tiap-tiap hak yang terkandung di dalam hakcipta Hasil Kerja ini kepada Universiti Malaya ("UM") yang seterusnya mula dari sekarang adalah tuan punya kepada hakcipta di dalam Hasil Kerja ini dan apa-apa pengeluaran semula atau penggunaan dalam apa jua bentuk atau dengan apa juga cara sekalipun adalah dilarang tanpa terlebih dahulu mendapat kebenaran bertulis dari UM;
- (6) Saya sedar sepenuhnya sekiranya dalam masa penghasilan Hasil Kerja ini saya telah melanggar suatu hakcipta hasil kerja yang lain sama ada dengan niat atau sebaliknya, saya boleh dikenakan tindakan undang-undang atau apa-apa tindakan lain sebagaimana yang diputuskan oleh UM.

Tandatangan Calon

Tarikh: 21 July 2020

Diperbuat dan sesungguhnya diakui di hadapan,

Tandatangan Saksi

Tarikh:

Nama:

Jawatan:

ABSTRACT

In today's heavy-vehicle accidents, one of the major contributors is emergency braking, particularly for vehicles without an anti-lock braking system (ABS), which is dominant in developing countries like Malaysia. As the heavy vehicle driver applies emergency braking, there is a high chance of wheel lock-up, at which point the vehicle will skid along the road, creating braking marks from the tires. These braking marks are often used in crash reconstructions. Braking marks are mainly used by investigators to examine the vehicle's pre-impact velocity. There are many models and formulations based on kinetic energy that show the effect of some parameters. Still, there has been less discussion about vehicle dynamics' and loading condition's effects on slip ratio and wheel lock-up. This study used a multi-body dynamics method to examine the braking process in emergency braking for a better understanding of the characteristics of heavy vehicle braking, the performance of heavy vehicles during emergency braking, wheel lock-up, and skidding as evaluated by the critical pedal force that triggers wheel lock-up, PF_{crit} . The findings generated from this study indicated that a minimum pedal force exists regardless of the factors involved. This inadvertently creates the PF_{crit} , which causes wheel lock-up and skidding. With that in mind, this study also highlighted the importance of PF_{crit} .

Two phases were involved. The first phase examined PF_{crit} . Here, the wheel lock-up data for various pedal forces of the heavy vehicle's loading condition, its speeds, and the road surface conditions were generated through a multi-body dynamic model. Then the parameters that have a significant effect on the heavy vehicle's wheel lock-up were validated through statistical analysis. The results showed that the vehicle's dynamic characteristics could change during emergency braking situations, particularly for overloaded vehicles. This change can affect the heavy vehicle's wheel lock-up and the ability to stop safely. These parameters are fundamental, and so should be considered when determining braking marks distances. The most important finding to be noted from this study is the difference detected in the skidding distance when the vehicle's gross vehicle weight (GVW) is changed.

The second phase of this study concentrated on the skidding distance and whether there is a contributory relation between skidding and vehicle dynamics. An alternative model was

developed and then subjected to various vehicle characteristics and road conditions for this purpose. The primary consideration for developing the new regression model was to look at how vehicle dynamics and road conditions may impact the wheel lock-up and skidding distance. A nonlinear model to estimate the skidding distance. This model was derived as a case study by considering the nonlinear effect of the vehicle loading condition, tire forces, and longitudinal tire slip. According to the data presented here, this model provides information on how heavy vehicle GVW affects vehicle performance during emergency braking.

Keywords: accident reconstruction, emergency braking, overloading, pedal force, multi-body dynamics, braking distance, braking mark, wheel lock-up

University of Malaya

ABSTRAK

Perangkaan kemalangan kenderaan berat pada hari ini, menunjukkan salah satu punca utama khususnya disebabkan oleh masalah brek kecemasan yang terdapat pada kenderaan berat tanpa sistem brek anti-kunci (ABS), yang dominan di negara-negara membangun seperti Malaysia. Semasa kenderaan berat menggunakan brek kecemasan, sekiranya berlaku kunci roda ia akan meluncur di sepanjang jalan dan menghasilkan tanda gelinciran di atas jalan raya. Tanda gelinciran yang disebabkan oleh tayar merupakan salah satu faktor penting yang digunakan untuk pembinaan semula kemalangan. Tanda gelinciran digunakan terutamanya oleh para penyiasat untuk memeriksa halaju pra-impak kenderaan. Terdapat banyak model dan formula berdasarkan Tenaga Kinetik yang menunjukkan kesan beberapa faktor lain, tetapi agak kurang perbincangan mengenai pengaruh muatan kenderaan pada nisbah slip dan kunci roda. Tesis ini menumpukan kajian pada prestasi brek semasa kecemasan melalui model dinamik pelbagai-badan yang dapat memberikan gambaran lebih baik tentang ciri-ciri brek kenderaan berat serta keadaan kenderaan semasa berlakunya brek kecemasan, kunci roda dan gelinciran. Sehubungan itu, ciri-ciri brek kenderaan berat diambil kira dengan mempertimbangkan daya kritikal pedal yang boleh mencetuskan kunci roda, PF_{crit} . Penemuan yang dihasilkan daripada kajian ini menunjukkan bahawa daya minimum pedal sentiasa wujud tanpa mengira faktor-faktor lain memandangkan PF_{crit} boleh menyebabkan kunci roda dan gelinciran berlaku secara drastik. Maka kesuluruhannya, kajian ini juga telah memberi penekanan tentang kepentingan PF_{crit} .

Kajian ini telah pun dijalankan dalam dua fasa. Fasa pertama mengkaji ciri-ciri PF_{crit} . Dalam hal ini, data kunci roda untuk pelbagai keadaan beban daya kenderaan berat, kelajuan dan keadaan permukaan jalan raya telah dihasilkan melalui model dinamik pelbagai badan. Kemudian, parameter yang mempunyai kesan signifikan terhadap kunci

roda kenderaan berat disahkan melalui analisis statistik. Hasil analisis menunjukkan bahawa ciri dinamik kenderaan boleh berubah ketika dalam keadaan kecemasan, terutama bagi kenderaan yang melebihi beban muatan. Perubahan ini boleh menjejaskan kunci roda kenderaan berat dan keupayaannya untuk berhenti dengan selamat semasa kecemasan. Parameter ini adalah teras utama yang perlu dipertimbangkan untuk menentukan tanda jarak gelinciran kenderaan berat. Penemuan yang paling penting untuk diambil perhatian daripada kajian ini adalah perbezaan yang didapati pada jarak gelinciran apabila Berat Kasar Kenderaan (GVW) diubah.

Fasa kedua kajian ini memberi tumpuan pada jarak gelinciran jika terdapat hubungan kausal yang mengaitkan sebab dan akibat di antara gelinciran dan dinamik kenderaan. Satu model alternatif kemudiannya telah dibangunkan untuk tujuan ini yang mana tertakluk kepada pelbagai ciri kenderaan dan keadaan jalan raya. Pertimbangan utama untuk mencipta model regresi baru adalah dengan melihat bagaimana dinamik kenderaan dan keadaan jalan raya boleh memberi impak pada kunci roda dan jarak gelinciran, yang juga menghasilkan model bukan linear bagi menganggarkan jarak gelinciran tersebut. Model ini merupakan kajian kes yang diperolehi dengan mempertimbangkan kesan bukan linear oleh keadaan muatan kenderaan, daya pada tayar dan gelinciran tayar secara membujur. Menurut data yang dikemukakan di sini, model ini hanya memberi maklumat tentang bagaimana berat kasar kenderaan berat GVW memberi kesan kepada kenderaan semasa membrek dalam kecemasan.

THIS THESIS IS DEDICATED

**In Loving Memory of
My Beloved Late Father**

♥♥*Ali Khan*♥♥

University of Malaya

ACKNOWLEDGMENT

First of all, I would like to express my deepest gratitude to my supervisors, Associate Professor Ir. Dr. Rahizar Ramli and Dr. Ahmad Saifizul Abdullah, from the Department of Mechanical Engineering, Faculty of Engineering, University of Malaya, for their guidance. I owe them my deepest appreciation for allowing me to work on such an innovative and exciting project. I am indeed thankful for their invaluable advice, the enlightening discussions, the timely and positive feedback, and also their encouraging words. Without their continuous support, help, and motivation, this project work would not have materialized. It is my good fortune to have this excellent opportunity to work and learn from them, with this fortifying my strength as a researcher.

Next, I would like to convey my utmost thanks to my colleagues at the Control Lab of the Faculty of Engineering, the University of Malaya, Dr. Airul Sharizli, Nurzaki Ikhsan, Sim Hoi Yin and Farah Fazlinda. My sincerest thanks go to Dr. Ming Foong Soong for his critical yet very insightful advice and his attentive curiosity. It has been an excellent opportunity for me to work with him. The support provided by him has been a great help for this research project.

I am also grateful to my husband, Mehdi, and my lovely daughter, Kiana, and my little son Kian for their great support and patience are given to me throughout these years.

Last but not least, I thank my parents, who taught me invaluable lessons about life and humanity in the world. Their unconditional love, support, prayers, and continuous encouragement is given to me during the whole duration of my academic pursuit cannot be measured. My only regret is that life did not allow me the opportunity to share this day of completing my Ph.D. with my beloved late father, **Ali Khan**. May God bless him.

TABLE OF CONTENTS

| | |
|--|--------------|
| ABSTRACT..... | iii |
| ABSTRAK... .. | v |
| ACKNOWLEDGMENT | viii |
| TABLE OF CONTENTS..... | ix |
| LIST OF FIGURES | xiv |
| LIST OF TABLES | xix |
| LIST OF SYMBOLS AND ABBREVIATIONS | xx |
| LIST OF APPENDICES | xxiii |
| CHAPTER 1: INTRODUCTION..... | 1 |
| 1.1 Heavy Vehicle Road Accidents..... | 1 |
| 1.2 Accident Reconstruction..... | 3 |
| 1.3 Stopping/Skidding Distance | 5 |
| 1.4 Problem Statement..... | 6 |
| 1.5 Research Objectives..... | 8 |
| 1.6 Limitations and Assumptions | 9 |
| 1.7 Research Definitions..... | 10 |
| 1.8 Scope of the Study..... | 11 |
| 1.9 Significance of Research | 12 |
| 1.10 Thesis Outlines | 15 |
| CHAPTER 2: LITERATURE REVIEW..... | 16 |
| 2.1 Heavy Vehicle Road Crashes | 17 |
| 2.1.1 Heavy Vehicle Road Crashes in Malaysia | 19 |
| 2.1.2 Heavy Vehicle Road Crashes with Skidding | 23 |
| 2.2 Fundamentals Factors Involved in Heavy Vehicle Crashes | 25 |

| | | |
|---------|--|----|
| 2.2.1 | Vehicle Conditions..... | 27 |
| 2.2.2 | Driver Factors..... | 27 |
| 2.2.3 | Environmental Factors | 28 |
| 2.3 | Risk Factors Involved in Heavy Vehicle Crashes | 28 |
| 2.3.1 | Vehicle Speed..... | 29 |
| 2.3.2 | Vehicle Overloading | 29 |
| 2.3.3 | Road Surface Condition | 30 |
| 2.4 | Accident Reconstruction..... | 30 |
| 2.4.1 | Objectives of Accident Reconstruction..... | 31 |
| 2.5 | Crash Reconstruction Phases..... | 31 |
| 2.5.1 | Crash Models and Methods..... | 32 |
| 2.6 | Straight Line Equation of Motion..... | 34 |
| 2.6.1 | Constant Deceleration | 34 |
| 2.6.2 | Heavy Vehicle Braking Behavior | 36 |
| 2.6.2.1 | Emergency Braking Fundamentals | 37 |
| 2.6.2.2 | Air Drum Brakes | 38 |
| 2.6.2.3 | Pedal Force..... | 40 |
| 2.6.2.4 | Braking Performance and Wheel Lock-up..... | 41 |
| 2.6.3 | Stopping and Skidding Distance | 42 |
| 2.6.3.1 | Tire Skid Mark and Its Importance | 43 |
| 2.6.3.2 | Estimation of Speed from Skid Mark..... | 44 |
| 2.6.3.3 | Speed from Skid Formula | 46 |
| 2.6.3.4 | Formula Practice Assumptions | 48 |
| 2.6.3.5 | Formula Application Issues and Uncertainties..... | 48 |
| 2.7 | Tire Forces Characteristics | 51 |
| 2.7.1 | Tire Mechanics..... | 51 |
| 2.7.2 | Tire Longitudinal Force | 52 |
| 2.7.2.1 | Tire Slip Ratio | 53 |
| 2.7.2.2 | Coefficient of Friction..... | 54 |
| 2.7.3 | Tire Lateral Forces | 55 |
| 2.7.4 | Tire Vertical Forces..... | 57 |
| 2.7.5 | Tire Dynamic Properties Due to Pure Longitudinal Slip..... | 58 |

| | | |
|-------------------------------------|--|-----------|
| 2.7.6 | Tire Traction and Braking Performance | 59 |
| 2.7.7 | Tire Models | 61 |
| 2.8 | Heavy Vehicle Dynamic Simulation | 64 |
| 2.8.1 | Multi-Body Dynamics..... | 65 |
| 2.8.2 | Heavy Vehicle Dynamic Simulation for Accident Reconstruction | 66 |
| 2.8.2.1 | Analytical Methods Limitations..... | 67 |
| 2.8.2.2 | Heavy Vehicle Simulation | 67 |
| 2.8.2.3 | Simulation and Animation | 68 |
| 2.8.2.4 | Simulation versus Real Testing..... | 69 |
| 2.8.2.5 | MSC.ADAMS | 69 |
| 2.8.2.6 | Modeling of Vehicle Systems | 72 |
| 2.8.2.7 | Tire Modeling..... | 72 |
| 2.8.2.8 | Road Modeling..... | 74 |
| 2.9 | Literature Review Summary..... | 75 |
| CHAPTER 3: METHODOLOGY | | 84 |
| 3.1 | Multi-Body Heavy Vehicle Model Development..... | 87 |
| 3.1.1 | Steering | 89 |
| 3.1.2 | Suspension | 90 |
| 3.1.2.1 | Steer_axle_suspension | 90 |
| 3.1.2.2 | Tandem_axle_suspension..... | 92 |
| 3.1.3 | Chassis | 93 |
| 3.1.4 | Braking System | 94 |
| 3.1.5 | Tires..... | 95 |
| 3.1.6 | Roads for the Simulation..... | 98 |
| 3.1.7 | Tire Model and Road Interaction | 101 |
| 3.1.8 | Full Vehicle Assembly..... | 104 |
| 3.2 | Multi-Body Heavy Vehicle Model Validation | 105 |
| 3.2.1 | Model Validation Experimental Test Plan (NHTSA)/ Braking Distance | 106 |
| 3.2.1.1 | Loaded Vehicle Tests | 108 |
| 3.2.1.2 | Un-Loaded Vehicle Tests..... | 113 |
| 3.2.2 | Model Validation with TruckMaker® (4-axle SUT) | 118 |
| 3.3 | Simulation of Emergency Braking | 120 |

| | | |
|---|---|------------|
| 3.3.1 | Emergency Braking Simulation | 121 |
| 3.3.2 | Braking Maneuver Setting | 121 |
| 3.3.3 | Wheel Lock-up and PF_{crit} | 123 |
| 3.3.4 | Tire Normal Force versus Longitudinal Force (F_x) at Pure Slip Condition | 127 |
| 3.3.5 | Braking Distance..... | 129 |
| | 3.3.5.1 Braking Simulation | 130 |
| | 3.3.5.2 Data Collection and Interpretation | 131 |
| 3.3.6 | Braking Marks and Skidding Distance Through The Braing Distance | 131 |
| 3.4 | Simulation Data Analysis | 135 |
| | 3.4.1 Steps to Create Data Plots..... | 136 |
| | 3.4.2 Data Setup and Scaled Data | 136 |
| CHAPTER 4: RESULTS AND DISCUSSIONS | | 138 |
| 4.1 | Critical Braking Pedal Force (PF_{crit}) | 145 |
| | 4.1.1 PF_{crit} Influential Factors and Their Significance | 146 |
| | 4.1.2 Assessment of Interactions among PF_{crit} Influential Factors..... | 150 |
| | 4.1.3 Modeling of PF_{crit} | 150 |
| 4.2 | Braking Distance, Braking Mark and Skidding Distance..... | 152 |
| | 4.2.1 Impact of GVW, Speed and Road Surface Condition on SD | 152 |
| | 4.2.2 Assessment of Correlation between the SD and Influential Factors... | 157 |
| | 4.2.3 Heavy Vehicle SD Prediction Model for Accident Reconstruction... | 158 |
| CHAPTER 5: CONCLUSION AND RECOMMENDATION | | 163 |
| 5.1 | Summary | 163 |
| 5.2 | Conclusions | 163 |
| | 5.2.1 Pedal Force Effect on Wheel Lock-up, PF_{crit} | 163 |
| | 5.2.2 Wheel Lock-up, Braking Mark and Skidding Distance | 164 |
| | 5.2.3 Influential Factors on Braking Distance or Braking Mark Model | 165 |
| | 5.2.4 New model | 165 |
| 5.3 | Contributions of Research | 166 |
| 5.4 | Recommendations for Future Work | 167 |

| | |
|--|------------|
| REFERENCES | 168 |
| APPENDICES | 183 |
| APPENDIX A SUT TRUCKS SPECIFICATIONS..... | 183 |
| APPENDIX B TIRE MODELS..... | 184 |
| APPENDIX C MSC ADAMS INPUT PARAMETERS | 188 |
| APPENDIX D MODEL PAC2002 TIRE PROPERTIES..... | 196 |
| APPENDIX E TEST VEHICLE SPECIFICATION | 203 |
| APPENDIX F BRAKING DISTANCE SIMULATION DATA SET..... | 205 |
| APPENDIX G DECELERATION DATA | 258 |
| APPENDIX H BRAKING DYNAMIC..... | 259 |
| LIST OF PUBLICATIONS AND PAPERS PRESENTED | 261 |

LIST OF FIGURES

| | |
|--|----|
| Figure 1-1: Accident Reconstruction Publication Since 2000 | 13 |
| Figure 1-2: Accident Reconstruction Research Growth Process Since 2000 | 13 |
| Figure 1-3: Research Growth for Tire Skid Marks Since 1992 | 14 |
| Figure 2-1: Forecast for Freight Transport in the EU until 2030 (Windhoff-Héritier, Kerwer, & Knill, 2001). | 16 |
| Figure 2-2: Heavy Vehicle Types Involved in sever Accidents during 2008-2012 in South Australia. | 18 |
| Figure 2-3: Truck Types Involved in Fatal Crashes (2008–2012) in New Zealand | 18 |
| Figure 2-4: Malaysian Perspectives for Accident Statistic | 19 |
| Figure 2-5: Road Accident Numbers by Road type | 21 |
| Figure 2-6: The adoption rate of ABS by Malaysia..... | 23 |
| Figure 2-7: Heavy Trucks in Single-Vehicle Crashes in Australia, 2003 to 2012 (Driscoll, 2013) | 24 |
| Figure 2-8: Heavy Trucks in Single-Vehicle Crashes with Unusual Factor, 2010 to 2012 | 24 |
| Figure 2-9: Single Vehicle Crash by Crash Frequency..... | 25 |
| Figure 2-10: Common Heavy Vehicle Crash Factors | 26 |
| Figure 2-11: The Relationship between Crash Frequency and Average Traffic Speed (Aarts & Van Schagen, 2006). | 29 |
| Figure 2-12: Typical Heavy Vehicle Braking System Layout (Nunney, 2007) | 39 |
| Figure 2-13: Schematic Drum Brakes (Nunney, 2007) | 40 |
| Figure 2-14: Braking Performance Diagram..... | 40 |
| Figure 2-15: Different Type of Tire Marks (Seipel & Winner, 2013a) | 44 |
| Figure 2-16: Typical Tire Forces | 52 |
| Figure 2-17: General Tire Longitudinal Force Variation with Slip Ratio (Clark, 1981) | 53 |

| | |
|--|----|
| Figure 2-18: General Variation of Road Friction Coefficient with Tire Slip | 55 |
| Figure 2-19: Tire Lateral deformation (Clark, 1981)..... | 56 |
| Figure 2-20: General Lateral Tire Force via Different Slip Angles..... | 57 |
| Figure 2-21: Tire normal Force Distribution in Contact with the Road (Gillepsi, 1992)..... | 58 |
| Figure 2-22: Tire Traction Circle (Clark, 1981) | 61 |
| Figure 2-23: Tire Model Basic Input and Output..... | 62 |
| Figure 2-24: Coefficient of Friction due to Tire Braking (Clark, 1981)..... | 63 |
| Figure 2-25: The General Schematic Flow of A Vehicle Simulation and Analysis with MSC.ADAMS..... | 72 |
| Figure 2-26: Schematic Tire Forces during Braking..... | 77 |
| Figure 2-27: Models of Schematic Tire Forces (Popov, 2010)..... | 79 |
| Figure 2-28: Typical Longitudinal Force versus Pure Slip Ratio (Nunney, 2007)..... | 80 |
| Figure 2-29: Tire Longitudinal Force due to Pure Slip Ratio | 81 |
| Figure 3-1: Research Methodology Flowchart | 85 |
| Figure 3-2: Model Development and Simulation Steps..... | 87 |
| Figure 3-3: Flow of Modeling and Model Verification | 88 |
| Figure 3-4: MSC.ADAMS Vehicle Model Compositions..... | 89 |
| Figure 3-5: The Model's Subsystems and Assembly..... | 89 |
| Figure 3-6: Sample MSC.ADAMS Steering System..... | 90 |
| Figure 3-7: Sample MSC.ADAMS Steering Suspension with its Leaf Spring..... | 91 |
| Figure 3-8: Typical MSC.ADAMS Tandem Axle Suspension..... | 92 |
| Figure 3-9: Schematic MSC.ADAMS Air Brake System..... | 94 |
| Figure 3-10: Typical MSC.ADAMS Input Parameters for Braking System | 95 |
| Figure 3-11: ADAMS/Truck Tire Data and Fitting Tool | 98 |
| Figure 3-12: ADAMS/Truck Road Builder, Coordination Input..... | 99 |

| | |
|---|-----|
| Figure 3-13: ADAMS/Truck Road Builder, the Coefficient of Friction Data..... | 100 |
| Figure 3-14: Tire Model and Experiment Comparison..... | 101 |
| Figure 3-15: Tire-Road Interaction Model..... | 101 |
| Figure 3-16: Research Model on the Road Profile in ADAMS/Truck | 103 |
| Figure 3-17: ADAMS/Truck road builder, Set Friction's data | 104 |
| Figure 3-18: Volvo 6x4, Experimental Vehicle..... | 107 |
| Figure 3-19: Comparison of Experiment and Simulation Results for Average BD's at Various Speeds (Fully-Loaded) | 112 |
| Figure 3-20: Comparison of Experiment and Simulation Results for Average BD's at Various Speeds (Unloaded)..... | 117 |
| Figure 3-21: Comparison of Simulation Results for Deceleration vs. GVW for Different Speeds | 120 |
| Figure 3-22: Slip Ratios for Straight-line Braking under Various Pedal Forces (Non-wheel Lock-up) | 123 |
| Figure 3-23: Slip Ratios for Straight-line Braking under Various Pedal Forces (Wheel Lock-up)..... | 124 |
| Figure 3-24: Wheel's Angular Speeds for Straight-line Braking under Various Pedal Forces (Non-wheel lock-up) | 125 |
| Figure 3-25: Wheel's Angular Speeds for Straight-line Braking under Various Pedal Forces (Wheel lock-up)..... | 126 |
| Figure 3-26: Longitudinal Vehicle Speeds for Straight-line Braking under Various Pedal Forces (Non-wheel lock-up) | 126 |
| Figure 3-27: Longitudinal Vehicle Speeds for Straight-line Braking under Various Pedal Forces (Wheel lock-up)..... | 127 |
| Figure 3-28: Tire Longitudinal Force with Slip Ratio Due to Different Tire Normal Force | 128 |
| Figure 3-29: Plot Tire Normal Force versus Longitudinal Force at Pure Slip Condition | 129 |
| Figure 3-30: Braking Simulation Window in ADAMS/Truck | 130 |
| Figure 3-31: Braking Simulation Flowchart | 131 |

| | |
|--|-----|
| Figure 3-32: Emergency Braking: Vehicle speed profile. | 132 |
| Figure 3-33: Emergency Braking Angular Velocity Profile during Wheel Lock-Up... | 133 |
| Figure 3-34: Braking Distance. | 133 |
| Figure 3-35: Workflow to Calculate Skidding Distance..... | 135 |
| Figure 3-36: Sample Data Set in SPSS | 137 |
| Figure 4-1: Pedal Force Effect on Braking Distance under Different Conditions..... | 141 |
| Figure 4-2: Brake Pedal Force Effect on Braking Distance..... | 143 |
| Figure 4-3: Simulation of the Effect of Speed and GVW on Braking Distance | 145 |
| Figure 4-4: Correlation Charts Relating Influential Factors to PF_{crit} | 147 |
| Figure 4-5: Effect of Speed on Mean of PF_{crit} | 149 |
| Figure 4-6: Effect of Heavy Vehicle's GVW on SD under Different Speed and μ Condition..... | 153 |
| Figure 4-7: Effect of Road Surface Coefficient of Friction on SD under Different Vehicle's GVW and Speed Condition | 155 |
| Figure 4-8: Effect of Heavy Vehicle's Traveling Speed on SD for Different μ and GVW | 157 |
| Figure 4-9: Comparison of Model, Simulation, and Traditional Formula average SD (V: 40-80 Km/h GVW: 11-41 tonnes)..... | 161 |
| Figure B-1.1: Description of Parameters in the Magic Formula (MSC.ADAMS, 2015) | 184 |
| Figure C-1.1: The Model Tandem Axle Hardpoints..... | 188 |
| Figure C-2.1: Tandem Axle Construction Frames..... | 189 |
| Figure C-3.1: Tandem Axle Subsystem Parts..... | 190 |
| Figure C-4.1: Tandem Axle Geometries | 192 |
| Figure C-6.1: MSC.ADAMS Template Roles in Template Builder..... | 193 |
| Figure C-6.2: MSC.ADAMS Tandem-Axle Template | 194 |
| Figure C-6.3: MSC.ADAMS Sub-System Builder..... | 194 |

University of Malaya

LIST OF TABLES

| | |
|--|-----|
| Table 2-1 Vehicle Dynamics Parameters and Braking Performance..... | 83 |
| Table 3-1 ADAMS/Tire Models and Their Applications | 96 |
| Table 3-2: Tire 315/80 R 22.5 Specification..... | 97 |
| Table 3-3: Road Coefficient of Friction vs. Vehicle Loading Condition (Experiment)..... | 103 |
| Table 3-4: SUT Model Subsystems | 105 |
| Table 3-5: Test Vehicle Configuration | 107 |
| Table 3-6: Test Vehicle Loading Conditions as Specified by NHTSA (Loaded)..... | 108 |
| Table 3-7: Test Vehicle Stopping Distance (Loaded)..... | 109 |
| Table 3-8: Braking Distance Analysis (Fully loaded)..... | 112 |
| Table 3-9: Test Vehicle Loading Conditions as Specified by NHTSA (Unloaded)..... | 113 |
| Table 3-10: Test Vehicle Stopping Distance (Unloaded) | 114 |
| Table 3-11: Braking Distance Analysis (Unloaded)..... | 117 |
| Table 3-12: Simulation Input Parameters | 122 |
| Table 4-1: Two-way ANOVA Test Results..... | 150 |
| Table 4-2: Regression Coefficients with a <i>p-value</i> for <i>a</i> and <i>b</i> | 152 |
| Table 4-3: Regression coefficients with a <i>p-value</i> for <i>C_i</i> | 152 |
| Table 4-4: Pearson Correlations between <i>SD</i> and Influential Factors | 158 |
| Table 4-5: Regression Coefficients <i>a</i> and <i>b</i> | 159 |
| Table 4-6: Regression Coefficients C1 to C4 | 160 |

LIST OF SYMBOLS AND ABBREVIATIONS

| | | |
|-----------------------------|---|---|
| ADAMS | : | Automatic Dynamic Analysis of Mechanical Systems |
| ANOVA | : | Analysis of Variance |
| ABS | : | Anti-lock Braking System |
| BD | : | Braking Distance |
| BITRE | : | Bureau of Infrastructure, Transport, and Regional Economics |
| FMCS | : | Federal Motor Carrier Safety |
| FMVSS | : | Federal Motor Vehicle Safety Standards |
| <i>GVW</i> | : | Gross Vehicle Weight |
| MAA | : | Malaysian Automotive Association |
| MDI | : | Mechanical Dynamics Inc. |
| MIROS | : | Malaysian Institute of Road Safety Research |
| NHTSA | : | National Highway Traffic Safety Administration |
| <i>PF</i> | : | Brake Pedal Force |
| <i>PFcrit</i> | : | Brake Pedal Force Critical (Wheel lock-up happen) |
| SD | : | Skidding Distance |
| SPSS | : | Statistical Package for the Social Sciences |
| SUT | : | Single Unit Truck |
| <i>v</i> | : | Vehicle Speed |
| μ | : | Road Coefficient of Friction |
| <i>d</i> | : | Skidding Distance |
| <i>F_x</i> | : | Tire Longitudinal or Braking Force |
| <i>F_y</i> | : | Tire Horizontal Force |
| <i>F_z</i> | : | Tire Vertical or Normal Force |
| <i>V</i> | : | Wheel Longitudinal Speed |

| | | |
|----------|---|------------------------------------|
| ω | : | Wheel Angular Velocity |
| W | : | Vehicle Weight Acting on the Wheel |
| M_b | : | Braking Torque |
| κ | : | Tire Longitudinal Slip |
| D_x | : | Linear Deceleration |
| F_{xt} | : | Total Longitudinal Force |
| M | : | Vehicle Mass |
| P_h | : | Hydraulic Line Pressure |
| A_{Mc} | : | Area for Master Cylinder |
| η | : | Braking Efficiency |
| i_p | : | Pedal Lever Ratio |
| P_h | : | Hydraulic Line Pressure |
| R | : | Effective Rolling Tire Radius |
| r | : | Effective Drum Radius |
| A_{WC} | : | Area of Wheel Cylinder |
| a | : | Deceleration Rate in g |
| BF | : | Braking Factor |
| ω | : | Angular Acceleration |
| I_t | : | Rotational Inertia |
| T_b | : | Brake torque |
| KE | : | Kinetic Energy at Start of Moving |
| F | : | Frictional or Braking Force |
| g | : | Gravity Acceleration |
| μ_p | : | Peak Friction Coefficient |
| μ_s | : | Sliding Friction Coefficient |

| | | |
|---------------------------|---|--|
| γ | : | Tire Camber (wheel inclination) Angle |
| B | : | Stiffness Factor in Magic Formula |
| C | : | Shape Factor in Magic Formula |
| D | : | Peak Factor or Dissipation Function in Magic Formula |
| E | : | Curvature Factor in Magic Formula |
| S_V | : | Vertical Shift in Magic Formula |
| S_H | : | Horizontally Shift in Magic Formula |
| a_1, a_2, a_3, a_4, a_5 | : | Defined Coefficients' in Magic Formula |
| a_6, a_7, a_8 | : | |
| K_{xk} | : | The Longitudinal Slip Stiffness in Magic Formula |

LIST OF APPENDICES

| | | |
|------------|--------------------------------------|-----|
| APPENDIX A | SUT TRUCKS SPECIFICATION | 183 |
| APPENDIX B | TIRE MODELS | 184 |
| APPENDIX C | MSC ADAMS INPUT PARAMETERS | 188 |
| APPENDIX D | MODEL PAC 2002 TIRE PROPERTIES | 196 |
| APPENDIX E | TEST VEHICLE SPECIFICATION | 203 |
| APPENDIX F | BRAKING DISTANCE SIMULATION DATA SET | 205 |
| APPENDIX G | DECELERATION DATA | 258 |
| APPENDIX H | BRAKING DYNAMIC | 259 |

University of Malaya

CHAPTER 1: INTRODUCTION

1.1 Heavy Vehicle Road Accidents

As a developing country, Malaysia has built many roads and highways within cities and rural areas. Yet some of Malaysia's best highways are consistently congested with heavy vehicles such as buses, trucks, and lorries. This observation has been endorsed by the Malaysian Automotive Association (MAA), which reported that the number of registered heavy vehicles increased in 2018 rose to 65,512 units from 61,950 units in 2017 (MAA, 2019). The association further stated that Malaysia's freight task was set to double in the next 15 years, meaning that Malaysian roads will be distended to include more heavy vehicles. Along with this increase in freight development and cargo tasks due to the movement of these heavy vehicles, the number of road accidents will inevitably increase. Reports indicate that 34,942 heavy vehicles were involved in road accidents with fatalities in the 12 months, graduating toward the end of 2015. This number is expected to increase to more than 80% by the year 2020 (Sarani, Allyana, Mohd Marjan, & Voon, 2012). Statistics further show that vehicle road accidents are the eighth major cause of death globally. By 2020, vehicle road accidents will become the third-largest cause of death. Among all the heavy vehicle crashes recorded, the majority involve single-unit vehicle (SUT class) crashes. The literature has argued that the reason for the numerous commercial road transport crashes has been due to speed (Noor Syukri, Rahim, Voon, & Sohadi, 2009). The most widely recognized factors causing road crashes can be classified as involving under-speed vehicle loading conditions, including overloading and substandard mechanical conditions, mainly brakes (Saifizul, Yamanaka, & Karim, 2011). Heavy vehicles that exceed the legal speed and mass limits increase the risk of traffic accidents (Grzebieta, Rechnitzer, & Simmons, 2015; Soole, Watson, & Fleiter, 2013; Vadeby & Forsman, 2014).

It is not advisable for heavy vehicles to speed because their movement can cause vehicle instability, loss of mobility and maneuverability, tire overheat, and brake failure. Despite the high statistics of such instances, only a few empirical studies have looked into the emergency braking situations, especially in cases when the wheel lock-up occurs.

It is difficult to safely perform checks on highly-trafficked roadways for overloaded heavy vehicles. With high traffic volume and an increase of heavy vehicles on the road, static weighing becomes ineffective to the point that it acts as a deterrent, with this low probability of heavy vehicles' being weighed and the low-level penalties and fines for weight limit violations, overloading practices have also increased. Karim et al. (2014) found that more than 21.5% of heavy vehicles surpass their permissible gross vehicle weight (GVW).

A heavy vehicle's braking failure causes many accidents, especially during emergency braking situations where the braking system starts the wheel lock-up and the vehicle skids along the road. Other factors contribute to road accidents, such as pavement–tire friction and road surface conditions. They are responsible for the grip vehicles' need to sustain the control of the vehicle and come to a safe stop. Many reports have statistically shown the significant correlations between the road surface condition and road accident severities (Mayora & Piña, 2009).

Thus far in the literature, accident causes and their contributing factors have been considered generally. A primary reason for heavy vehicle crashes on highways is the possibility of skidding and an inability to stop safely, especially during emergency braking. During such an event, wheel lock-up occurs, causing vehicles to skid before they can come to a complete stop. During that, the driver of the heavy vehicle has no control of the vehicle's path. Therefore, understanding a heavy vehicle's braking characteristics and its performance is crucial for understanding how a wheel lock-up occurs to help in the reconstruction of accidents.

1.2 Accident Reconstruction

Accident reconstruction is a scientific investigation that explores, investigates, and arrives at conclusions regarding traffic accident causation and the influential factors behind it, such as the role of the vehicle drivers, the condition of the vehicle, and road conditions (Fricke, 1990). There are many developed techniques in the field of accident reconstruction that use the post-accident vehicle state and information to determine the vehicle's pre-accident state. One of the fundamental elements estimated by the road accident investigator is the evaluation of the precrash speed and the vehicle's dynamic specification. This is performed by applying the law of physics. The estimate is made by calculating the tire braking marks left on the road in the accident scene. Based on the measured and estimated values, an investigator can evaluate the possibility of different vehicle collision scenarios, such as with pedestrians and vehicles (Nagurnas, Mitunevičius, Unarski, & Wach, 2007).

To determine the traffic's crash nature and the responsibility of those involved in the accident, the vehicle's instantaneous speed identification is critical. The precise speed estimation reflects the bold role of vehicle drivers, which is used by judicial authorities to make decisions. To know the length of the braking marks, the accident reconstruction engineer can use one of the most well-known methods for the reconstruction, the "speed from skids" formula. This is often used to determine the vehicle speed that caused the vehicle to skid along the road after a sudden braking maneuver applied before stopping.

In general, the formula is derived from the moving vehicle's kinetic energy equation, which changes to frictional work during the slowing of the skidding vehicle when the braking force is applied. In other words, the moving vehicle's kinetic energy is equal to the frictional work caused by the skidding vehicle upon braking.

Therefore, the problem to be solved is the speed of the accident vehicle determined by the skid marks gathered through the speed from skids formula, as described in Equation 1.1:

$$v = \sqrt{30 \cdot \mu \cdot d} \quad (\text{mph}) \quad \text{Eq. 1.1}$$

where v = vehicle speed (mph), μ = coefficient of friction, d = skidding distance (ft)

Given the importance of this formula, due to the use of kinetic energy formulation, a point-mass model for the vehicle is considered to create the equation.

Limitations of the existing model in determining the critical speed are restricted to only the kinematic variables, such as speed and the road coefficient of friction. Other important independent parameters for heavy vehicles such as vehicle classification, GVW, and tire-road nonlinear behavior, which may have a direct impact on vehicle braking performance, have not been explicitly considered. This point-mass model has some limitations. It ignores force differences seen on different tires and axles of the same vehicle, and this model is independent of vehicle configuration and characteristics such as the braking system, suspension system, and tire mechanical behavior. This point-mass model might be suitable for non-articulated vehicles such as passenger cars, but it is not precise enough for heavy vehicles (Varunjikar, 2011).

Although several publications validating the uncertainties initiate from accident reconstruction methods and models, Brach (1994) worked on the change in the velocity calculation uncertainty and the crash energy, which are the investigation uncertainties that come from the variations in the crash stiffness (Karim, Saifizul, Yamanaka, Sharizli, & Ramli, 2013). In particular, the importance of vehicle inertial properties and vehicle mass properties effects on speed calculation were emphasized in 2002 when the new method for measuring the inertia tensor of rigid bodies has been developed and used for vehicle system dynamics applications in accident reconstruction (Sharizli, Ramli, Karim, &

Saifizul, 2014; Paultan.org, 2016). Vehicle characteristics and tire behavior have been slowly gaining more importance in the accuracy of vehicle speed estimated from tire marks; recent studies have been made in the direction (Seiler, Song, & Hedrick, 1998).

1.3 Stopping/Skidding Distance

The braking of a heavy vehicle is performed many times by every driver during their driving journey. This braking is considerable; it becomes a critical issue during emergency situations. "Braking" refers to the process of stopping a vehicle, and this must be done as fast as possible to remain a safe distance. It is a severe issue for drivers. Accident investigators and automotive engineers need to have a precise awareness of the time and distance that a heavy vehicle takes upon braking to stop the heavy vehicle at a specific primary speed. This means that investigators have to decide what the limit for speed is when drivers stop the vehicle within a safe time and at a safe distance. Investigators have to finally make their decisions as to what has dominated the skidding phenomenon. In the case of heavy vehicles, the braking process involves a series of sequenced operations. The sequence starts from the driver's response to an observed hazard, and it finishes by bringing the vehicle to a stop.

To determine the vehicle's stopping distance, we must know the vehicle's dynamics and its braking mechanisms. After the braking performance, based on the first pedal brake contact, the kinetic energy of motion of the vehicle starts to transform to friction energy. In other words, as soon as the brakes are applied, the braking system slows down the vehicle's speed. During the braking process, the tire-road interaction is essential because the connection of the vehicle with the road is made through its tire traction forces. This means that the friction's coefficient between the tire and the road surface affects the braking distance.

If the wheels of the vehicle are not rotating during the hard-braking maneuver (i.e., the wheels are locked), this inaction can result in the tire's sliding and causing a visible skid or brake marks on the induced by friction, which is important evidence for the reconstruction of traffic accidents. These marks enable investigators to draw their conclusions about the speed the vehicle was traveling at when it made the marks.

Many studies talk about crash analysis, where investigations have reported tire braking mark types, their formation, and their different characteristics. This information can be useful for police and investigators as a means to identify and manually measure tire marks (Carter, Beauchamp, & Rose, 2012; Seipel, Winner, Baumann, & Hermanutz, 2013a; Wang, 2007). Because simulation tools are increasingly being used for reconstruction purposes, there is a need to acquire knowledge of the preconditions for the development of the tire marks and the parameters that affect their intensity. Such knowledge is important for the validity and transferability of simulation results.

Many researchers have studied braking marks in accident reconstructions. However, few studies have specifically addressed the influential factors affecting the braking distance and the braking mark length. These factors can be used to present a practical model to predict more effectively how crashes occur.

1.4 Problem Statement

Many different factors, including drivers, vehicles, and other environmental factors, can, as a whole or in part, be responsible for heavy vehicle crashes. Accidents involving heavy vehicles are an important topic concerning road safety in Malaysia. Many technologies have been used to improve heavy vehicle road safety and accident investigations so as identify the major factors causing these accidents. Thus, the development of methodologies for the analysis and reconstruction of such accidents is vital for research purposes.

Heavy vehicle accidents with skidding are a common type of road crashes. They happen when the drivers do not pay attention to the traffic, when the vehicle is in poor condition, or when the weather is bad such as with heavy rain or wind.

Of the accidents caused by heavy vehicles, tire braking/skid marks, or skidding distances are used as evidence for accident reconstruction by engineers and investigators. In this regard, the determination of an accurate precrash speed is a fundamental step in developing a reliable accident reconstruction calculation and crash judgment. Therefore, the success of estimating a vehicle's real speed depends on whether the model or formula used can calculate the vehicle's speed with precision.

The formula currently used to forensically analyze road vehicle collisions' speed is based on the theory that a moving vehicle's kinetic energy at the beginning of the wheel lock-up is equivalent to the work performed by the braking force applied to the vehicle through the skidding distance. In other words, the vehicle's kinetic energy is converted to heat between the tires and the road while the energy that is dissipated by the skidding heats the surrounding air.

Such input data for the method mentioned are frequently obtained from ephemeral evidence at the scene, which usually is tire marks from which the post-impact trajectories and velocities can be determined. Overloading has long been recognized as a considerable safety problem for vehicles. It is considered to be even more important in this context than braking distance during accidents, particularly with high velocity (Aliakbari & Moridpoure, 2016).

This is an important aspect to be taken into account because it also contributes to the impact of accident reconstruction. In this regard, it would be useful to develop a model that measures the velocity of the vehicles causing those accidents by considering the vehicle loading conditions. Such a model can show a better understanding of estimating the vehicle's velocity by taking into account the vehicle condition, the driver, and the road

conditions. Further, the application of this model leads to a better assessment of vehicle loading condition application in precrash speed estimation and of vehicle loading conditions regarding vehicle safety.

1.5 Research Objectives

Based on the problem statement described, this study will thus assess the vehicle driver's brake pedal force characteristics for different situations. The aim of doing this is to formulate an empirical model that is capable of predicting the vehicle's braking characteristics to a reasonable degree of accuracy, particularly when the vehicle is placed in different vehicle and road conditions. Following this, the study will use the results obtained to investigate the braking marks left by different vehicles under several road conditions to develop a method that contains more parameters that can be used for heavy-vehicle crash reconstruction. The list shown below outlines the individual objectives of this study, and they are categorized as the following:

- a) To develop a heavy vehicle multi-body dynamic model with air drum brakes and without ABS.
- b) To simulate a heavy vehicle straight braking test under different vehicle and road characteristics to account for the tire longitudinal dynamics in hard-braking performance.
- c) To incorporate the model and simulations, and investigate the effect of the brake pedal force on the heavy vehicle wheel lock-up;
- d) To determine the possibility of wheel lock-up occurrence under different vehicle and road conditions;
- e) To quantify factors such as GVW, speed, and road coefficients of friction, affecting heavy-vehicle braking distance with wheel lock-up and predict braking distance and braking mark; and

- f) To develop a regression model to correlate braking marks (during wheel lock-up) with vehicle GVW, speed, and road coefficient of friction and assess improvement in the accuracy of vehicle speed estimated from the wheel lock-up braking mark model using multi-body dynamics; vehicle loading is used to determine the braking force and finally estimating the skidding distance during the emergency braking of a truck.

1.6 Limitations and Assumptions

To make the research findings more efficient, the limitations and assumptions of the research are defined as below:

- a) Since the majority of heavy vehicles in Malaysia and many other countries are non-ABS-equipped, the heavy vehicle used in this thesis was restricted to the analysis of a 4-axle SUT (single unit truck) with an air-drum braking system without ABS. The developed model will be limited to this type of truck only, but the methodology should be compatible with different truck configurations.

With the use of ABS systems due to a reduction in wheel slip and to avoid wheel lock-up (100% slip), tire marks are becoming less common.

- b) While, traditional crash reconstruction method for calculating the precrash speed from tire skid is based on a rigid body and lumped mass parameters, that are independent of the vehicle configuration and characteristics (such as the suspension system, nonlinear tire dynamic), resulting in the vertical tire reactions to be independent of the motion of the vehicle and its characteristics; In this research, the vehicle characteristics took into consideration by employing a multi-body dynamic model to analyze the braking behavior of heavy vehicles.

Therefore, an alternative braking mark formulation can be established by considering vehicle characteristics and nonlinear tire behavior with varying loading conditions.

- c) The research road surface is to be level without any grade (Grade = 0). The simulations with all wheels locked up are considered for analysis, so the drag factor equals the coefficient of friction on a level road (Fricke, 2010).
- d) The expected model is based on a single heavy-vehicle crash behavior without any collision, and not a multi-vehicles or vehicle-barrier crashes with collision and contact forces between them (Fricke, 2010).
- e) The research-supposed model is based on the tire braking marks during wheel lock-up; in situations where there are no tire braking marks, the model cannot succeed. This research considers single-vehicle crashes without impact and where there are tire braking marks.
- f) The Pacejka tire model was used to calculate the tire forces and moments, but any tire model that is designed for braking analysis can be used. The set of tire variables can be easily updated through the attached MATLAB code if any variable is needed to be changed for the review (Varunjikar, 2011; Dugoff, Fancher, & Segel, 1970).

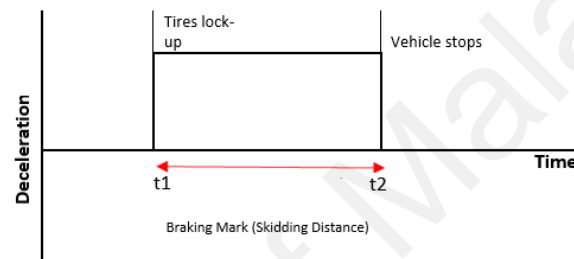
1.7 Research Definitions

In this research:

- a) *Stopping distance*: Perception reaction distance + Braking distance
- b) *Perception reaction distance*: The distance a vehicle travels in the time it takes the driver to react to a hazard and step on the brakes.

Perception reaction time is from around 1.0–2.5 seconds depending on the experience and alertness of the driver but commonly adopted as 1.5 seconds. Perception reaction time for this study supposed 1.5 seconds.

- c) *Braking distance*: The distance a vehicle covers after the driver applies the full brake until it has stopped moving.
- d) *Braking Mark*: The tire mark length from when wheel lock-up happens until the vehicle has completely stopped moving (with all wheels locked up).



Stopping distance: The distance from when the wheels commence braking until the vehicle has completely stopped moving (maybe some or all wheels are locked).

1.8 Scope of the Study

Proper braking performance is essential in preventing a heavy vehicle from having a crash. Many techniques and methods in crash reconstruction use braking output to learn more about the crash causes. The most critical parameters useful for learning about braking performance include the vehicle's braking distance, which refers to the vehicle's distance to stop at a safe distance. During a hard-braking operation or an emergency braking situation, if wheels lock-up happen, then one or more tires lose their grip, the skid may happen, and tires start to create braking marks. This study aims to investigate about tire braking marks further by using multi-body dynamic simulations. The analysis will offer a detailed understanding of the factors that influence wheel lock-up, vehicle braking, and the tire braking marks of heavy vehicles.

Through vehicle dynamics, we can see a strong correlation between braking mark lengths with speed, road coefficient of friction, and vehicle GVW. The braking mark for this study has been simulated for a heavy vehicle within a multi-body dynamic commercial software, generating braking distance data for various vehicle loads and speed with different road conditions. Finally, we study wheel lock-up and skidding cases.

In general, the first part of this study examines the influence of the vehicle type, its speed, the GVW, the road condition, and their interactions on the brake pedal force, which is all the wheel lock-up under different conditions. In exceptional cases where a wheel lock-up occurs, the skid distance is recognized, and the braking mark lengths are predicted. This study offers an alternative braking mark model to be used for heavy-vehicle crash reconstruction for more reliable results.

As a case study, this model considers the variation in vehicle dynamics parameters such as speed and GVW with road surface conditions. It will allow the crash engineers to have more consideration for speed estimation with the additional factor of vehicle GVW.

1.9 Significance of Research

The bar charts shown in Figure 1-1 to Figure 1-3 were taken from the web of science to illustrate the number of publications looking at crash reconstruction and their sum of times cited per year since the year 2000. There is a clear upward trend in this area. The pattern also reveals the importance of research in the crash reconstruction area. In that regard, this study contributes to knowledge and progress in theory and practice in the crash reconstruction engineering discipline.

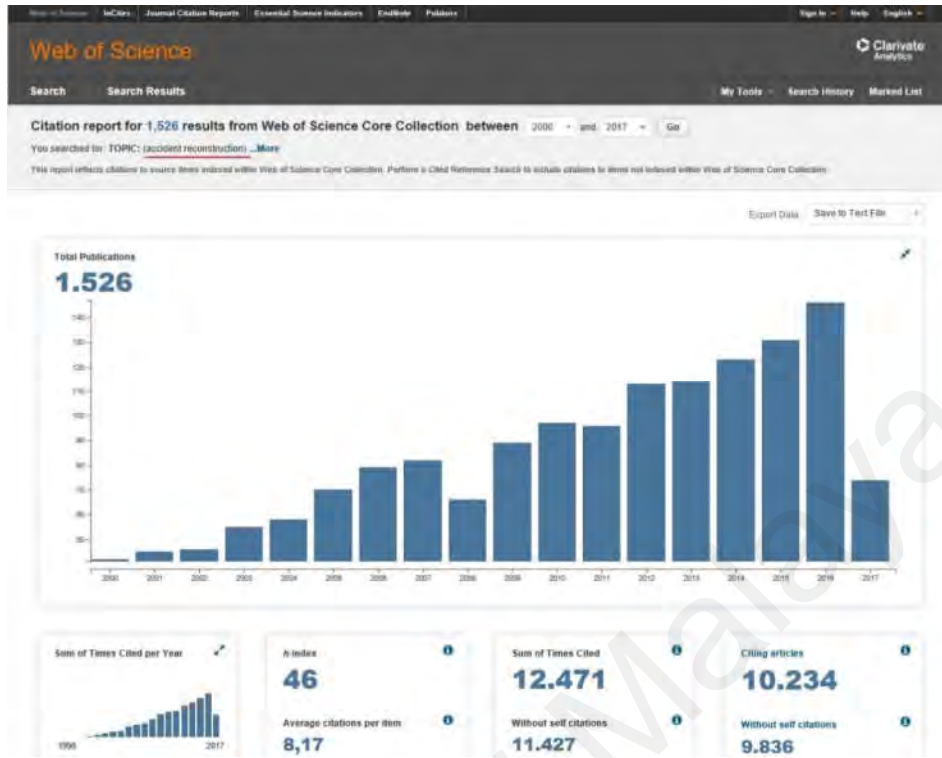


Figure 1-1: Crash reconstruction publication since 2000

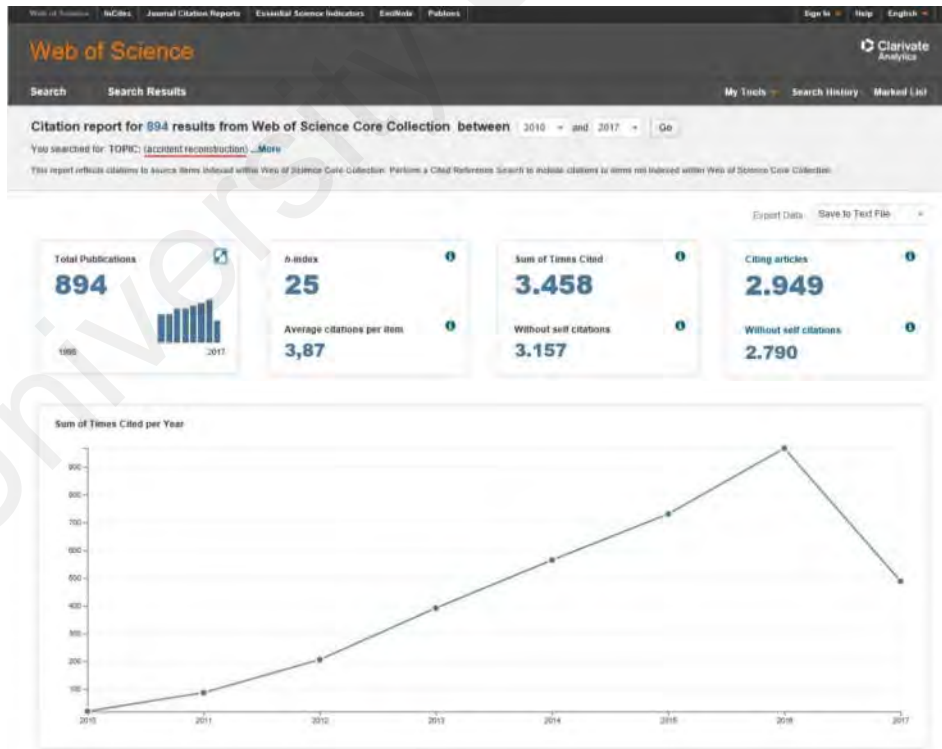


Figure 1-2: Crash Reconstruction Research Growth Process Since 2000

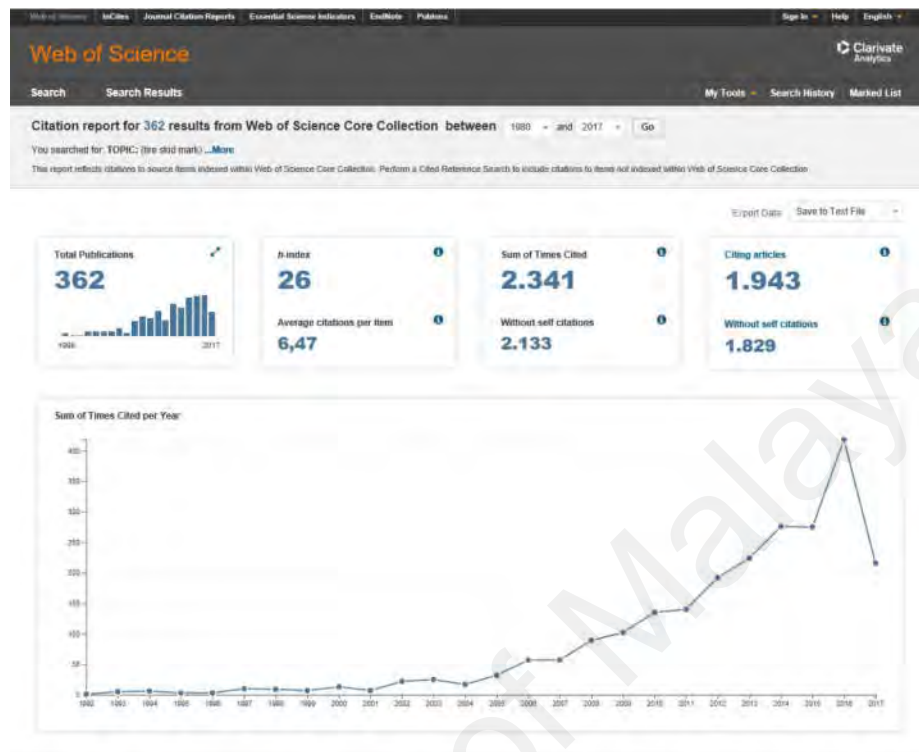


Figure 1-3: Research Growth for Tire Braking Marks Since 1992

Vehicle dynamics, or vehicle characteristic such as the GVW, affects skidding distance. Although some studies have emphasized the effect of the GVW on crash severity, results relating it to skidding distance are thus far unclear. By focusing on the theoretical perspective, this study has developed and validated a new model to measure braking marks by including more influential factors (vehicle GVW) for crash reconstruction. The new model can have a dramatic effect on the results of the reconstruction. The most important finding to be noted from the conclusions drawn from this study is the difference in output obtained when the vehicle's GVW is changed.

1.10 Thesis Outlines

This thesis is organized into five main chapters.

Chapter 1 outlines the research goals and motivation. It sets the scene for the objective of this research by projecting the problem statement. Following this, the research questions formulate the scope of the study and the significance of the study.

Chapter 2 reviews the available studies on the main factors involved in heavy vehicle crashes. Crash reconstruction methods and models, tire properties and modeling, vehicle dynamics, and their applications in crash reconstruction are also explained.

Chapter 3 describes the research procedure, the process of performing the study, and how the required data were generated for the skidding distance through a multi-body dynamic model created in the commercial software MSC.ADAMS. The developed model was then used to examine the influence of speed, GVW, road conditions, and their interactions regarding brake pedal force. This is followed by another process that investigates the wheel lock-up under different conditions. Then the skid distance is noted for the individual cases where wheel lock-up happens, and the braking mark lengths are predicted and examined. These data are then used in Chapter 4 for analysis.

Chapter 4 uses the data generated from Chapter 3 to recommend a new skidding distance or braking mark model. The model details are further described. The full research results are then explained accordingly.

Chapter 5 lists the research conclusion of developing a new model for examining the tire braking marks noted in crash reconstructions. This model will allow a better understanding of the parameters that come from vehicle dynamics and road surface conditions. This model will enable investigators to determine the braking marks by giving focus to the GVW. The results derived from developing this model will be of use to crash reconstruction engineers who can use the model to estimate the vehicle's pre-crash speed. The opportunities and recommendations for future research efforts are also provided.

CHAPTER 2: LITERATURE REVIEW

In recent years, many countries have begun to take targeted steps to promote higher efficiency within their heavy vehicle fleets. Heavy vehicles are of economic importance most of the world's roads. Statistics show that in the coming years, the volume of heavy-vehicle traffic on the roads will increase significantly. The roadworthiness of commercial vehicles is, therefore, becoming more critical than ever. However, traffic crashes are also a global phenomenon, so it is vital to look for measures to prevent vehicle crashes. Figure 2-1 demonstrates that in Europe, heavy vehicle numbers on the road will increase sharply by the year 2030.

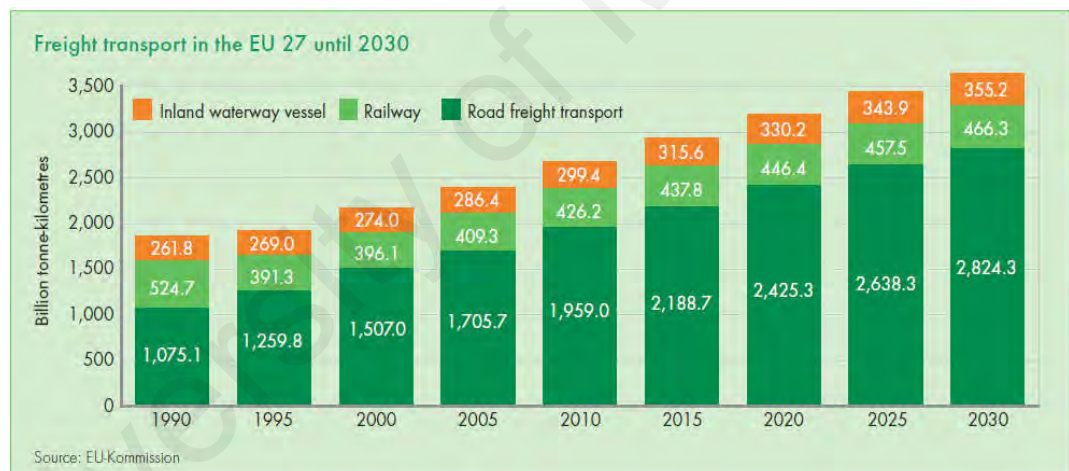


Figure 2-1: Forecast for Freight Transport in the EU until 2030 (Windhoff-Héritier, Kerwer, & Knill, 2001).

With the growth of the population, which creates various needs such as food, transportation, household products, and clothing, dependence on the trucking industry has also escalated. There are now more heavy vehicles on the road, so it is also inevitable that collisions on the roads involving heavy vehicles will increase.

According to the University Technology Malaysia (UTM), Integrated Occupational Safety Health and Environment Management case study, the growth of heavy vehicle usage has led to more crashes, which have resulted in the loss of 6,000 lives every year with about 1,000 of these fatalities involving car occupants and motorcyclists involved in collisions with heavy vehicles (Sarip, 2018; Huzaifah & Wong, 2010).

According to the experts, a primary factor leading to all these is crash compatibility. It appears that the large dimension and heavy mass of these heavy vehicles contribute to the crashes. Thus, more safety measures have been taken, especially during festive seasons, to alleviate these accidents from occurring. As a developing country, Malaysia has tried its best to improve road transportation safety. Unfortunately, statistics highlight that regardless of all applied road safety regulations and even technological advancement, road accidents involving heavy vehicles are worsening. This rise in the number of accidents will continue to affect economic growth and social issues if steps are not taken to divert this possibility.

2.1 Heavy Vehicle Road Crashes

Throughout the world, one of the main concerns for governments regarding heavy vehicles is their over-representative share in fatal crashes. As seen in Figure 2-2, the total number of road crashes involving heavy vehicles in South Australia is high, and of the fatal crashes involving heavy vehicles from 2008–2012, 41% involved heavy vehicles over 4.5 tons (Zhang, Meuleners, Chow, & Govorko, 2014).

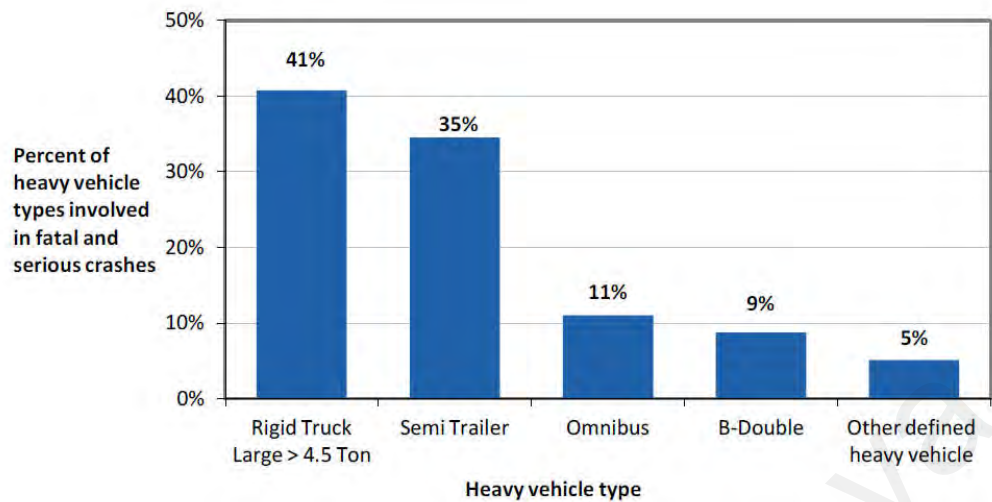
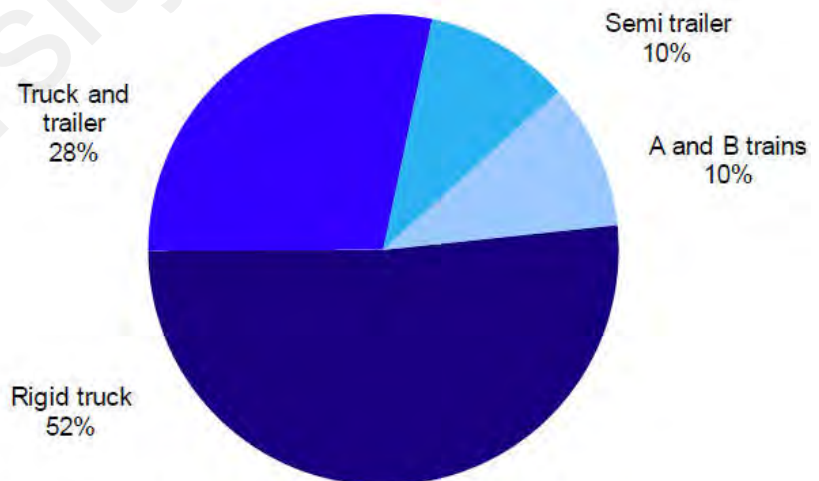


Figure 2-2: Heavy Vehicle Types Involved in Severe Crashes during 2008-2012 in South Australia

Figure 2-3 reflects a similar scenario involving heavy vehicles causing high rates of occupational crashes in New Zealand.



Note: A Train: A towing vehicle towing a semi-trailer followed by a full trailer.
B Train: A towing vehicle with two semi-trailers attached.

Figure 2-3: Truck Types Involved in Fatal Crashes (2008–2012) in New Zealand

2.1.1 Heavy Vehicle Road Crashes in Malaysia

Heavy vehicles are a big part of the transportation system in Malaysia. They are used for various transportation purposes and are commonly seen in central cities, highways, and rural roads. Thus, it is inevitable that the number of road crashes in Malaysia involving heavy vehicles will rise along with their use. As long as these heavy vehicles are being used for transportation purposes, other road users will risk being involved in road crashes and road crashes. Due to the high number of fatalities caused by crashes involving heavy vehicles, the Malaysian government has also resorted to banning heavy vehicles on the road during festive seasons. The Road Transport Department (RTD) announced a ban on heavy vehicles from all roads for five days during the Chinese New Year, from February 2–4 and February 9–10, 2019. The objective of the restriction was to minimize road crashes involving heavy vehicles and lorries (TheStar, 2019; Sarip, 2018; Huzafah & Wong, 2010).

According to the Transport Statistics of Malaysia 2010 (Ministry of Transport, Malaysia), the road crashes rate involving heavy vehicles has been increasing since 2001. The statistics for the crashes rates in Malaysia from 2001–2015 are presented in Figure 2-4.

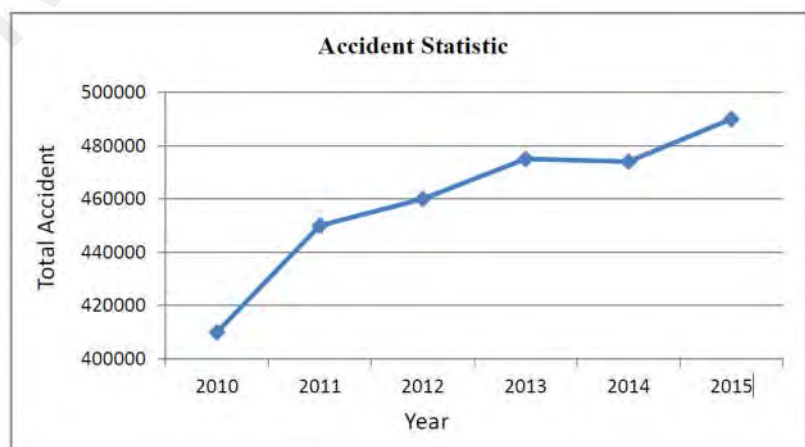


Figure 2-4: Malaysian Perspectives for Crashes Statistic

The RTD revealed that the number of road crashes is growing rapidly, as evidenced by Figure 2-4, indicating the growth rate from 2010–2015 (Krishnan, Hizam, Firdhaus, Sarah, & Taufiq, 2017). These statistics noticeably highlight the necessity of studying heavy traffic crashes so that improvements can be made to ensure the safety of local transportation systems.

According to the 2005 NHTSA statistics on traffic safety facts, more than 67% of rural crashes and about 81% of urban crashes happen on straight roads. Precautions were taken by drivers at points of danger such as curved roads, but it seems that on straight roads, the drivers' attention is diverted to the end of becoming careless. High speed is also a significant cause of crashes because drivers tend to drive faster on straight roads. Figure 2-5 shows that an ambitious plan was set in Malaysia to prove that the straight road type is the most dangerous, and it has the highest percentage of road crashes in Malaysia (Mustafa, 2005).

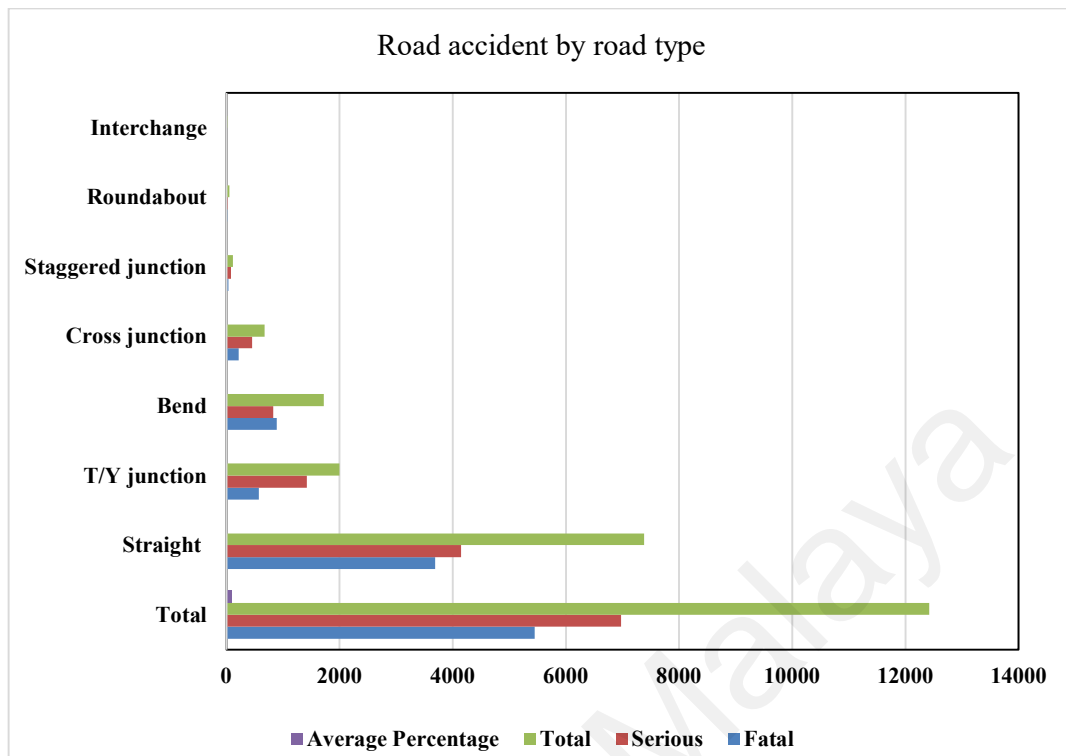


Figure 2-5: Road Accident Numbers by Road type

The heavy vehicles' safety system in Malaysia is being given attention. While 70% of road crashes in Malaysia are due to brake failure, the Malaysian Institute of Road Safety Research (MIROS) has reported that due to minimal government regulation, vehicles often lack crucial safety equipment because manufacturers sacrifice such items to keep prices low. In other words, ABS in heavy vehicles is not mandatory, thus risking skidding in the event of emergency braking. Most of the commercial vehicles, such as lorries and trucks, are built using a traditional braking system, mostly with old braking technology. This means wheel lock-up will increase the risk of skidding on the roads when the brakes are applied hard.

Furthermore, MIROS reported while the heavy vehicle speed is limited to 30–80 km/h on the federal and state roads and a maximum of 90 km/h for the expressway, more than 98% of trucks exceeded the speed limit, increasing the chance of single-vehicle crashes

(Ho & Manan, 2019; MIROS, 2017) and other studies report overloading in Malaysia is common and a serious problem for road safety.

Figure 2-6 shows the ABS adoption rate in Malaysia compared to the world and neighboring countries. In 2015, just 36% of total vehicles included passenger cars, and light-heavy vehicles were equipped with the ABS braking system, while narrow-heavy vehicles were less than 1% (Paultan.org, 2016).

Many countries, mostly in Asia, have not made ABS mandatory for commercial vehicles. The Indian government made ABS compulsory for all new cars in April 2019, but there are many old cars and heavy trucks without ABS (Nair & Shankar, 2017).

In Australia, the first attempt for mandating ABS was started in the early 2000s and was unsuccessful. Just 3% of the total registered vehicles in Australia were equipped with ABS in 2017, which accounts for 8% of the total vehicle kilometer on the public roads. In other words, more than 92% of Australian vehicle kilometers were recorded for vehicles without ABS braking systems. Heavy vehicle crashes need more consideration from the heavy vehicle industry and Australian policymakers (BITRE, 2017, 2019).



Figure 2-6: The adoption rate of ABS by Malaysia

2.1.2 Heavy Vehicle Road Crashes with Skidding

Road crashes can happen in many ways and are usually described using two categories. One is the single-vehicle crash that occurs between an object and a vehicle. The other is a multi-vehicle crash where two or more vehicles collide with each other. Single-vehicle crashes are significant over the multi-vehicle types (Qin, Ivan, & Ravishanker, 2004). In single-vehicle crashes with heavy vehicles, a skidding vehicle is one of the most common causes. Due to its direct effect on traffic safety, it is thus a crucial factor that should be considered in crashes studies. According to the New South Wales (NSW) Center of Road Safety, in Australia, single-vehicle crashes are substantially more frequent (75.9%) along straight roads, as shown in Figure 2-7.



Figure 2-7: Heavy Trucks in Single-Vehicle Crashes in Australia, 2003 to 2012 (Driscoll, 2013)

It was further established that single heavy vehicle crashes with skidding or sliding caused more than 72% of heavy vehicle crashes (Figure 2-8).

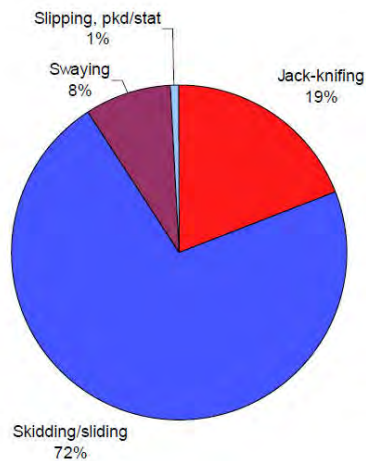


Figure 2-8: Heavy Trucks in Single-Vehicle Crashes with Unusual Factor, 2010 to 2012

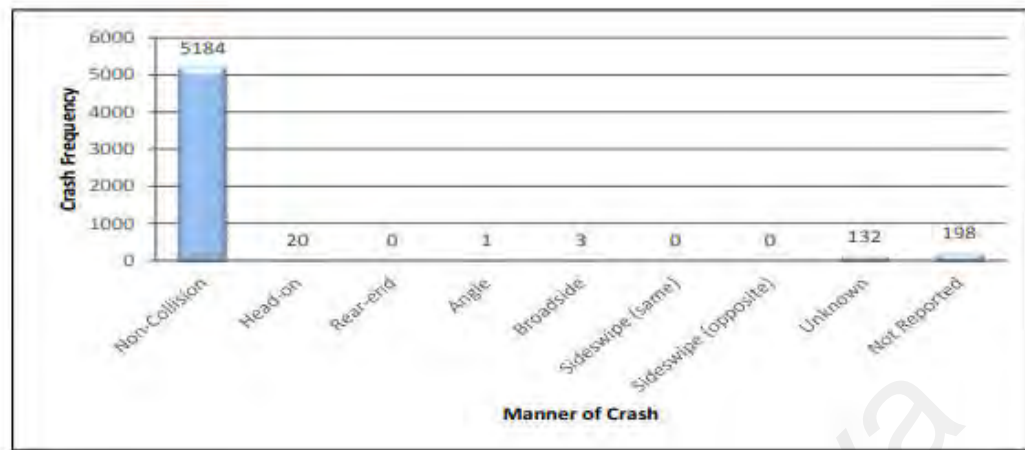


Figure 2-9: Single Vehicle Crash by Crash Frequency

Similarly, in the United States, as shown in Figure 2-9 for single-vehicle crashes from 2007–2012, the most common reason is a non-collision event (Cerwick, 2013). Single-vehicle crashes occurring on Malaysian roads are also of significant concern. This was reported with statistics provided by the Traffic Police Department, Malaysia. All these statistics from Australia and Malaysia highlight the importance of studying heavy vehicle crashes and understanding the related factors that caused these crashes to improve the road system.

2.2 Fundamentals Factors Involved in Heavy Vehicle Crashes

Many studies have shown that various factors can influence heavy vehicle crashes, and they are complicated events to study. Every heavy vehicle crash may be caused by different factors, such as factors that may have taken place just before the crash or even a long time before the crash occurred. These factors encompass conditions of the vehicle,

driver, and weather that can affect the road surface specifications (Clarke & Robertson, 2005).

Furthermore, various experimental tests have explored the relation between heavy vehicles' physical characteristics and crash scenarios. The severity of their impact on the other vehicles revealed that the heavy mass and large dimensions could be very active contributors to these types of crashes. Other factors, including road characteristics and environment, cannot be neglected due to their significant effect on the crashes' severity (Fancher, 1986; Priddy, Jones, & Sandu, 2013).

In sum, as Figure 2-10 shows, common heavy vehicle crash factors related to vehicle safety relationships with the environment, the driver, and the vehicle must be better understood to reduce crashes. The literature generally concludes that road crashes are very complicated outcomes from many combinations of these three main factors. An extensive search of the scientific research and industry publications was undertaken here to include the road environment effects of the crash (Ewing & Dumbaugh, 2009; Mooren, Grzebieta, Williamson, Olivier, & Friswell, 2014).

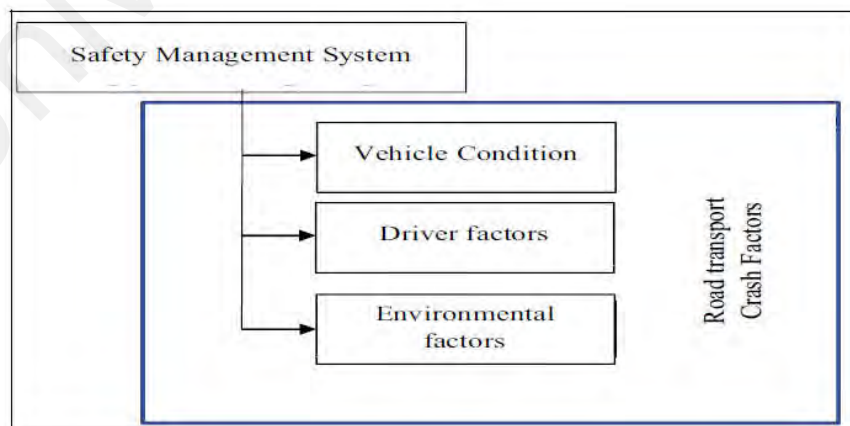


Figure 2-10: Common Heavy Vehicle Crash Factors

2.2.1 Vehicle Conditions

The vehicle motion is related to its tires' connection with the road. Any changes in speed or vehicle driving conditions will affect traction forces of the vehicle's tires and may ultimately cause severe crashes. There is a considerable body of research on the different aspects of vehicle effects on severe crashes and injuries. They suggest that many vehicle factors are significantly related to traffic violations. Factors such as handling, braking, stability characteristics, configuration, overloading, and tire conditions are also critical factors. As an example, emergency braking may be the only cause of a single-vehicle crash involving wheel lock-up and loss of directional stability.

2.2.2 Driver Factors

Many studies have demonstrated that attempts to reduce heavy vehicle crashes must be focused on driver behaviors because crash reports indicate that human factors are the principal cause of nearly 90% of all road traffic crashes. Research on a specific group of factors such as driver recognition, fatigue, and decision errors have been reported by the Federal Motor Carrier Safety Administration (FMCS, 2015).

McKnight (2004) listed comprehensively the range of driver factors that caused heavy truck causation, and they include factors related to physical, performance, emotional, experience, fatigue, carrier relation, recognition, and decision-making. Other studies highlighted that aggressive driving (Habtemichael & de Picado Santos, 2014), falling asleep, age (Lee & Li, 2014), night driving (McKnight & Bahouth, 2009), distraction (Zhu & Srinivasan, 2011), and fatigue (Driscoll, 2013; Häkkinen & Summala, 2001) are other common factors. Taking the driver's perspective, we can see that it is the driver who determines the direction and the speed of the vehicle by accelerating, speeding, or braking (Every, 2015).

2.2.3 Environmental Factors

The road can also affect vehicle motion through its surface condition and shape. Road surfaces can be affected by weather conditions, and it is this kind of road change that has always been identified as one of the contributing factors that lead to the severities and frequencies of road crashes. Brodie (2009) reported that more than 80% of crashes happen on dry highways, and 85% of crashes occur in the usual weather. In fact, drivers try to be more cautious in the adverse weather conditions than in normal conditions. This means that the severity of crashes on highways will most likely be high under normal circumstances when the road is completely dry (Brodie, Lyndal, & Elias, 2009).

In the last few decades, researchers and experts have been keen on determining how the chances of a crash happening are affected by weather conditions. Several researchers have investigated the relationship between weather conditions and crash occurrence rates. Studies have looked at the effect of weather elements such as snow, fog, rainfall, temperature, and wind on crash severity, primarily through affecting tire traction and braking performance (El-Basyouny, Barua, & Islam, 2014; Jaroszweski, Chapman, & Petts, 2013).

2.3 Risk Factors Involved in Heavy Vehicle Crashes

Any heavy vehicle crash is preceded by one or more critical conditions or risk factors. Thus, it is essential to recognize them as significant in crash causation. This can be used as a procedure to process proper documentation for future crash reconstructions. Identifying causation factors is an integral part of a crash scene.

2.3.1 Vehicle Speed

Speed has been identified as a factor in many heavy vehicle crashes. Figure 2-11 shows that it is one of the most significant factors that contribute to the severity of crashes and the intensity of the crashes.

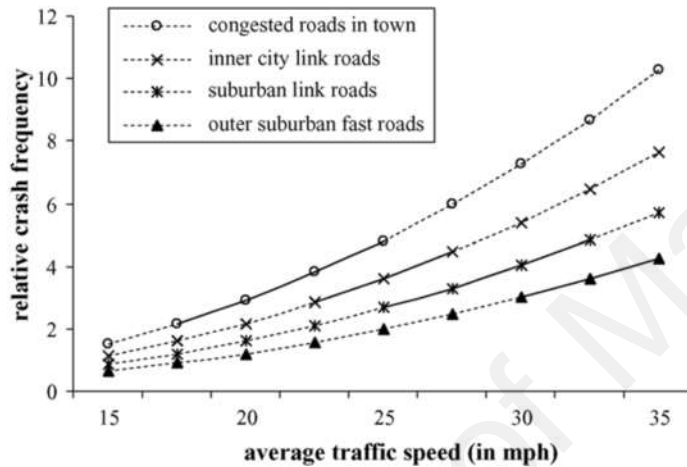


Figure 2-11: The Relationship between Crash Frequency and Average Traffic Speed (Aarts & Van Schagen, 2006).

The severity of the crash can be directly estimated through calculations of kinetic energy that relate the vehicle speed as a function of mass properties. It means the amount of kinetic energy that will be released during the crash will be affected by vehicle speed on different roads.

2.3.2 Vehicle Overloading

Many researchers have been investigating heavy vehicles weigh specification and its impact on the crash happening and its frequency (Gobbi, Mastinu, & Previati, 2014; Saifizul et al., 2011). It was found that illegally loaded heavy vehicles were the cause of

relatively high portions of the road crashes. In other words, heavy vehicle loading conditions and its carrying weights are critical factors in determining road crash severities and intensities (Taylor, Lynam, & Baruya, 2000).

The overloading of heavy vehicles can cause the loss of vehicle maneuverability and mobility because the kinetic energy is higher for the more massive vehicle, so this can result in more considerable damage to the other vehicles or infrastructure due to higher impact forces (Karim, Saifizul, Yamanaka, & Ramli, 2013). A sudden decrease in nonlinear tires or road friction caused by increasing speed tends to cause more crashes (Gunaratne, Bandara, Medzorian, Chawla, & Ulrich, 2000; Hartman & Alam, 2014).

2.3.3 Road Surface Condition

The literature has highlighted that the probability of a heavy vehicle traffic crash is significantly linked to the frictional coefficient of the road surface with the tires. This means that the number of crashes will dramatically increase due to more friction fall (Al-Mansour, 2006; Rogers & Gargett, 1991; Viner, Sinhal, & Parry, 2005). Theoretical and experimental studies on the effect of the friction coefficient on road safety have revealed that improving the friction coefficient through improving vehicle traction and braking ability can influence the frequency and severity of crashes (Andrey, Mills, & Vandermolen, 2001; Prato, Kaplan, Patrier, & Rasmussen, 2017).

2.4 Accident Reconstruction

Accident reconstruction is a practical assessment of vehicle accidents by employing advanced science and engineering principles and rules. It commences with technical evaluation and estimation of the existing physical evidence that may consist of primary measurements and data collection. In most cases, accident reconstruction engineers judge

an accident by investigating and reconstructing it based on gathered information accumulated from the vehicle's deformations and tire braking marks. These crash specialists are either police officers, road authorities' engineers, or specialists from independent organizations.

Their final reconstruction reports are used in court rulings on the road accident-related cases. Accidents are also reconstructed, for example, by vehicle manufacturers to examine the efficiency and potential of their new safety designs and devices. They then use the accident reconstruction reports to help them to learn more about the different accident mechanisms.

2.4.1 Objectives of Accident Reconstruction

Road accident reconstruction is being used increasingly in the courts to review the accident failure analysis based on the evidence before the court issue penalties. The fundamental objective of accident reconstruction is to use systematic methods and advanced mathematical science to process the experimental results and to identify the influential primary factors causing the accident by the vehicle or the road.

The method developed for road accident investigation and accident reconstruction encompasses state parameter calculations of the vehicle concerning the road environment. This is calculated based on the types of accidents and characteristics, such as where the accident happened. The final accident assessment for vehicle accidents is derived from the investigator's reports and technical analysis (Chen & Wei, 2011; Evtiukov, Kurakina, Lukinskiy, & Ushakov, 2017).

2.5 Crash Phases

A crash from the perspective of a crash investigation can be considered in three main phases: (a) where the vehicle moves before impact, (b) the impact phase where the vehicles interact with each other, and (c) postimpact where the vehicle moves till comes to a stop. Harriot's theory of impacts is one of the oldest references, from 1619 (Pepper, 1976). Later, Newton published his theory, which formed the basis of impact and started modern crash investigation (Stronge, 2000). During the three crash phases, vehicles move on the ground and dissipate energy. During the pre- and postcrash phases, ground forces and elevation changes dominate, and aerodynamics forces are generally ignored.

To summarize, there are some assumptions to use Newton's second law in crash reconstructions; out of plane effects are small, impulse due to external forces is low, and changes in physical geometry are either small or insignificant (Struble, 2020; Brach, 1998).

2.5.1 Crash Models and Methods

Many techniques and models are used for analyzing different phases of the crash scene, but the most common aspect of all vehicle crashes is the vehicle velocity.

There are two main models currently used to analyze vehicle collisions. The first models, such as Brach's model, are based on linear and angular momentum where an input receives the vehicle's initial velocities and predicts the result. The Ishikawa model has 2D models that calculate different types of vehicle collisions (Chen, Zhang, Huang, Wang, & Tarefder, 2016; Ishikawa, 1993; Raymond Brach, 1998; Yilmaz & Aydin, 2016), and the others are based on the crash algorithm as defined by Smith (1998) and Steffan and Moser (1996).

The second type as described by McHenry and Smith is the CRASH algorithm (McHenry, 1981)

Looking at the several physical models and algorithms used for the vehicle's accident reconstruction, some complex computer programs have been established. These were developed based on various physical models that calculate motion and the impact of the vehicle. An overview of some typical computer programs for accident reconstruction is addressed below:

SMAC: simulating vehicle motion before and after a collision, giving a damage profile for each vehicle as output (Solomon, 1974).

IMPACT: creating a simple analysis of an angled collision (Woolley, 1985).

CRASH: conserving the input from the vehicle crash scene, estimating the Delta-V of the vehicle that was involved in the accident and vehicle impact velocity (Woolley, Warner, & Perl, 1986).

EDSMAC4: calculating two vehicles' impact velocities and Delta-V (Day, 1999).

PC-CRASH: considering all three accident phases: pre-collision, collision with impact, and post-collision (Datentechnik, 1999).

CARAT: simulating for different vehicle types such as cars, trucks, and trailers as well as stages (precrash, crash, and postcrash dynamics) by using a 2D momentum-based collision algorithm (Fittanto, Ruhl, Southcombe, Burg, & Burg, 2002).

MADYMO: simulating safety systems and occupant injuries (Tass, 2010).

TBS: Tractor Braking and steering is a simulating commercial vehicle tool to predict the directional response to different maneuvers such as braking, steering, and their combination (Woolley, 1986).

2.6 Straight Line Equation of Motion

The primary objective of this section is to come up with mathematical expressions that will help in describing the motion of the vehicle by using three kinetic variables: velocity, displacement, and time. These variables can be paired in three ways: time-displacement, velocity-displacement, and velocity-time. These pairings are brought up according to the three laws of motion, that is, the first, second, and third equations of motion.

2.6.1 Constant Deceleration

Vehicle braking performance general equation may be obtained from Newton's second law written for the x-direction (Appendix H). Then Newton's 2nd law is shown in:

$$M a_x = -\frac{W}{g} D_x = -F_{xf} - F_{xr} - D_A - W \sin \theta \quad \text{Eq. 2.1}$$

Where:

W= vehicle weight

g= gravitational acceleration

$D_x = -a_x$ =linear deceleration in the x-direction

F_{xf} = front axle braking force

F_{xr} = rear axle braking force

D_A = aerodynamic drag

θ = uphill grade

The front and rear braking forces arise from the brakes' torque along with the rolling resistance effects and driveline drags.

The fundamental assumption used to derive the relations is that through a brake application, the forces acting on the vehicle are completely constant. The primary relationships that control the braking of the vehicle can now be understood by using the derived equations (Gillespie, 1992). As seen in Equation 2.2:

$$D_x = \frac{F_{xt}}{M} = -\frac{dV}{dt} \text{ (ft/sec}^2\text{)} \quad \text{Eq. 2.2}$$

Where:

D_x = linear deceleration in x direction (ft/sec²)

V= forward velocity (ft/sec)

M= vehicle mass (lb)

F_{xt} = the total of all longitudinal deceleration forces on the vehicle in the x-direction

Now integrate the Equation 2.2 from initial velocity to a final velocity, due to constant F_{xt} .

$$\int_{V_o}^{V_f} dV = -\frac{F_{xt}}{M} \int_0^{t_s} dt \quad \text{Eq.2.3}$$

$$V_o - V_f = \frac{F_{xt}}{M} t_s \quad \text{Eq.2.4}$$

Where:

t_s = time for the velocity change (sec)

$$V_o - V_f = \frac{F_{xt}}{M} t_s \quad \text{Eq.2.5}$$

Distance and velocity are related to each other by $V = dx/dt$ (ft/sec), so substitute it in Equation 2.2, then integrate and obtain Equation 2.6:

$$\frac{V_o^2 - V_f^2}{2} = \frac{F_{xt}}{M} X \quad \text{Eq.2.6}$$

In this equation:

X= total distance traveled during the deceleration (*ft*)

If in case the deceleration is caused to the full stop, then $V_f = 0$ and X is the total braking distance in (*ft*).

In the case where the deceleration is a full stop, then V_f is zero, and X is the braking distance in ft, BD. So:

$$BD = \frac{V_o^2}{2\frac{F_{xt}}{M}} = \frac{V_o^2}{2D_x} \quad (ft) \quad \text{Eq.2.7}$$

To calculate the time that vehicle needs to be stopped:

$$t_s = \frac{V_o}{\frac{F_{xt}}{M}} = \frac{V_o}{D_x} \quad (sec) \quad \text{Eq.2.8}$$

Therefore, with all other things being equal, the time that a vehicle needs to stop is proportional to its velocity, but the distance that is traveled is equivalent to the speed squared. This means that if the speed is doubled, the stopping time will be doubled, but the braking distance will be quadrupled. Generally, the deceleration is assumed to be uniform over the entire braking maneuver.

2.6.2 Heavy Vehicle Braking Behavior

Vehicle braking characteristics are important criteria for determining vehicle safety. The braking system should decelerate the vehicle to be stopped as quickly as possible while retaining its directional control and stability.

During the braking process, a complicated energy conversion happens where kinetic energy is changed into the braking system's thermal energy through the vehicle and at the tire-road interface. When a driver applies some force on the brake pedal, the inserted force is transmitted through a mechanical, hydraulic system, and this causes each of the wheels on the vehicle to experience a retarding torque.

The friction force between the tire and the road surface and the inertia of the wheel oppose the braking torque, which causes the vehicle to decelerate. The braking torque created at the wheel is defined by the features of the mechanical system. In contrast, the deceleration forces are determined by the frictional coefficient between the tire–road interface together with the heavy vehicle mechanics.

Consequently, deceleration of a heavy vehicle after the application of some force on the brake pedal would rely on many factors like the static and dynamic characteristics of the whole braking system.

The braking system on heavy vehicles is comprised of many components, with the major being the master cylinder, booster, brake lines, wheel calipers, brake pads, and drums. To brake the vehicle, the driver depresses the brake pedal attached to the master cylinder, thereby creating fluid pressure on the brake lines. This is transferred to the brake cylinders and then to the calipers that press the brake pads against the brake drum.

2.6.2.1 Emergency Braking Fundamentals

Real testing in heavy vehicle accident reconstruction can be used for accident replication. However, actual tests are expensive, and due to uncontrollable variables, many repetitions may be necessary to determine an average response. However, real testing is used to provide essential data to calibrate and tune the mathematical models, so their validity and accuracy can be reasonably estimated. In industry, real testing and simulation work hand-in-hand. Because simulation in the truck industry is vastly less expensive than real testing, simulation significantly reduces design costs by cutting back on the number of actual real tests that must be run (Ruhl, 2006). During emergency maneuvers, the driver's reaction to a sudden option is made by pushing hard on the brake pedal to stop the vehicle as soon as possible and as fast as they can. Depending on the vehicle and road conditions, when a brake is applied, the most likely situation that occurs

is that some wheels would most possibly lock up, and the vehicle will then leave braking marks. In the evaluation of driver behavior, many reports following scenarios of collisions have noted that steering away from a crash is the most underused tactic of collision avoidance. The required distance needed to make a controlled lane change is generally less when compared to that distance required to stop.

It is well recognized that driver performance plays a vital role in traffic crash causation (Markkula, Benderius & Wahde, 2014). Many studies followed the drivers' initial reactions or maneuvers to the emergency, typically in near-crash situations. They reported a tendency of drivers not to apply steering to the full stability limits of their vehicles. They thus brake and collide in situations where steering could have avoided the collision (Markkula, Benderius, Wolff, & Wahde, 2012a). The low expectancy for crashes, lack of driver experience, or critical braking may limit the magnitude of avoidance maneuvering employed by the driver (Wu et al., 2015). This means that drivers who steer away to avoid a collision have a lower chance of hitting an obstacle than drivers who brake suddenly. In the event where both braking and steering together are applied, the probability of avoiding a collision is even higher (Prynné & Martin, 1995). There are many driver behavior models used in simulation and crash simulators based on drivers' tendency to brake rather than steer in emergencies. Such models can offer great improvements in many simulation-based approaches (Plöchl & Edelmann 2007; Markkula, Gustav 2014; Markkula & Benderius, 2012b).

2.6.2.2 Air Drum Brakes

In current commercial vehicles, the braking system is composed of pneumatic and mechanical subsystems. The pneumatic subsystem is made up of a compressor, storage reservoir, pneumatic valves, brake chamber, and pipes for linking the components. A typical air braking system for a heavy vehicle brake system is displayed in Figure 2-12.

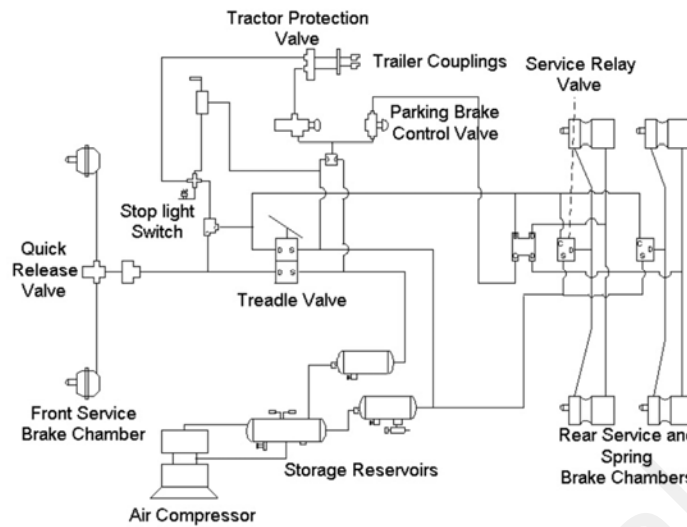


Figure 2-12: Typical Heavy Vehicle Braking System Layout (Nunney, 2007)

Air pressure in the system is converted into an actuating force on the brake by the brake chamber. Typically, the air pressure displaces a piston/diaphragm assembly through a distance called the “stroke.” This displacement produces the force necessary for brake application; its force can be ideally computed by the product of the pressure times the piston/diaphragm area.

As shown in Figure 2-13, the mechanism of the drum brakes is to decelerate the vehicle by pushing the friction pads into the inner surface of the drum where the drum is fixed to the wheel. Brake shoes hold the friction pads in place, which pivot at an anchor post. National Highway Traffic Safety Administration (NHTSA) investigations showed that the type of braking system had no statistically significant effect on driver behavior before braking (Nunney, 2007).

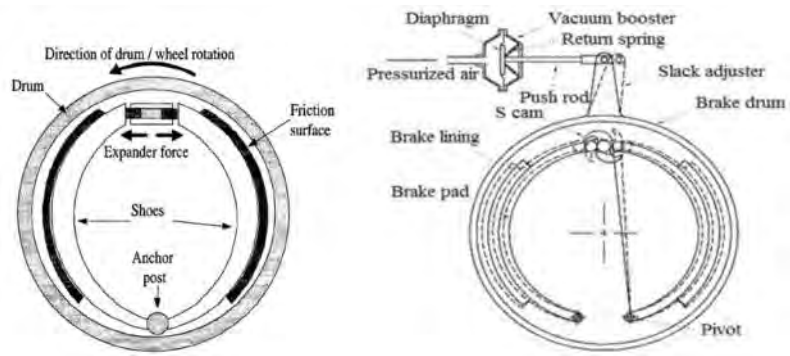


Figure 2-13: Schematic Drum Brakes (Nunney, 2007)

2.6.2.3 Pedal Force

Pedal force in heavy vehicles refers to the magnitude of the acting foot force on the brake pedal, which is determined by the heavy vehicle driver's braking efforts measured by the pedal force and reaction time. Figure 2-14 is usually used for heavy vehicles as a way to summarize the relationship between pedal force (PF) and brake factors (Fancher & Mathew, 1987; Mortimer et al., 1970):

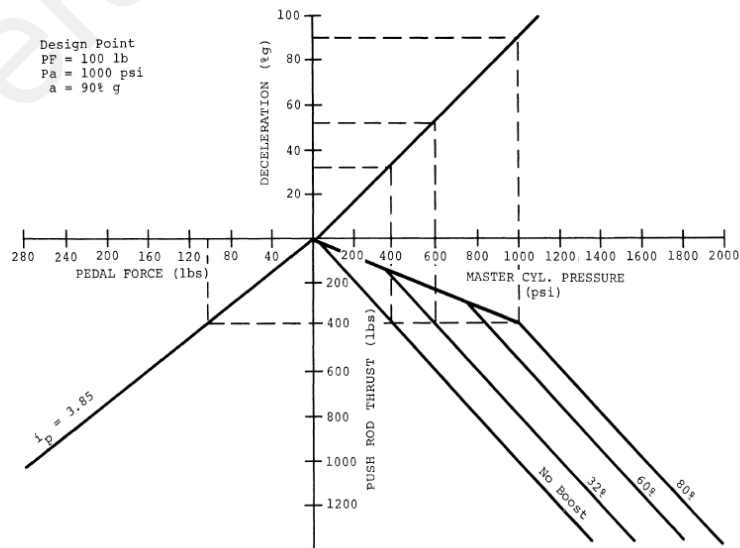


Figure 2-14: Braking Performance Diagram

$$PF = \frac{P_h \cdot A_{Mc}}{i_p \cdot \eta} \quad \text{Eq.2.9}$$

Where in this equation:

PF = brake pedal force

P_h = hydraulic line pressure

A_{Mc} = area for the master cylinder

η = braking efficiency

i_p = pedal lever ratio

P_h = hydraulic line pressure

$$P_h = \frac{W \cdot a \cdot R}{[(A_{WC} \cdot BF \cdot r)_F + (A_{WC} \cdot BF \cdot r)_R] \cdot 2\eta} \quad \text{Eq.2.10}$$

R = effective tire radius

r = effective drum radius

A_{WC} = area of the wheel cylinder

a = deceleration rate in g

BF = braking factor (for the most drum brake designs are listed by (Limpert, 1992))

(Paul S Fancher, 1986; Surblys & Sokolovskij, 2016; Wu et al., 2015, 2017).

2.6.2.4 Braking Performance and Wheel Lock-up

The equation for dynamics of a rotating wheel is given as below:

$$\omega = \frac{1}{I_t} [F_x \cdot r - T_b] \quad \text{Eq.2.11}$$

Where:

ω = angular acceleration (rad/sec²)

I_t = rotational inertia (kg.m²)

F_x = longitudinal wheel force (N)

r = rolling radius (m)

T_b = brake torque (N/m)

In Equation 2.11 for a positive T_b such that T_b is greater than $F_x \cdot r$, the angular acceleration in the next integration step would decrease to a smaller value compared to the prior step. This represents the correct physics, but only until the wheel is locked. Numerically, the integrator used in the model would allow $\omega < 0$ if T_b is greater than $F_x \cdot r$. However, this is not physically possible. To curb this, when the wheels are locked ($\omega = 0$), the equations for rotational dynamics are altered. In this case, when the wheel locks, the brake torque T_b is matched to the equilibrium torque $F_x \cdot r$ so that the resulting ω remain zero (Khekare, 2009).

2.6.3 Stopping and Skidding Distance

A driver's inability to decelerate and stop the vehicle safely is a major attribute of accidents, especially during sudden braking under unforeseen circumstances. In other words, braking becomes critical at the time when stopping the vehicle should be done as fast as possible so as to avoid any crashes. During such a situation, the driver's action is generally to push the pedal with a panicked force. When this occurs, the driver could be applying excessive brake pedal force in the effort to stop the vehicle quickly. This extreme braking might result in one or more wheels of the vehicle being locked even though the vehicle is still carrying an absolute forward velocity (Limpert, 1992).

The stopping distance in the above scenario is composed of two main parts: the distance that the vehicle travels before wheels lock-up and the skidding distance as the vehicle with those wheels locked-up stop skidding. Skidding occurs when a vehicle experiences wheel lock-up, particularly during emergency braking. For many heavy vehicles that are typically not equipped with an anti-lock braking system (ABS), this wheel lock-up phenomenon will cause some of the vehicle wheels to skid, leaving

physical evidence such as the tire marks on the pavement. Furthermore, vehicle engineers, traffic accidents officers, and road safety engineers need to examine how high the vehicle speed is before braking and finally skidding in the case of wheel lock-up.

2.6.3.1 Tire Braking Mark, Skid Mark and Its Importance

A friction mark made on the road by a vehicle's nonrotating tire is called a "braking mark or skid mark". Braking marks differ considerably in their appearance depending on the vehicle condition and the road condition.

Braking marks are useful in crash reconstruction as a means of measuring a vehicle's sudden braking and slowing and help calculate impact location, vehicle condition, driver behavior, minimum speed before the accident, and post-collision trajectories. Among all the principal applications and critical use of such data is the need to identify whether the vehicle is speeding (Ong & Fwa, 2009; Wach, 2016).

Road and crash engineers use some skills such as identifying the relative distance and the orientation between the stopped vehicle and any braking marks created and the vehicle heading based on the driver's descriptions. Such judgments are provided by the investigator's experience and understanding based on the driver's description, which frequently causes disagreements, especially when the driver has inconsistent statements or when the investigator faces a more complex accident scenario (Tseng & Liao, 2012).

In many crash reconstructions, simulation software is being developed to provide the precondition information of the tire braking marks and the parameters that may affect them. This helps the investigators to generate more reliable simulations.

2.6.3.2 Estimation of Speed from Braking and Skid Marks

Estimating the vehicle speed based on braking marks left on the road in accident scenes is very important for crash investigators and road traffic and vehicle engineers (Fricke, 2010). Many studies have been carried out in different areas of vehicle dynamics and crash scenes to correlate the vehicle's initial speed with deceleration variation for both the preskid and the skidding intervals through the analysis of braking marks (Heinrichs, Allin, Bowler, & Siegmund, 2004; Ryu, Lee, Jung, & Cheon, 2010). Various studies on different tire marks suggest a significant difference between the dynamic limits of tire marks. Seipel (2013) then categorized all the tire marks into two main groups based on vehicle dynamics and road properties, as displayed in Figure 2-15 (Seipel & Winner, 2013a,b).

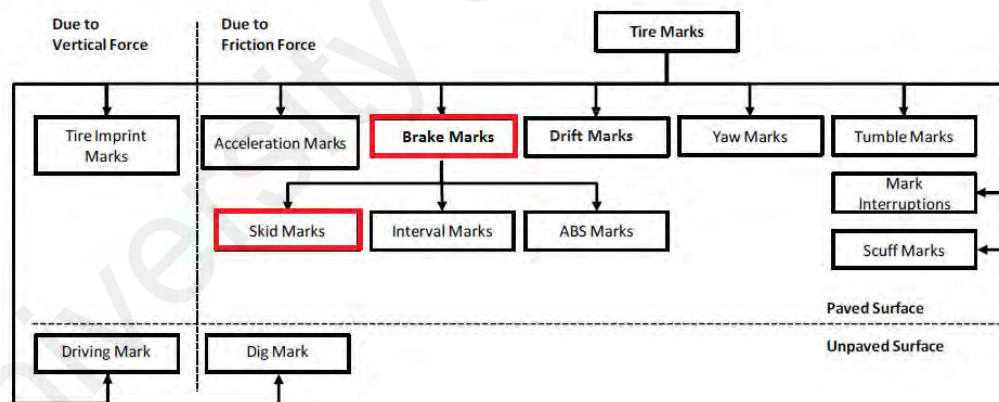


Figure 2-15: Different Type of Tire Marks (Seipel & Winner, 2013a)

Among all the different tire marks noted on the road, brake marks, especially skid marks, stand out as a factor for describing the accident cause. Brake marks play an important individual role among all the other tire marks because they are created during wheel lock-up in an emergency situation. Brake marks are used to calculate the vehicle's

speed before braking for crash analysis and reconstruction purposes. That is, speed calculation before braking is made based on skid marks' length, and this is done according to the speed from skid traditional formula (Seipel et al., 2013a).

In view of the importance of the tire skid marks in crash reconstruction, the mentioned crash risk factors have not been addressed explicitly in the existing practices of determining skidding distance, a significant component of braking distance. Several numerical and field studies have been carried out to determine the vehicle and road parameters affecting the emergency braking distance. The literature data and author's experience show that as the vehicle mass changes, the emergency braking distance changes as well due to the tire contact area. In other words, when the load increases on the tire, the tire footprint will increase, which could affect the adhesion changes (Shirazli, & et al., 2014; Gobbi, Mastinu, & Previati, 2014; Berjoza, 2019; Skrúcaný, Vrabel, Kendra, & Kažimír, 2017). However, changes in the road friction coefficient also significantly will affect the braking distance during emergency braking (Ismael, & Razzaq, 2017; Greibe, 2007). In particular, there have been many investigations revealed that among other factors, the parameter that mostly affects the resulting the vehicle braking distance is speed (Tang, & et al., 2017). Hence less discussed is these factors' impact on the skidding vehicle during emergency braking. Presently, only a few studies have been carried out on heavy truck skidding distance and skid mark length, concerning the mentioned accident risk factors. To the author's knowledge, this lack of information leads to a lack of detailed understanding of the effect of these factors on skid mark length (Bedsworth, Butler, Rogers, Breen, & Fischer, 2013; Qian, Shi, Wang, & Lv., 2007). Past studies on skidding and skid marks have been primarily restricted to experimental field tests and analysis of accident data with a gap left by the comprehensive examination of various factors. This is because comprehensive empirical tests consume a lot of cost and time. Despite improvements made in the techniques of skid mark measurements in recent

years, there is still a need to develop a better measure of skid marks. This is particularly relevant to heavy vehicles such as trucks as past researchers mostly focused on passenger cars and not heavy vehicles where not all wheels lock up. Among the related studies, Ong and Fwa (2008, 2009) recommend a robust analytical model for heavy trucks using the finite element method. Yet even this analytical simulation model focusses on the skid resistance behavior of heavy truck tires only rather than concentrating on skidding distance.

2.6.3.3 *Speed from Skid Formula*

One typical formula in crash reconstruction is the speed from skid formula, although misgivings have been expressed concerns about its accuracy. It is used for estimating vehicle speed while the deceleration remains constant as the vehicle completely comes to a stop without striking an object. It is useful for single-vehicle and multi-vehicle crashes (Fricke, 2010).

To obtain this formula, the initial energy of the moving vehicle before skidding is taken to be equal to the amount of the energy dissipated by the skidding. In other words, all of the vehicle's kinetic energy is converted to heat the tires and road, and the air it creates is equal to the work that would have to be done to stop the skidding vehicle. The kinetic energy conversion to heat is done by the work of friction, so the following will obtain:

Energy at start = Energy at End

Motion Energy = Frictional Energy

$$KE = Work \quad \text{Eq. 2.12}$$

$$KE = \frac{1}{2}(m V^2) \quad \text{Eq.2.13}$$

$$Work = F d = (m a) d \quad \text{Eq.2.14}$$

$$\frac{1}{2}(m V^2) = F d = (m a) d \quad \text{Eq.2.15}$$

Where:

KE = kinetic energy at the start of moving

m = vehicle Mass

a = acceleration (ft/sec^2)

V = vehicle longitudinal speed (ft/sec)

F = frictional or braking force (lb)

d = skidding distance (ft)

It is supposed that the vehicle is skidding to stop without any impact on objects or other vehicles along the road. The kinetic energy is then replaced with friction force based on Coulomb's law of friction, which defines frictional force as a function of the normal force. This means that it converts Equation 2.15 to Equation 2.16.

$$\frac{1}{2} (mV^2) = mad = m (fg) d = m f (32.2) d \quad \text{Eq.2.16}$$

Where:

f = coefficient of friction between tire and road

g = gravity acceleration = $32.2 (ft/sec^2)$

The weight and mass relationship is replaced with the relationship between the weight and mass, instead of the weight on the right side of the equation.

$$\frac{1}{2} (V^2) = (32.2) f d \quad \text{Eq.2.17}$$

$$V^2 = (64.4) f d \quad \text{Eq.2.18}$$

$$V = \sqrt{(64.4) f d} \quad (ft/sec) \quad \text{Eq.2.19}$$

To convert $V (ft/sec)$ to (mph)

$$K = \frac{3600}{1} \left(\frac{sec}{hr} \right) * \frac{1}{5280} \left(\frac{mile}{ft} \right) = 0.6818 \quad \left(\frac{sec.mile}{hr.ft} \right) \quad \text{Eq.2.20}$$

$$K^2 = 0.46488 \quad K^2 * 64.4 = 29.94 \quad (mile^2/hr^2)$$

Finally, it was extracted the final formula as:

$$V = \sqrt{(29.94) f d} = \sqrt{30 f d} \text{ (mph)} \quad \text{Eq.2.21}$$

$$V = \sqrt{254 f d} \text{ (km/h)} \quad \text{Eq.2.22}$$

(Gary, 2006; Xu & Jun 2009; Smith, 1991; James & Nordby, 2002).

2.6.3.4 Formula Practice Assumptions

There are some assumptions for the speed from skid formula, which may be modifications required for other usages of this formula. These include a flat road, constant drag (when all wheels locked with maximum braking efficiency), constant deceleration, a straight-line path with the uninterrupted tire marks. Tire forces are assumed to be negligible, so the whole momentum is converted to friction work.

The spectrum limits the kinematic equations used to establish this formula, the vehicle as to the center of mass. This specific point behaves all vehicle mass is concentrated in it, without considering the vehicle configuration. The model has some limitations in that it discounts force differences on different tires and axles of the same vehicle, and it is independent of vehicle features such as braking system, suspension system, and tire mechanical behavior (Varunjikar, 2011; Gobbi, Mastinu & Previati, 2014).

Furthermore, the conservation of energy always holds true, but we can't still account for all assumptions well enough to apply this type of analysis.

2.6.3.5 Formula Application Issues and Uncertainties

All current methods and formulas used for accident analysis and reconstruction carry some uncertainties depending on their assumptions and applications. Generally, three types of uncertainties have been considered in accident reconstruction analysis: measurement, calculation, and modeling. The value of these uncertainties is crucial

because some factors are essential in accident severity but are sometimes not considered in the reconstruction (Brach, 1994; Chao, 2017; Wach & Unarski, 2007).

- *Measurements:* The essential hands-on measurements for accident reconstruction is typically done by professionals and police officers who work in the field. They illuminate it with standard measurement deviations for skid marks, and the value is assumed for the road coefficient of friction, driver reaction time, and deceleration rise time. Their measurement tools can be another source of uncertainty (Bartlett et al., 2002; Randles et al., 2010; Han & Park, 2010).
- *Calculation:* The calculation uncertainty in accident reconstruction can be related to the computing models and data assumed in the models. (Li, Yuan & Chen, 2004; Batista, 2011; Guzek, 2016).
- *Modeling:* For accident reconstruction, there is an adopted range of modeling, with kinetic or dynamic assumptions, and different parameters as input, which come from driver behavior, the vehicle, and the surrounding environment. Variation of models, analytical or simulation, assumptions, and the input data directly affect the values of outcome such as braking distance (Brach, Guzek & Lozia, 2007; Wach, 2016).

The objective of this research is to focus on vehicle dynamics, particularly tire longitudinal force affected by the vertical force on the tire, to calculate the precrash speed from braking marks. The current formula is based on an energy method considering the vehicle as a point mass, which states that all the kinetic energy of a moving vehicle is lost by the friction to stop it, so the pre-skidding speed is calculated by just measuring the braking mark length and the road friction coefficient.

Many studies have reported the influence of heavy vehicle loading conditions on the severity of the accidents (Gobbi & Massimilano, 2014; Melnikov & Gennady, 2015; LuTy, Witold, 2018), and investigated the effect of the uncertainties in the information of vehicle mass properties, in the accident reconstruction to point out the solid impacts of such parameters (Sztwiertnia & Guzek, 2017; Heinrichs & Bradley, 2012; Metz & Daniel, 1998; Brach, 1994).

As noted previously, one of the objectives of this research is to focus on the vehicle loading conditions' impact on heavy vehicle single accidents with wheel lock-up and skidding. Many studies have reported the influence of heavy vehicle loading conditions on the severity of the accidents. The idea is that a change in vehicle loading will cause different tire behavior and thus affect wheel lock-up and skidding.

A review of the present methods indicates that the formula that calculates the precrash speed from skid marks is based on kinetic energy, and a conversion method that states all the kinetic energy of a moving vehicle (considered as a single mass-point) is lost by the friction to stop it. The amount of information about the vehicle speed calculation that can be gleaned from this formula is limited (Aliakbari & Moridpoure, 2016).

Later, through the theories of tire forces and vehicle dynamics, this study will investigate how vehicle loading conditions can be taken into account in modeling tire braking marks. This implies that it is vital to estimate the sensitivity of such standard speed calculations by the variation of vehicle weight. The dissimilar findings of this research are due to considering vehicle dynamics methods rather than kinematic and considering vehicle and tire properties effects (i.e., by using the dynamics of the rigid body and the magic formula (Pacejka, 1992) for tire model). This research proposes a vehicle model representation that includes both dynamic and kinematic vehicle models.

2.7 Tire Forces Characteristics

The tire plays a critical role in road safety. The crucial factor for vehicle safety is to ensure that the tire grip with the road is sufficient under all applicable working conditions. Tire performance can be categorized into structural and mechanical performance, and both are essential in accident reconstruction.

The structural performance is mostly related to static and dynamic loading conditions, and mechanical performance is related to the tire driving functions, such as acceleration, braking, rolling resistance, and ride comfort. Both structural and mechanical performance are essential elements for accident analysis and reconstruction.

2.7.1 Tire Mechanics

The fundamental duty of any tire is to support the vehicle weight and the load that it is carrying, followed by the appropriate longitudinal force transmission during braking or accelerating. The lateral force it needs to exert to create directional stability and to control the vehicle's steering. Due to the tire's contact with the road and its elastic deformation, the applied forces it exerts can be categorized into three types: F_x longitudinal tire force (tractive, frictional force or braking), F_y lateral tire force, F_z vertical, and normal tire force.

Figure 2-16 illustrates the typical tire forces (Baffet, Charara, & Lechner, 2009)

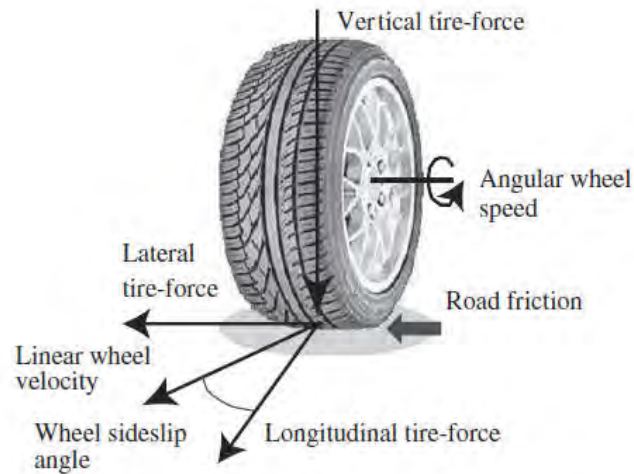


Figure 2-16: Typical Tire Forces

2.7.2 Tire Longitudinal Force

The tire's longitudinal force is produced by every accelerating or braking behavior of the vehicle. Many studies have proven that a longitudinal tire force is significantly dependent on the tire's vertical load and slip ratio. F_x longitudinal tire force versus the tire slip ratio can be seen as a nonlinear function with a different slope for different values of tire normal load. The typical relation is displayed in Figure 2-17, and from here, it can be derived that the longitudinal tire force or braking linearly peaks at a low slip ratio, and then it drops. When the tire is fully sliding (nonlinear area), a smaller braking force is available. Therefore, a decrement in braking distance is expected if the tire slip ratio is retained around this peak.

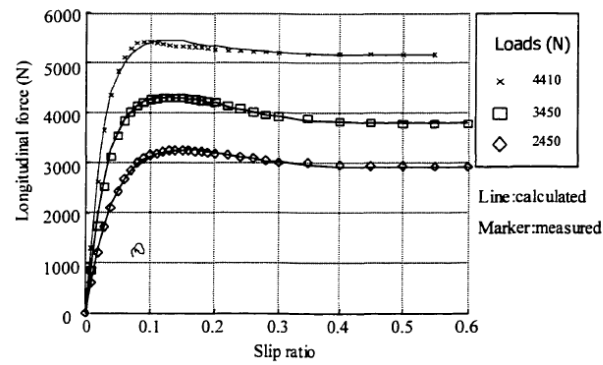


Figure 2-17: General Tire Longitudinal Force Variation with Slip Ratio (Clark, 1981)

During the braking operation, depending on the braking system's air drums or disks, the brake shoes or brake pads are pressed to generate a frictional force. The driver of the vehicle can use the brake pedal forces to regulate the amount of this force. Every force applied to the brake pedal causes the shoes to press against the brake drums (when drum brakes are used) or the disk brakes (where the brake pads are pressed against the disks). Frictional forces are also produced depending on the total force that is exerted on the pedal by the driver. The braking torque, MB , is provided by the frictional force or braking force, which is then multiplied by the distance at which they act from the wheel's rotation axis. The braking torque acts on the circumference of the tire.

2.7.2.1 Tire Slip Ratio

The tire slip ratio is specified as the percentage of the difference between a vehicle's longitudinal speed and its wheel angular velocity. The mathematical definition of slip ratio during braking is shown in Equation 2.23. It should be noted that although various literature shows the equation in slightly different forms (Delaigue & Eskandarian, 2004; Tanelli, Ferrara, & Giani, 2012; Johansen, Petersen, Kalkkuhl, & Ludemann, 2003), the basic definition remains the same.

$$\text{Slip Ratio}\% = \sigma = \left(\frac{r\omega - V}{V} \right) \quad \text{Eq.2.23}$$

where ω is the wheel's angular velocity, V is the vehicle traveling speed, and r is the effective tire radius. The slip ratio can be used as an indicator of the locking status of a wheel. The zero slip ratio is characterized by the coefficient of friction decreasing to its minimum while the wheel has a free motion with no longitudinal tire force acting on the tire contact patch. This is called "free-rolling" (Petersen, Johansen, Kalkkuhl, & Lüdemann, 2001). Whenever there is deceleration due to a braking maneuver, the braking torque acting on the wheels will reduce the rotational or angular velocity of the wheels before the tire compliance generates the opposing longitudinal tire force that overcomes the linear, longitudinal speed. Consequently, a small but non-zero slip ratio exists. However, if this value reaches its maximum magnitude (slip ratio = -100%), then the wheels have come to a standstill even though the vehicle still carries a longitudinal speed. Of the three states, it is only when the slip ratio reaches -100% that wheel lock-up is said to exist. This justifies why it is used as an indicator in this study. Otherwise, wheel lock-up can also be identified indirectly by a sudden decrease in wheel speed (Johansen et al., 2003; Petersen et al., 2001; Tanelli et al., 2012).

2.7.2.2 Coefficient of Friction

The traction performance of the tire is usually expressed by friction coefficient and braking distance, presented as a popular μ -slip ratio diagram. First, one determines the relationship between the speed and the coefficient of friction. As shown in Figure 2-18, it is necessary to understand the major characteristic values related to friction. It explains the behavior of the friction coefficient when the brakes are applied, and the progression of the coefficient of friction under braking. In the beginning, the degree of brake slip is zero, but it increases steeply and reaches its peak from 10 to 40% of brake slips, which

are determined by the tires and the state of the road surface. After attaining its peak point, it begins falling again.

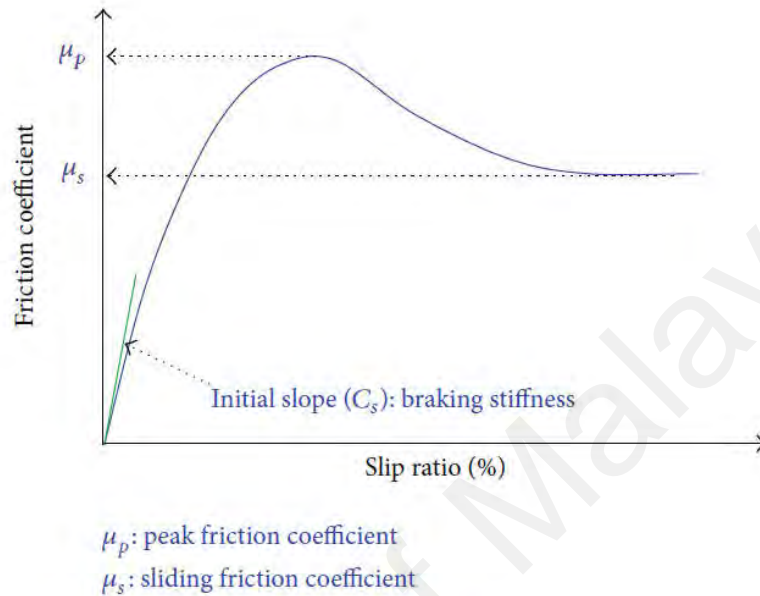


Figure 2-18: General Variation of Road Friction Coefficient with Tire Slip

As shown in Figure 2-18, the slip ratio (abscissa axis) is determined as the speed ratio between the car and the wheel. The highest value of friction coefficient produced due to changes in slip ratio is indicated as the peak friction coefficient (μ_p). The friction coefficient obtained when a locked wheel slide occurs referred to as sliding friction coefficient (μ_s) (Goudie, Bowler, Brown, Heinrichs, & Siegmund, 2000; Leiss, Becker, & Derian, 2013; Noon, 1992; Oh & Lee, 2014; Tanelli et al., 2012).

2.7.3 Tire Lateral Forces

Tire lateral forces (i.e., cornering or slide force) are created due to the steering or when there is a crosswind that causes the vehicle to change direction. The lateral force can also be a reaction to a cornering maneuver, which is called a cornering force, which is

necessary to hold a vehicle through a turn. It is mostly generated by the lateral tire deformation in the contact patch, as illustrated in Figure 2-19.

The cornering force depends highly on the tire's vertical load. This means that when the tire's normal or vertical load increases under the same cornering operational condition, the cornering force also increases. Meanwhile, during cornering maneuvers, a higher vertical load is exerted on the cornering direction tires due to lateral load transfer. Therefore, higher cornering forces are also applied to the same cornering direction tires.

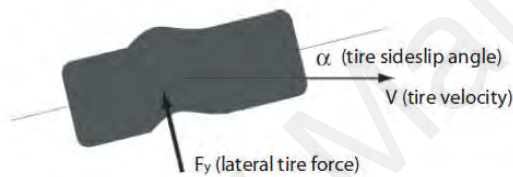


Figure 2-19: Tire Lateral deformation (Clark, 1981)

Besides all these factors, the tire's lateral force, as shown in Figure 2-20, is related to the slip angle of the tire. As much as the slip angle is increasing under the same tire normal load on the tire, the related cornering force also increases. However, when the cornering force reaches a certain level, it does not significantly increase any further. Instead, it tends to converge to an asymptote which is a road surface adhesion limit (Albinsson, Bruzelius, Jonasson, & Jacobson, 2014; Doumiati, Victorino, Charara, & Lechner, 2010; Lian, Zhao, Hu, & Tian, 2015; Ludwig & Kim, 2017).

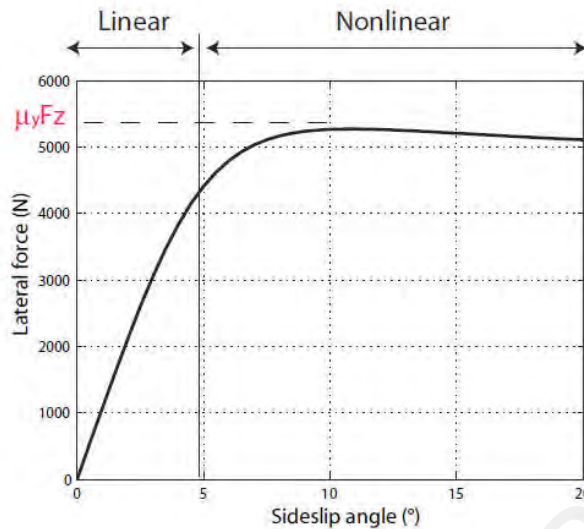


Figure 2-20: General Lateral Tire Force via Different Slip Angles

2.7.4 Tire Vertical Forces

The vertical force, F_z , or normal force, N , is defined as the vertical force acting downward on the tire's footprint. It shows the force exerted between the tire and the road surface. This type of force is always working on the tires even when the vehicle is not in motion.

The payload acting on each vehicle wheel plus the vehicle weight determines the vertical tire force. The vertical force is affected by the additional acting forces on the vehicle (e.g. heavier load). For example, during cornering, the normal force exerted on the inner wheels will be less than the force on the outer wheels.

The degree of the road gradient in which the vehicle is moving or standing on, whether upward or downward, affects the vertical tire force. Nonetheless, it should be considered that the vertical force reaches its maximum peak when the road surface is flat (i.e., when the gradient is zero).

As shown in Figure 2-21, the tire's normal or vertical force deforms the part of the tire in contact with the road surface. This deformation is not uniform and depends on the tire's sidewall properties, which are affected by that deformation. The vertical force cannot be evenly distributed, and this depends on the applied normal force magnitude, where the deformation shape will be different.

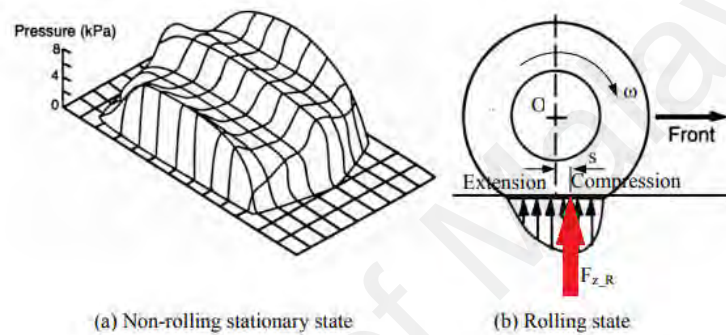


Figure 2-21: Tire normal Force Distribution in Contact with the Road (Gillespi, 1992)

2.7.5 Tire Dynamic Properties Due to Pure Longitudinal Slip

Tires have to experience a specified level of the slip in their footprint or contact area with the road to be able to create enough traction or grip with the road surface.

Braking experiments are the most common way to characterize a tire's response to a longitudinal slip. Figure 2-22 illustrates the general curve shape for F_x and highlights three parameters commonly used to describe the reaction of tires to slip ratio. For any amount of force transmitted by the tires, a certain level of the slip will be created in the contact area. Therefore, a slip is a critical parameter concerning tire forces, and tire forces versus tire longitudinal slip or even slip ratio curves are generally used in automotive engineering specifically for skidding or sliding vehicle behavior. Any increase in the tire

forces increases the tire deformation to a level where the whole contact patch slips. When the extra torque enforces the tire to spin freely, it is known as a full or 100% slip, and when the slip ratio in braking becomes -1.00, the wheel is locked.

2.7.6 Tire Traction and Braking Performance

One of the critical sections of road safety is the heavy vehicle's braking performance. When brakes are applied in a vehicle, frictional force or braking force created in the tire tread connection with the road surface is one of the most critical and essential variables that affect the braking performance. Tire traction, or frictional force, depends on many variables that come from the vehicle features and the road surface specifications. Every driving activity such as steering, accelerating, or braking has a different effect on the tire traction due to the forces that generate at the tire–road surface interface.

Different conditions that come from the tire, such as tire inflation pressure, normal force changes and road surface variation, can also have a maximum force on the tire generated at the contact area. This maximum tire force is the result of two different types of forces produced by the tire (longitudinal and lateral). The sequential and the total force of the tire for the various driving conditions is illustrated by a renowned circle called the “tire traction circle,” as shown in Figure 2-22. The traction circle represents the resultant and the total available force at the tire.

The forces on each tire or the whole vehicle, can be illustrated by a traction circle. In a situation where the vehicle is traveling on a straight path, it only uses longitudinal traction, which is demonstrated by using a vertical arrow. A similar arrow that points in the opposite direction would represent braking. When there is no longitudinal acceleration in a vehicle during cornering, braking would be located along the horizontal axis on the traction circle. The exact position (left/right) would rely on the direction of the corner.

Movement along the boundary of the traction circle, therefore, means that the traction limits of the tires have been reached while a vehicle driving outside the traction circle indicates no traction or even stability. The normal driving scenario happens within the defined traction circle.

If a vehicle is accelerated longitudinally within the traction circle's longitudinal limit, no lateral force can be produced. Now, supposing a vehicle with the lateral acceleration swerves into a corner, it necessarily causes a decrement of the longitudinal force due to the traction state movement along the traction circle in the lateral direction. For a combined vehicle driving and braking condition or even during driving and cornering, the traction is shared between the two conditions. Thus, the main observation from the traction circle is that the magnitude of the traction has to be shared between the lateral and longitudinal tire forces. In the absence of each of these forces, traction force would be only along one axis, x or y.

Furthermore, the presented traction circle can be characterized by more than three or even more dimensions due to its changes under different conditions. Different parameters could be a third dimension, such as vehicle speed (as engine performance and aerodynamics effects come into play) or tire normal force. An expansion nearly linearly outward will most likely occur on the traction circle of each tire whenever there is an increase in the tire's normal load. The traction circle may sometimes be called the "traction ellipse" or "friction ellipse" because experimental data gathered from real vehicles have revealed that the traction circle assumes a more elliptical shape than a circle (Clark, 1981; Nantais, 2006).

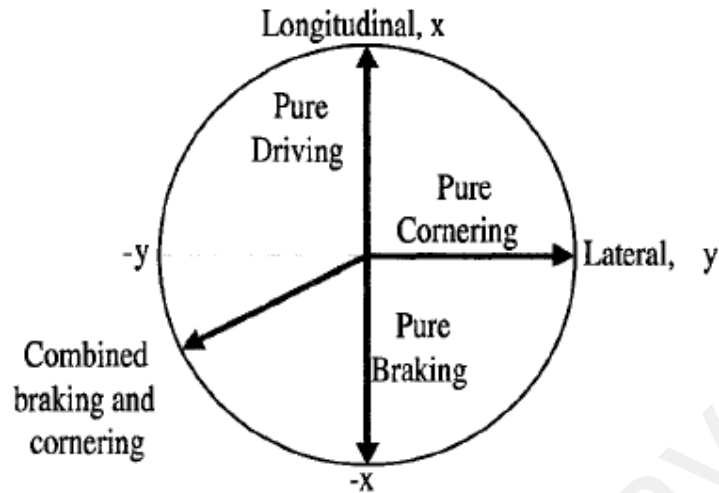


Figure 2-22: Tire Traction Circle (Clark, 1981)

2.7.7 Tire Models

The tire is known to be one of the most complicated and important parts of vehicle dynamics. Various studies have shown that tires have a nonlinear behavior; they react to forces generated in their interaction with the road. This mainly occurs because of the complexity of the tire structure and other constitutive compounds that make up the different properties, so these make tire modeling for simulations a challenging job. Studies examining the modeling of tires have typically used experimental or analytical approaches to this issue (Captain, Boghani, & Wormley, 1979; Pacejka & Sharp, 1992; Rill, 2006; Svendenius, 2003)

Much research has tried to precisely model tire behaviors, but nonlinear rubber properties do not allow an accurate model to be formulated. Instead, the empirical curve fitting for various tires has created a database to stand for representative tires to be used in simulations (Guo & Sui, 1996; Velenis, Tsiotras, & Canudas-de-Wit, 2002).

A general tire model is shown in Figure 2-23 where the tire's longitudinal force calculation is commonly expressed as a function of the different parameters such as tire normal force, slip ratio, and the coefficient of friction (Mokhiamar & Abe, 2004; Villagra, D'Andréa-Novel, Fliess, & Mounier, 2011), i.e.,

$$F_x = f(\mu, \kappa, F_z) \quad \text{Eq.2.24}$$



Figure 2-23: Tire Model Basic Input and Output

Here, μ is the tire-road coefficient of friction, which means the peak; it takes approximately a value in the interval of [0,1]. Therefore, it may be good enough to perform a simplification for Equation 2.24 and describe the tire's longitudinal force as follows:

$$F_x = \mu \cdot f(\kappa, F_z) \quad \text{Eq.2.25}$$

where the described model serves as one of the most common models that were suggested by Pacejka to be the “magic tire formula” (Appendix B), equation 2.25 indicates that the road coefficient μ is a scaling factor that can be factorized as a fixed value. Many studies have comprehensively examined the friction coefficient for different road surfaces (Dorsch, Becker, & Vossen, 2002; Hall et al., 2009; Henry, 2000; Savkoor, 1986).

Due to the complex friction mechanics that are composed of a consequence of many interacting phenomena, many researchers prefer to experimentally determine the friction between different tires and road surfaces. Many research projects have been conducted to examine the interacting friction of the tire and road under different conditions (Wang, Al-Qadi, & Stanciulescu, 2010).

Consequently, many studies have resulted in accurate and reliable data for the coefficients of friction (Lee & Tomizuka, 2003; Tanelli et al., 2012). Figure 2-24 shows some coefficient amplitude for the different road surfaces. A typical road coefficient of friction for various road surfaces involving slip ratio changes can be observed in the following graph.

The graph shows that at zero tire slip (non-acceleration or braking, just a tire free rolling), all curves start at μ zero. Following this, no matter how much the slip is increasing, there is also a linear growth occurring at the maximum tire longitudinal force followed by a drop to the 100% slip ratio, which means that as the wheel lock-up is happening, the tire is no longer rotating and the vehicle is skidding.

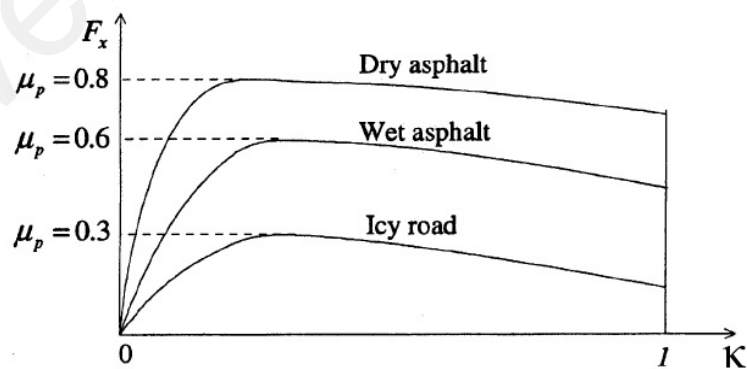


Figure 2-24: Coefficient of Friction due to Tire Braking (Clark, 1981)

2.8 Heavy Vehicle Dynamic Simulation

In the 1970s, computers became sufficiently developed to make the necessary calculations to simulate heavy vehicles and their subsystems. Digital simulations were written at the Highway Safety Research Institute (HSRI) at the University of Michigan. The first heavy vehicle simulation was done in 1971 from the HSRI program, and it was designed to simulate the straight-line braking of heavy vehicles with air drum brakes. The next simulation was done for directional responses of heavy vehicles. In 1980, the simulation programs evolved with the concept of multi-body models, which can more readily handle increasingly complex simulations with larger elements (Sayers, Michael William, 1990).

Heavy vehicle dynamic simulation generally involves motions such as acceleration, braking, ride, and handling characteristics, but the final behavior for any vehicle is influenced by many parameters such as interactions between the tire and the road, gravity, and aerodynamics.

Heavy vehicle dynamics computer simulation has now become an accepted methodology that enables engineers to test and optimize vehicle behavior and to investigate the specifications of future vehicles. Numerous tests maneuvers like braking, double lane changing, acceleration, and rollover can be simulated during the conception phase so as to examine the vehicle's response to any new design, change, or optimization such as changes in subsystems, parts, parameters, or mass distribution on different axels. The main objective of the vehicle simulation is to save design time and cost and to prevent unwanted phenomena such as the skidding of heavy vehicles during emergency situations.

Historically speaking, heavy vehicle dynamic simulations have been used for several vehicle designs and testing applications for at least three decades. Through simulation,

engineers can easily evaluate new designs, both on the component and system level, without building a prototype. Although full-scale prototype testing remains the factual test of any product, but simulations can be used for the initial evaluation of the new design, thereby eliminating several potential problems that may arise and ultimately leading to a more refined design that can be built and tested as a prototype. In the long run, these simulation toolsets greatly reduce time and cost for the entire design process.

Most aspects of vehicle dynamics simulation behavior are comprehensively investigated based on analytical studies, experimental tests, and computer simulations. Recently, safety-related goals have become the major objectives of the vehicle design. Among all these goals, the bold concern is for the accident reconstruction. Concurrently, the vehicle design concept is drawn from the technical view to use the virtual modeling and simulation to save time and cost.

To sum up, many automotive engineers, researchers, and investigators can choose from heavy vehicle computer simulations that span a range of model complexity to determine the best approach to solving problems.

2.8.1 Multi-Body Dynamics

A multi-body mechanical system is defined as a collection of interconnected rigid bodies that can move relative to one another; it is inter-connected with joints that limit the relative motion of pairs of bodies. Multi-body dynamics is the study of the dynamic behavior of such systems as they undergo large displacements caused by external forces.

When dealing with multi-body dynamics, vector and matrix algebra play an essential role because the necessary mathematical foundation for the kinematics and dynamics is formed. Matrix notation makes it easy to represent a system of equations, and matrix operation makes it easy to develop and organize the solutions of the system of equations.

Vectors represent the positions, velocities, and accelerations of points of bodies. In analyzing the equations of motion or when implementing the equations in a computer formulation, vector and matrix algebra are essential tools for solving multi-body dynamic problems.

A full heavy vehicle model can be created through a multi-body system (MBS) software, allowing different simulations to get the desired results. However, depending on the complexity of the defined model and the type of simulation, there needs to be a more computational operation that may also take a long time.

As described in many studies, multi-body simulation has been repeatedly used for vehicle dynamics simulations to validate vehicle dynamic behavior during traveling on different roadway surfaces.

2.8.2 Heavy Vehicle Dynamic Simulation for Accident Reconstruction

The technical heavy vehicle accident investigation is the application of scientific principles to reach conclusions regarding how an accident occurred, why it happened, and perhaps how it might have been avoided or could be avoided in the future. Accident reconstruction engineers have an array of calculation methods available to them for the analysis of heavy vehicle accidents and reconstruction. The spectrum spans kinematic equations that model the vehicle as a point mass without dimensions, to 3D computer simulations that model the exact kinetics or dynamics of the heavy vehicle with a high degree of realism and can directly output 3D visualization of the heavy vehicle's motion.

In recent years, vehicle dynamics' simulation software has been used for accident reconstruction as a means to analyze vehicle safety and highway safety issues. Various software programs (e.g., SMAC, IMPAC, PC-Crash) have been used for reenacting a

vehicle's response during a crash. Based on the data gathered at the scene of the incident, these programs are used to recreate the event and so complete a full analysis of the accident causation in the attempt to prevent similar crashes. In some comprehensive studies, the outcomes of the simulations are compared to the experimental data to show a greater agreement in the linear and nonlinear range of the vehicle's responses (refer to the goals of the research project; Lang, Tao, & Qiang, 2003; Xu, Li, Lu, & Zhou, 2009; Xiaoyun et al., 2007).

2.8.2.1 Analytical Methods Limitations

Analytical methods with analytical solutions are taken from a manual calculation that exists for accident reconstruction, including all categories of vehicles, involving heavy vehicles. A better approximation of accident reconstruction can be made by using computer technology to check the effects of vehicle characteristics and vehicle dynamics. In other words, where analytical calculation methods are limited, computer simulations may be used to determine reliable solutions.

2.8.2.2 Heavy Vehicle Simulation

Simulation programs (e.g., MSC.ADAMS) use numerical methods to solve equations that represent mathematical models of real-world systems. In heavy-vehicle dynamics, the system is the vehicle, and the solution is the response of the vehicle over time to the forces and vehicle, which include suspension, braking system, engines, and tire mechanical properties. Unlike manual analytical methods, simulations don't generate a single answer to the equations. Instead, the equation is solved for a small change in time. The variable outputs from this calculation, are then used as inputs for calculation in the next time step, and so on to the end of simulation time. The time steps must be small, resulting in numerous calculations that require significant computational power. The simulation outputs are the values of all variables at each time step or the time history of

the variables. Thus, the response of the vehicle over time can be predicted. Mathematical models can vary widely in their complexity. Commercially available vehicle dynamics simulation programs (e.g., MSC.ADAMS) can model the vehicle in either 2D or 3D. It may assume to be a rigid body or include subsystems such as suspensions, braking systems, tires, powertrain, and steering depends on the result that the researcher is looking for. It can vary from a straightforward model to highly realistic models. The sophistication of the tire model is particularly essential to the accurate modeling of the heavy vehicles during the different driving phases, where essentially all forces (e.g., accelerating, braking, steering) all occur at the tires.

Inputs to the computer simulations used in accident reconstruction include inert properties, such as driver input, vehicle weight, dimensions, tire, road, and environmental parameters that can be modified relating to steering, suspension, powertrain, and braking systems. Computer simulation can provide a time history on every variable that is part of the underlying equations for the model and subsystems. Variables of the interest can be reviewed by the investigator in tables or graphs.

2.8.2.3 Simulation and Animation

The terms “simulation” and “animation” are often used together, but in fact, they have individual explanations. Animation in forensic engineering usually means the 3D representation of a dynamic process displayed on a 2D display. The data source on which the depicted motion is based may come from the manual calculation, experimentation, or the output from another individual computer simulation. In many cases, the vehicle motion data are entered manually into the animation software.

A simulation is a predicted result determined through a physics-based model that represents the anticipated dynamic behavior. The simulation variable outputs are computed based on fundamental mathematical and physical laws. The graphics associated

with the simulations are determined by the calculated movement and are not explicitly operated by the investigator. These graphical interpretations of the vehicle reactions can be termed “displays” or “visualizations”. Some program manufacturers refer to visualizations created as an output to simulation as “animation” because they animate the vehicle calculated motion, hence the overlapping of the terms.

2.8.2.4 Simulation versus Real Testing

Heavy vehicle simulation is the prediction of dynamic behavior based on mathematical models. The mathematical models include the use of physics equations describing the known behavior of vehicles and data derived from previous tests. In heavy vehicle accident reconstruction, the output of the simulation is a prediction of what would occur in a specific case.

In a world with unlimited resources and full-scale vehicle testing for purposes of vehicle design, safety studies and accident investigation would be routine. In reality, it is not practical to implement full-scale testing to analyze every aspect of vehicle design and certainly not for the investigation of every vehicular accident (Ruhl & Laura, 2006).

2.8.2.5 MSC.ADAMS

Mechanical Dynamics Inc. (MDI) developed the MSC.ADAMS, the automatic dynamic analysis of mechanical systems, in the late 1970s for analyzing general multi-body dynamic systems. In 2002, the MSC Software Corporation acquired Mechanical Dynamics Inc., and so ADAMS is now part of the MSC Software Corporation.

MSC.ADAMS is a recognized leader in the automotive industry. It has been used in almost every design, from small passenger cars to buses and heavy trucks. It provides the best class optimization and modeling tools. Many prominent car manufacturing and components and subsystem suppliers use MSC.ADAMS to design and develop their

products. They use MSC.ADAMS as an integral part of their design process and incorporating dynamic analysis into their designs because it allows immediate feedback. It is the most-used multi-body dynamics and motion analysis software in the world.

MSC.ADAMS, as a complex simulation program, can have hundreds of variable responses available as output. As a run is executed, a 2D or 3D graphical representation of the vehicle and its predicted motion based on the calculated variables can be generated.

Today, MSC.ADAMS, heavy vehicle dynamic simulations with 2D/3D highly rendered graphics allow for effectual demonstrative output immediately after the simulation completion. The improvements to the graphic output of simulations in recent years have led to some confusion between simulations and animations

It helps automotive engineers to study the dynamics of moving parts, see how the forces and loads are distributed throughout mechanical systems, and optimize the performance of their products. Uses of MSC.ADAMS vary between OEMs. For instance, Volvo relies mainly on ADAMS/Car, Audi for ride and handling, and BMW for durability (Liu & Ramnath, 2016; ADAMS, 2005).

The MSC.ADAMS is recognized as the most popular software for analyzing multi-body systems. It automatically converts a topological model to a set of dynamic equations at each step and solves the equations by using a numerical solver (ADAMS, 2005).

The topological model is defined graphically within the MSC.ADAMS environment and the topology is based on the components used to describe the model. The MSC.ADAMS can perform both the kinematic and dynamic analysis as well as the static equilibrium analysis. There is also no restriction in the topological interconnection between bodies. Thus, open-loop, closed-loop, and multiple loop topologies can be analyzed.

MSC.ADAMS has the capability to:

- Construct a complete parametric model for complicated mechanical systems;
- Apply motion, forces and moments to proposed parts of our mechanical system to analyze the system behavior; and
- Measure distances, velocities, and acceleration of the system.

By a selection of correct values for input parameters in MSC.ADAMS, the influence on the results (e.g., tire–road friction coefficient) are subject to the same analysis as any parameter in the analytical method. Many experts have agreed that science is reliable, as simulations have been widely accepted across North America in vehicle accident cases (Sapietová et al., 2016).

MSC.ADAMS/TRUCK is an industry-specific module for modeling heavy vehicles and trucks. It helps to create a virtual model of a full heavy vehicle by creating and assembling the subsystems to analyze the virtual model rather than the real physical model. The model has enough ability to move over different road types, so various behaviors such as tire forces, stopping distance, and acceleration can be measured in the MSC.ADAMS post-processor module.

MSC.ADAMS/TRUCK has two different user graphical interfaces except for the post-processor. The first interface is the “template builder” where different vehicle parts and templates can be created. The second interface is the “standard” environment where subsystems and assemblies can be created and modified.

The general schematic flow of a vehicle simulation, and analysis with MSC.ADAMS is shown in Figure 2-25.

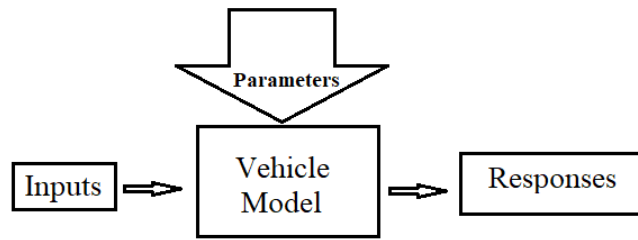


Figure 2-25: The General Schematic Flow of A Vehicle Simulation and Analysis with MSC.ADAMS

2.8.2.6 Modeling of Vehicle Systems

The mechanical parts of the vehicle system are usually made of either rigid or movable multi-body system models that work together with the electrical, hydraulic, and other systems in the vehicle. The validity of the results obtained from the system, depends mostly on the accuracy of the modeling of the vehicle systems that used. Hence, an accurate vehicle model is critical for every study.

A reliable vehicle dynamic system model comprises empirical data, physics-based algorithms, and engineering concepts. There are many well-developed commercial vehicle simulators like the MSC.ADAMS or TruckMaker, which provide a databank of different vehicle's categorized parts and many data sets that specify them. Later, according to the user requirements, the components can be assembled to create subsystems such as the chassis, suspension, powertrain, cab, braking system, and a full-vehicle model.

2.8.2.7 Tire Modeling

The response of vehicle systems to the road conditions is mostly based on the interaction between tire and road, as seen through the forces and moments in the contact area (Cebon, 1993; Hernandez & Al-Qadi, 2017; Klein & Anfosso-Ledee, 2004). The

only other major external forces that act on vehicle systems are related to the aerodynamics (Baker, 1991). The tire-road interaction is subjected by deformation of both the tire and the ground, in each of the contact patches developed between the tire and the ground. There are four different possibilities to model the deformation and contact between the two bodies. They are through using: a rigid tire and a rigid ground; a deformable tire and a rigid ground; a deformable tire and a deformable ground; and a rigid tire and a deformable ground (Li, Wang, & Zhou, 2006; Mousseau & Hulbert, 1996; Schmeitz, 2004; Xia & Yang, 2012). The most commonly used model for vehicles and on-road studies includes a pneumatic tire and a road considered as a solid surface with some irregularities (Gustafsson, 1998; Ray, 1995).

Tire models are most widely used in the vehicle dynamic studies because they predict the longitudinal and lateral forces of the tire as well as the moments that arise between tire and road surface contact area (Van Oosten, 2007).

Throughout the years, different tire forces and moments and many varieties of models have been used to formulate and simulate the tire behavior to be as close as possible to real tires. Based on the tire application, accuracy, and the computational cost of development, tire model definition, and the degree of complexity will be changed. Among all the elements, the empirical models for tires are primarily the best choice for vehicle dynamic simulation (Li, Yang, & Yang, 2014).

The empirical models are commonly defined based on experiments collected from indoor and outdoor tire test results, which correlate to the system's influential parameters, as noted from the existing mathematical equations. To evaluate the vehicle's behavior and performance in the conditions very similar to the real test environment and reach reliable results, tire empirical models become helpful tools, especially for issues related to the vehicle and its contact with the road.

The PAC 2002 tire model is a recognized tire model. It is highly complex and is based on a large set of data (Pacejka & Bakker, 1992). There are also many simplified tire models, such as the FIALA tire model, that can be used to estimate the tire forces and moments through a small set of parameters that describe the tire (Brach, 2009).

2.8.2.8 Road Modeling

The road model plays an important role in the calculation of the tire forces and moments where the vehicle dynamics simulation is conducted, especially for accident reconstruction due to tire interactions with the road. To model the road, there are two common ways to model it as a solid or a deformable surface. Many studies showed that because the vehicle is equipped with tires, one must determine the deformation profile and the contact area or footprint of the tire with road surface by proper definition of the tire specification and properties. An accurate definition of tire contact with the road surface and its related behavior, especially the deformation of the tire, can create more accurate results revealing the tire forces and the tire moments calculation (Doumiati, Victorino, Charara, & Lechner, 2011).

A solid road surface is the most common component in the road models that are broadly used to investigate vehicle behavior. This implies that in most analyses, the vehicle is driven on different solid surfaces such as pavement, asphalt, or cement. There are multiple ways of defining the road as a solid surface.

To conclude, if the road model is defined properly, the footprint or contact area can be effectively estimated for the tire and the road as an important input for vehicle dynamic analysis (Ray, 1995).

2.9 Literature Review Summary

Many technologies have been increasingly used to improve heavy vehicle road safety, but there is a moderate increase in heavy vehicle accidents due to extra weight or overloading. Of the crashes caused by heavy vehicles, tire skid marks, and skidding distance are being used as evidence for accident reconstruction by engineers and investigators.

In this regard, the determination of an accurate precrash speed is a fundamental step in developing a reliable accident reconstruction calculation and crash judgment. Therefore, the success of estimating a real vehicle's speed would depend on whether the model or formula used can calculate the vehicle's speed with precision. The lack of a generalized conclusion and the absence of studies on the impact of heavy vehicle weight limit increases show that the relationship of loading conditions with accidents should be further explored.

In heavy vehicle emergency braking studies, the tire and vehicle dynamics can be defined with different models, from very simplified lumped mass models that consider the vehicle longitudinal braking with a single-wheel model, which is only accurate when the tire inertia is very compared to the vehicle (Olson, Shaw & Stépán, 2005; Peng & Huei, 1996; Colli, Tomassi & Scarano, 2006). front and rear wheel model (two-wheel), to full-vehicle models considering nonlinear tire dynamics (Gim & Nikraves, 1991; Ko & Song, 2010). In this regard, different models are often considered for longitudinal brakings, such as the speed from skid formula given in Equation 2.26 and Equation 2.27. It is one of the traditional and basic formulas used for determining the precrash vehicle's speed that created skidding along the road prior to stopping. This formula is frequently used by road engineers, police officers, or investigators to assess precrash speed from skid marks.

$$V = \sqrt{254 f d} \text{ (km/h)} \quad \text{Eq.2.26}$$

$$V = \sqrt{30 f d} \text{ (mph)} \quad \text{Eq.2.27}$$

Where:

V = pre-crash Speed

f = coefficient of friction

d = skidding distance

The formula was established from the Newtonian laws of physics that a moving vehicle's kinetic energy at the beginning of the wheel lock-up is equivalent to the work performed by the braking force that is applied to the vehicle through the skidding distance.

Experimental evidence shows that the longitudinal tire force, or friction force, is proportional to the tire normal force at the contact point with the road, so the simple equation 2.28 can model the tire's longitudinal or frictional force with the coefficient friction serving as the constant of proportionality (Gillespie, 1992; Wong, 2008; Aly, Zeidan, Hamed & Salem, 2011).

$$F_x = \mu \cdot F_z \quad \text{Eq.2.28}$$

F_x = tire longitudinal or braking force

F_z = tire vertical or normal force

μ = road coefficient of friction

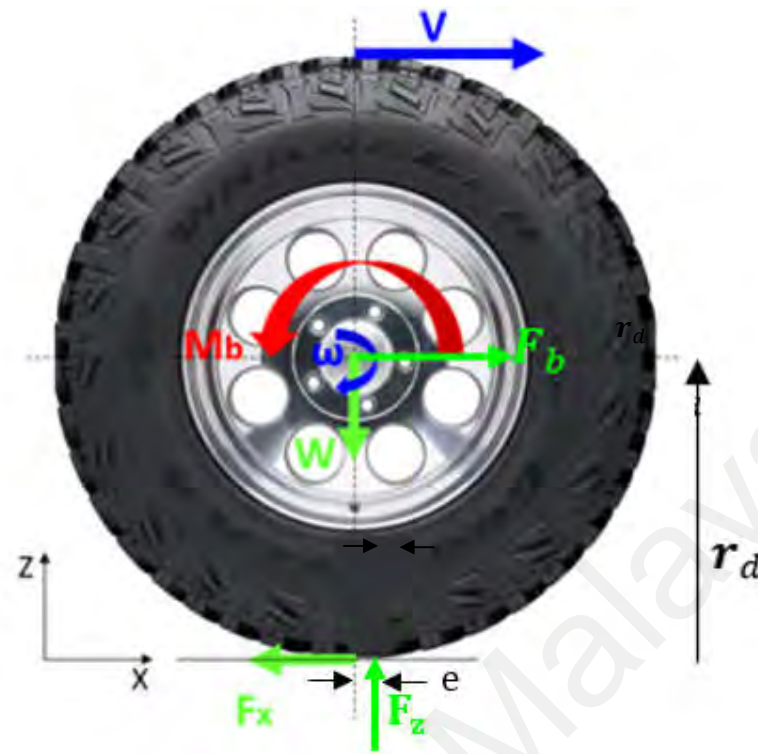


Figure 2-26: Schematic Tire Forces during Braking

Figure 2-26 shows the schematic tire forces during braking. In a real vehicle, the dynamics are $F_x \neq \mu F_z \neq \mu w \neq \mu mg$. This means that a typical assumption for F_x as a linear function of F_z is just a good approximation when the slip ratio is small. In other words, for the high tire slip ratio, more complicated modeling is required due to the strong nonlinear behavior of the longitudinal tire force with the normal tire force. The friction coefficient and tire normal force can be modeled in an empirical manner that depends on the slip ratio (Milani, Marzbani, Khazaei, Simic & Jazar, 2019; M'sirdi, Rabhi, Zbiri & Delanne, 2005).

The linear model of the tire has been used widely in vehicle dynamics applications. This model of the tire is very efficient in the primary simulation of normal driving conditions where the tire slip is small. Because vehicles operate in this region, the longitudinal and normal force of the tire is close to the linear involving the tire slip.

However, when a vehicle maneuvers at severe conditions, the tire slip can become large, and the tire force generation may acquire a nonlinear behavior. In this condition, the linear tire model is similar to the one that was noted in the traditional skid to stop formula. Tire modeling in hard vehicle maneuvers during emergency braking has always been a challenge because of the high nonlinear nature of tires (Berntorp, Quirynen & Cairano, 2019).

Based on the schematic diagram in Figure 2-27, longitudinal tire rotational motion can be formulated as:

$$I\dot{\omega} = -M_b - F_z e + F_x r_d \quad \text{Eq.2.29}$$

Where:

V = wheel longitudinal speed

ω = wheel angular velocity

W = vehicle weight acting on the wheel

M_b = braking torque

F_b = Inertia force during braking process

r_d = Tire effective radius

c_0 = Circumferential tire stiffness

I = Total moment of Inertia

t_{nh} = rise time in longitudinal tire force to reach F_{max}

and

$$t_{nh} = \frac{I\omega_0}{5(M_H + F_z f_t r_d - F_z^2 \frac{\mu}{2c_0} - F_z \frac{\mu r_d}{2})} \quad \text{Eq.2.30}$$

Figure 2-27 shows typical linear and non-linear models for a tire force (Popov, 2010).

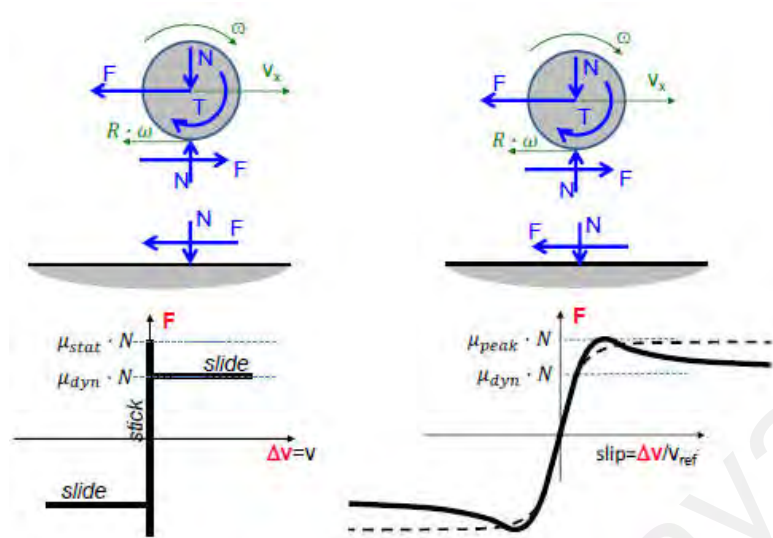


Figure 2-27: Models of Schematic Tire Forces (Popov, 2010)

Through the coefficients of friction, the linear model is simply relating F as the braking force with N as the tire's normal force, $F=\mu \cdot N$. But several different models were developed to study the characteristics of longitudinal tire force as a nonlinear function with multiple inputs, especially slip ratio and F_z functioning as the tire's normal force, so that they can be analyzed and evaluated mathematically. However, these are generally based on multiple inputs. To describe F_x with different inputs, several approaches, including the Pacejka model, have been suggested.

The magic formula parameters are derived from empirical tests, and the common formula to relate the tire's longitudinal force with the slip ratio and the tire's normal force has been widely addressed by many studies.

In general, the formula describes F_x as the tire's longitudinal force in pure longitudinal slip conditions, and it serves as a function of κ , the tire's longitudinal slip. Its shape is a sine arctangent curve shape, which is generally represented by an equation as proposed in Equation 2.31.:

$$F_x = D_x \sin[C_x \arctan\{B_x - E_x (B_x - \arctan(B_x))\}] \quad \text{Eq.2.31}$$

The B_x , C_x , D_x , and E_x parameters vary with the tire normal force, F_z . Some empirical studies have revealed that the tire's longitudinal force, F_x , depends on the slip value and F_z as the vertical or normal tire force. Thus, it should be mentioned that the road surface coefficients of friction that affect the tire's longitudinal force cannot be neglected.

The longitudinal slip ratio (i.e., traction slip ratio or braking slip ratio) is governed by the tire's operating condition. This depends on the vehicle's forward velocity and angular velocity, F_z , which has a variable value that depends on the vehicle's mass distribution and which can be altered by any load transfer in the lateral or longitudinal direction.

The general form of this dependency between the longitudinal tire forces, F_x , with the normal tire forces, F_z , for different tire slips, is shown in Figure 2-29. It is noted that the maximum longitudinal tire force reached a relatively low value of the wheel slip, thereby decreasing to a limited value at full slip. This occurs when the slip ratio is one and when the wheels are locked with zero angular velocity (Carlson & Gerdes, 2003; Pacejka, 2006).

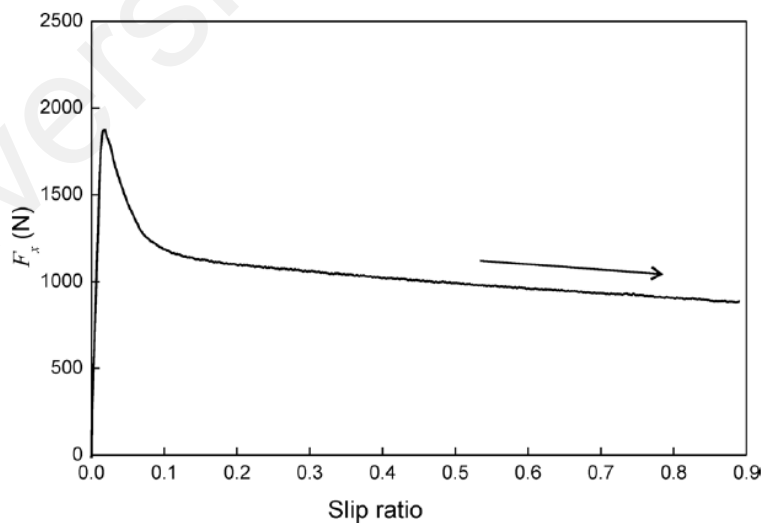


Figure 2-28: Typical Longitudinal Force versus Pure Slip Ratio (Nunney, 2007)

From Figure 2-29, it can be concluded that when the longitudinal tire force is at a very low slip ratio, the relation is approximately linear. However, beyond the linear area, additional forces are generated at every unit of the slip ratio, which starts to drop until it finally reaches its peak, after which the tire force will decrease, and the braking behavior becomes unstable.

Figure 2-30 shows the typical longitudinal tire force against the pure slip ratio under different normal tire forces where F_z is applied during braking. Specifically, in slip ratio 1 (wheel lock-up), the longitudinal and normal forces have a linear relationship. When the normal force is small, the tire's higher normal forces make the relation more nonlinear (Miller, Youngberg, Millie, Schweizer, & Gerdes, 2001; Rittmann & Manem, 1992).

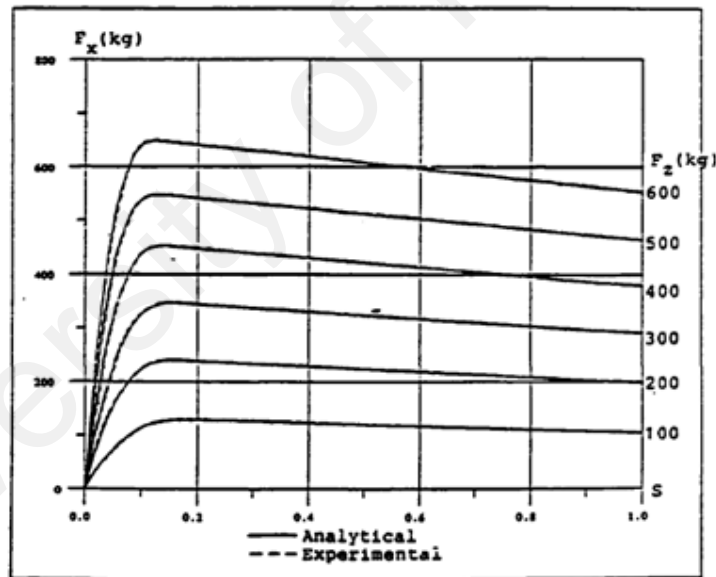


Figure 2-29: Tire Longitudinal Force due to Pure Slip Ratio

From the above explanation, it is clear that varying the vehicle loading conditions (tire normal force) changes the tire footprint, longitudinal forces with the slip ratio. As the load on the tire increases, the area of tire contact with the road also increases, but the relation is nonlinear. Following physics laws, due to mass point assumptions, the nonlinear tire

behavior was ignored in the studies of vehicle braking performance. Aiming to address that gap, the present study thus strives to investigate the different vehicle loading conditions that may affect wheel lock-up and finally predict the skidding distance through a multi-body dynamics with nonlinear tire behavior. The existing theoretical model is mainly simplified, steady-state linear models that assume the tire as a single body with the vehicle when it is in contact with the road and ignoring nonlinear deformations that will affect its footprint.

Hence, this study deduced the nonlinear change of longitudinal tire force with slip ratio and tire normal force to describe the importance of loading condition in heavy vehicle wheel-lock up and provide valuable insight into the vehicle safety and accident reconstruction (Olson, 2001, Zheng, Huang, Zhang, Zhao & Zhu, 2018).

Through the literature studied, the direction of this study has been focused on analysing the most used variables that considered on the reviews pointed above as the reason for heavy vehicle crashes. Understanding the uncertainties resulting from overlooking the vehicle dynamics in the analysis and reconstruction of heavy vehicle crashes that is important and necessary in order to improve crash reconstruction uncertainties. Having considered the work from previous researchers, this research will establish a statistical model to investigate the impact of different vehicle dynamic parameters such as weight and tire performance on the braking characteristics during emergency braking, that is often explored for crash reconstruction reason. Table 2-1 listed the most recent publication that studied the importance of vehicle dynamics in braking performance and accident reconstruction.

Table 2-1 Vehicle Dynamic Parameters and Braking Performance

| Authors | Title | Year | Journal/Conference |
|---------------------------------------|--|------|---|
| Žuraulis, V., & et al. | Vehicle velocity relation to slipping trajectory change: an option for traffic accident reconstruction | 2018 | Promet-Traffic&Transportation |
| Han, I | Analysis of vehicle collision accidents based on qualitative mechanics | 2017 | Part D: Journal of Automobile Engineering |
| Gobbi, M., & et al. | Modelling the tyre forces for a simulation analysis of a vehicle accident reconstruction | 2014 | International journal of crashworthiness |
| Shvets, A. O. | Influence of the longitudinal and transverse displacement of the cargo gravity center in gondola cars on their dynamic indicators | 2018 | Bulletin of Dnipropetrovsk National University of Railway Transport |
| Skrucany, T., & et al. | The influence of the cargo weight and its position on the braking characteristics of light commercial vehicles | 2020 | Open Engineering |
| Moreno, G., & et al. | Rollover of long combination vehicles: Effect of overweight | 2017 | Mechanisms and Machine Science |
| Zebala, J., & et al. | Determination of critical speed, slip angle and longitudinal wheel slip based on yaw marks left by a wheel with zero tire pressure | 2016 | SAE Technical Paper |
| Skrúčaný, T., & et al. | Impact of cargo distribution on the vehicle flatback on braking distance in road freight transport | 2017 | In MATEC Web of Conferences |
| Vrabel J, & et al. | Influence of Emergency Braking on Changes of the Axle Load of Vehicles Transporting Solid Bulk Substrates. | 2017 | Procedia Engineering |
| Vrábel, J. & et al. | Influence of Emergency Braking on Changes of the Axle Load of Vehicles Transporting Solid Bulk Substrates | 2017 | Transportation and technology |
| Nogowczyk P., Pałka A., Szcześniak G. | The influence of mass parameters of the body on active safety of a fire engine in terms of the selection of chassis | 2017 | The Archives of Automotive Engineering |
| Anupam, K., & et al. | Study of Influence of Operating Parameters on Braking Distance | 2017 | Transportation Research Record |
| Han, I. | Analysis of vehicle collision accidents based on qualitative mechanics | 2018 | Forensic science international |
| Shrestha, S., & et al. | Friction condition characterization for rail vehicle advanced braking system | 2019 | Mechanical Systems and Signal Processing |
| Seyedi, M., & et al. | A comprehensive assessment of bus rollover crashes: integration of multibody dynamic and finite element simulation methods. | 2020 | International Journal of Crashworthiness |
| Morrison, G., & Cebon, D. | Combined emergency braking and turning of articulated heavy vehicles | 2017 | Vehicle system dynamics |
| Melnikov, G. I., & et al. | Parametric identification of inertial parameters | 2015 | Applied Mathematical Sciences |
| Tang, T., & et al. | Study of influence of operating parameters on braking distance | 2017 | Transportation Research Record |
| Amoroso, D., & et al. | A Preliminary Study for the Comparison of Different Pacejka Formulations Towards Vehicle Dynamics Behaviour | 2019 | Italian Association of Theoretical and Applied Mechanics |
| Berjoza, D.,& et al. | Testing Automobile Braking Parameters by Varying the Load Weight. | 2019 | 7th TAE Conference |

CHAPTER 3: METHODOLOGY

The characteristics of heavy vehicles play important dynamic roles during emergency braking, particularly in accident scenarios and skidding possibilities. Further, the road conditions also need to be considered as they are equally important for predicting the possibility of skidding accidents. As mentioned previously, extensive studies have reported that the vehicle's high speed, its overloading, tire properties, and road surface conditions contribute to the number of accidents caused by heavy vehicles. In that regard, this study advances the understanding of the wheel lock-up that causes heavy vehicles to skid by developing a verified and reliable heavy vehicle model to assure the accuracy of the results. Additionally, the multi-body dynamic model consisting of different heavy vehicle characteristics, such as, loading conditions, tire forces, speed, and road surface conditions, all of which affect the wheel lock-up, is evaluated when the heavy vehicle's pedal force is changed. The simulations help us to understand what is happening to the heavy vehicle during emergency braking situations.

When all the simulations and wheel lock-up situations are determined (by considering wheel lock-up during emergency braking situations), then an evaluation of the vehicle's conditions, such as the GVW or speed and the road surface Mu is performed; to see if these have any significant effect on the wheel lock-up or skidding. The evaluation can also determine at which point more pedal force is expected to be less effective.

Finally, from the solid simulation results of data analysis, the braking situations are extracted precisely, and an empirical model for the braking mark or tire skid mark length (based on nonlinear multiple regression) is introduced. The regression model is a compact mathematical representation of the relationship between the skidding distance and the

input parameters gained from the vehicle and the road conditions. The regression model can be widely applied to obtain estimates of the different parameter significance and to calculate the skidding distance.

Figure 3-1 shows the research methodology developed by combining the experiment and the simulation to improve the theory.

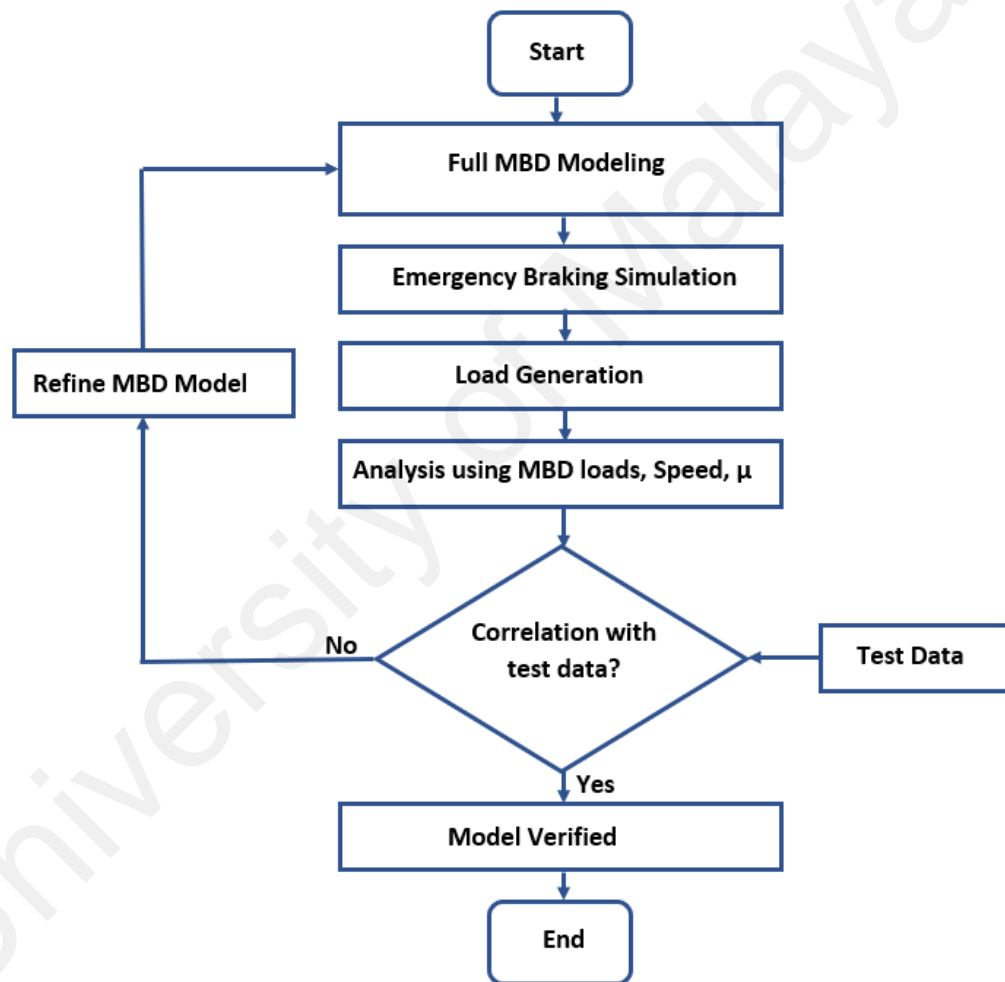


Figure 3-1: Research Methodology Flowchart

The evaluation of heavy vehicle responses to essential conditions and tests are discussed based on the multi-body dynamics simulation approach using the

MSC.ADAMS or Truck. With the advent of computational technology, heavy vehicle dynamics can be fully utilized in multi-body dynamics simulation to obtain simulated vehicle responses as a viable alternative to actual vehicle tests (Schiehlen, Guse, & Seifried, 2006). Many studies have employed the MSC.ADAMS as an approach for vehicle simulations to evaluate the different dynamic behaviors of heavy vehicles and to show how the virtual vehicle models can better model the physical experimental scenarios (Bao, 2014; Hegazy & Sandu, 2010; Li & Kota, 2001; Yao, Huang, Wei, & Sun, 2010).

In this chapter, the research first investigates the effect of the brake pedal force on the heavy vehicle's wheel lock-up by using the multi-body dynamics simulation approach. The virtual heavy vehicle model is subjected to a straight-line braking test by taking into account the GVW, road coefficient of friction, and vehicle speed as the influential factors. Next, evaluation of the braking characteristics is performed by examining the critical pedal force that triggered the wheel lock-up, PF_{crit} . Then the wheel lock-up data under various combinations of conditions are compiled to find the particular circumstances that caused the heavy vehicle's skidding.

As shown in Figure 3-2, the research simulation steps to determine PF_{crit} involve four main steps.

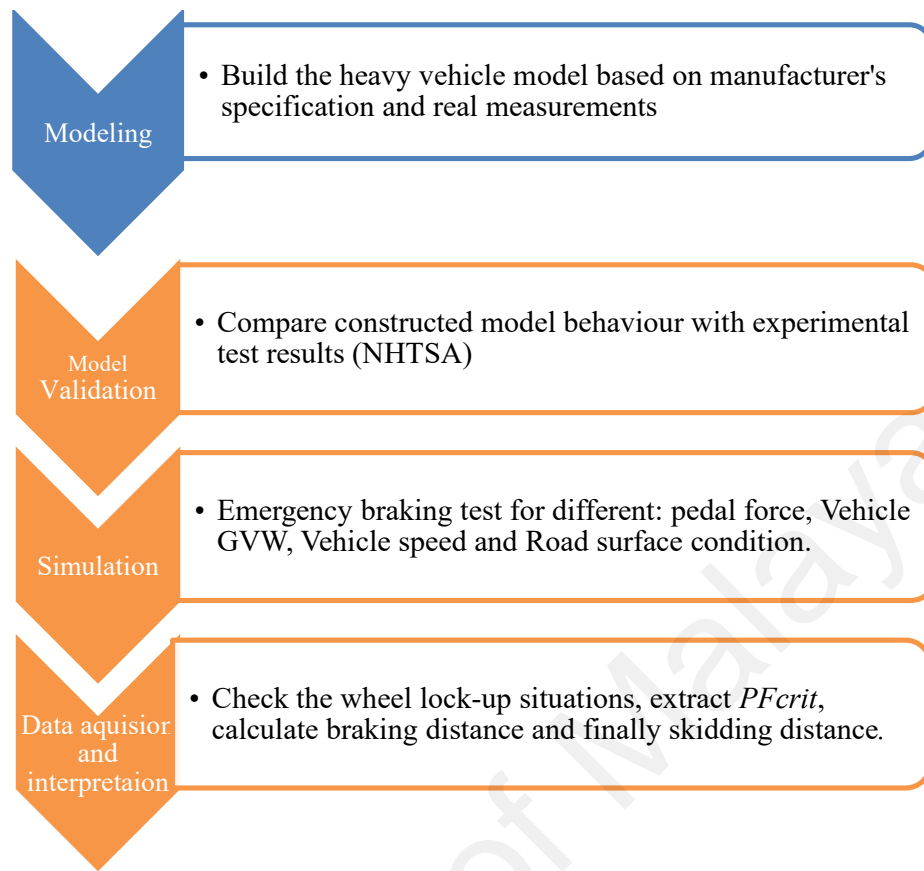


Figure 3-1: Model Development and Simulation Steps

3.1 Multi-Body Heavy Vehicle Model Development

In a vehicle dynamics simulation, a good model can eliminate related problems for the next simulation stage. The flow of modeling in the research is, as shown in Figure 3-3.

In Malaysia, there are differently designed heavy vehicles on the road. They can be categorized as single-unit trucks and trucks with semi-trailers. They may differ in the number of axles. This study focuses on a model of a four-axle single unit truck (SUT) as a case study in an attempt to undergo a series of straight-ahead braking simulations with all brakes functioning correctly as a means to determine the wheel lock-up possibility and to investigate the skidding phenomenon. As explained in the literature review, four-axle SUT is one of the most common commercial vehicles used in Malaysia with high-risk accidents involving skidding.

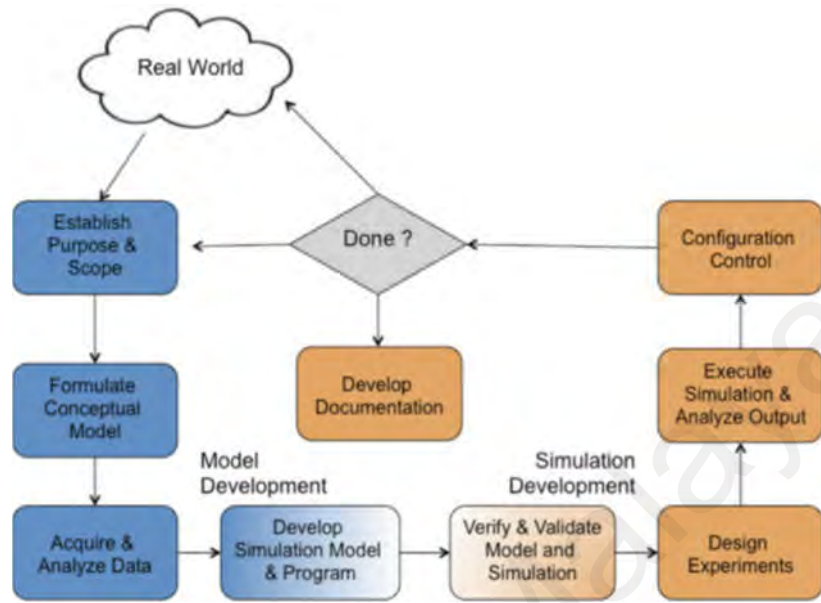


Figure 3-3: Flow of Modeling and Model Verification

The study begins with the modeling of a heavy vehicle in the MSC.ADAMS/Truck, using the graphical user interface of the ADAMS view system, based on a real commercial heavy vehicle model's measurements and manufacturer's specifications (Appendix A). To ensure great compatibility with reality, the multi-body full vehicle assembly in the MSC.ADAMS/Truck system was created with as many details as possible. The goal is to match the model carefully to the heavy vehicle experimental tests to reflect actual behavior during simulation. This made the model's creation a complicated and time-consuming process.

This four-axle SUT is a rear axle-driven vehicle equipped with air drum brakes for three axles. The front suspension system is the combination of a shock absorber with anti-roll bar and parabolic leaf spring, and the rear suspension system consists of multi-link suspension and a shock absorber with the airbag.

As shown in Figure 3-4, three particular classifications create any ADAMS model.

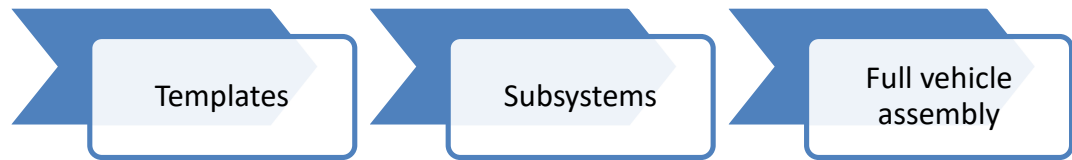


Figure 3-4: MSC.ADAMS Vehicle Model Compositions

Figure 3-5 displays the model's corresponding subsystems and assembly, which are explained in detail in the next sections and more in Appendix C.

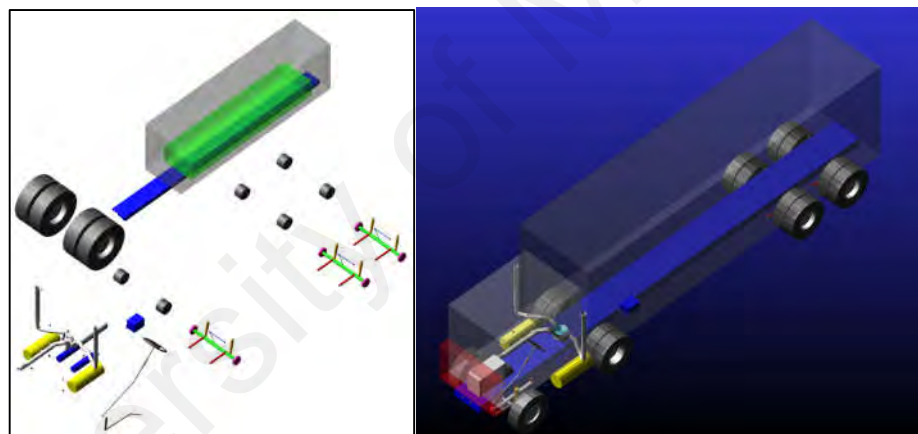


Figure 3-5: The Model's Subsystems and Assembly

The major subsystems that are required to model our SUT in the MSC.ADAMS/Truck is listed below:

3.1.1 Steering

The steering subsystem is one of the most important parts of the vehicle due to its role in controlling the vehicle. The steering system has to properly link the front wheels, preserve an appropriate toe, and produce the necessary steer angles during cornering

maneuvers (Thomas D Gillespie, 1992). There are many different designs for the steering system, but the most common, especially for heavy vehicles and pickups, is the rack-and-pinion and Pitman arm designs. Typically, if the heavy vehicle has straight axles, Pitman arms steering is used. Otherwise, the designers suggest the rack-and-pinion system. Both steering systems can be operated with a hydraulic or power-assisted system. The model steering system is shown in Figure 3-6.



Figure 3-6: Sample MSC.ADAMS Steering System

Any steering wheel move by the driver can be a steering shaft input that causes the steering shaft rotation. The steering shaft is attached at the end with a ball screw through a torsion bar. The ball screw transmits the motion via a coupler to the rack. In turn, the rack also rotates the Pitman arm with a coupler. Finally, the Pitman arm is connected to a steering link, and accordingly, the steering link is connected to the input arm, which is the trigger factor of the left and then the right wheel via a tie rod.

3.1.2 Suspension

3.1.2.1 Steer_axle_suspension

The subsystem for the steer or front suspension has many different parts, such as the front axle, steering knuckles, tie rods, leaf springs, and shock absorbers. Different revolute and spherical joints connect the suspensions parts. Figure 3-7 shows the steer

suspension and its leaf spring. In this study, the stiffness parameters used for the compression and extension of the spring were taken from the National Highway Traffic Safety Administration (NHTSA), and the damping coefficient for the shock absorbers was aimed at 30 KN-s/m for both the left and right sides.

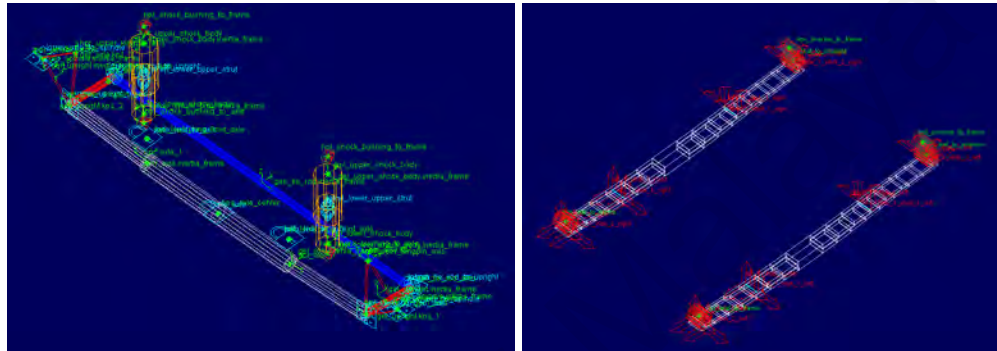


Figure 3-7: Sample MSC.ADAMS Steering Suspension with its Leaf Spring

The front axle is the only steerable suspension in the model. In front suspension, the axle is modeled as a rigid body, and air springs connect the axle to the chassis using mount parts for the frame attachment. Air springs are modeled as an Sforce element, which is defined using I and J parts for the suspension. The suspension I part is an axle, and J is the mount part, which also acts as a place holder for the chassis in the suspension system. Then we select trim load in ADAMS/Solver to solve the related differential equation and set the air spring trim load based on the trim length that is defined in the air spring property file. The differential equation calculates the trim load that corresponds to the desired trim length during static equilibrium analysis. Its value is then locked to the last value calculated during static analysis for all the subsequent simulations. The damper is modeled as a force base on a nonlinear spline between force and velocity. This file is created in ADAMS using the curve manager and then referenced for the front dampers at

the subsystem level. The tire is attached to the hub, and the axle is attached to the hub by revolute joints. Tierod and knuckles from the steering parts for the front suspension help steer the front tires of the vehicle.

3.1.2.2 Tandem_axle_suspension

The tandem_axle_suspension, as shown in Figure 3-8, is a multi-link suspension that is equipped with a shock absorber and an airbag. This tandem drive axle is located at the rear part of the vehicle, and it is attached under the rigid tractor. Since this vehicle is rear axle-driven, there are two actuators from the powertrain subsystem attached to both center axles in this tandem drive axles. This axle is connected to the dual tire template in the model.

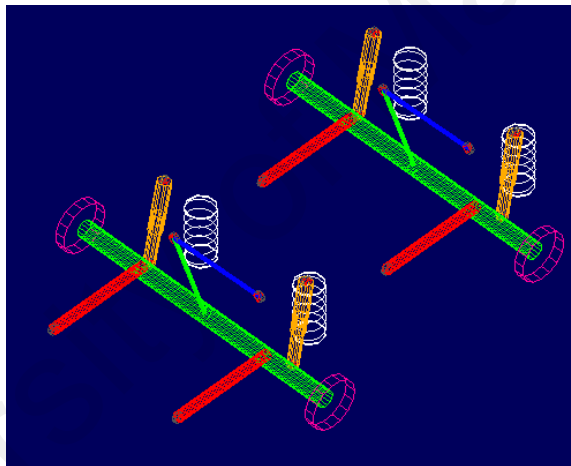


Figure 3-8: Typical MSC.ADAMS Tandem Axle Suspension

Antiroll bars also were assembled on all the SUT axles to make the chassis more stable during hard braking. The bars are connected through their drop-links to the suspension with spherical joints. The primary duty of the drop-links is to transmit suspension motion to the end of the bars and to increase the suspension roll rate.

For the tandem axle, the total vertical and roll stiffness must be split into two coupled axles. The data for the vertical stiffness, and auxiliary roll stiffness was provided by the

manufacturer in the study. The roll stiffness for the springs obtained in the roll and vertical force analysis was verified using Equation 3.1:

$$K_{\theta} = 0.5K_s s^2 \quad \text{Eq. 3.1}$$

where,

K_{θ} = roll stiffness of the suspension

K_s = vertical rate of each of the left and right spring

s = lateral separation between the spring

The total roll stiffness for any suspension is the sum of roll stiffness provided by the springs and the roll stiffness due to the torsion bars, torque rods, rubber bushings, and frame stiffness. As the frame was modeled as a rigid body, all the auxiliary roll stiffness for each axle was provided using anti-roll bars.

3.1.3 Chassis

The heavy vehicle chassis (sprung mass) was modeled as a single rigid body, and the geometry (shell) for the chassis was modeled in MSc.ADAMS/View and then imported to the MSc.ADAMS/Truck. The mass and inertia values for the chassis included the cab and frame combine to make the sprung mass of the model at GVW. The data for the mass and inertia coming from the real vehicle catalogs received from the vehicle manufacturer is in the appendix A. It was respected with the center of gravity of the parts; and the CG position was given concerning a fixed coordinate system below the front axle of the vehicle. The aerodynamic forces were not included in the modeling of chassis. The chassis included several output communicators that helped the chassis get connected to the axles' mount parts. Input mount parts in other subsystems were required to match with the output mount parts in the corresponding subsystems to generate a correct assembly. These output communicators were created to correctly attach the assembly to the other subsystems of the model.

3.1.4 Braking System

The air drum braking subsystem in the model works as a torque on the wheels. To insert the torque, the braking system model was first simulated in ADAMS/View, and its corresponding outputs were then transferred and used in ADAMS/Truck. The schematic of MSC.ADAMS air brake system is shown in Figure 3-9. When the pedal force is applied by the driver's foot, a pushrod between the brake pedal and the master cylinder actuates the master cylinder in response (Park, 2005). In the model, the brake chamber, the brake drum, the camshaft, and the brake pads were modeled with fixed joints. The S-cam, the slack adjuster, and the brake pad pivot were also assigned to the hinged joints. The contacts were attached at the brake pads, the brake drum, the S-cam, and the rollers.

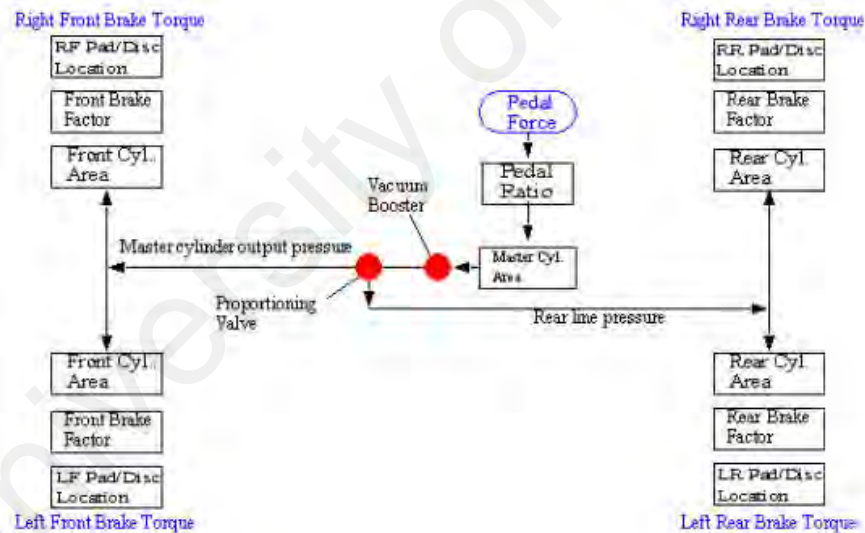


Figure 3-9: Schematic MSC.ADAMS Air Brake System

The brake chamber pressure values measured during the brake application were converted to the corresponding forces on the pushrod and input to the model. With this brake model, the brake input will be the brake pedal force converted into the brake

torques. This means that the parameters of the brake model will calculate the torques based on the pedal force. (See the model *.bst file for the brake system parameters as shown in Figure 3-10.) The mechanical brakes are defined as a single-component torque element applied at each wheel. It is assumed that the actual torque values of each wheel are equal and are received from the MATLAB/Simulink s mechanical brake logic via ADAMS/Control.

| | real_value | remarks |
|------------------------------------|------------|---------|
| pvs_brake_mu | 0.4 | (none) |
| pvs_demand_to_pressure_cnvt | 1.0 | (none) |
| pvs_drive_axle_load_at_max_braking | 8.0E+004 | (none) |
| pvs_drum_radius | 150.0 | (none) |
| pvs_drum_width | 200.0 | (none) |
| pvs_front_axle_load_at_max_braking | 5.0E+004 | (none) |
| pvs_hub_wheel_offset | 150.0 | (none) |
| pvs_pressure_to_torque_cnvt | 4.0E+005 | (none) |

Figure 3-10: Typical MSC.ADAMS Input Parameters for Braking System

3.1.5 Tires

As the tires are the communicators of the heavy vehicle to the ground, correct tire modeling is essential. To know and predict vehicle behavior during the different maneuvers, especially during braking and acceleration, all forces and moments are transferred through the tire's contact footprint to the vehicle model. Therefore, creating tire models according to the real data and tests is very important; it has a significant share of the simulation. In the simulation, the wheel is modeled firstly as a rigid body, but all tire deformation behavior should also be considered.

The ADAMS/Tire consists of many different tire models due to its application. Further, ADAMS provides a chance to users, which allows them to develop their own designed tires. Different tire models with their features are shown in Table 3-1.

Table 3-1 ADAMS/Tire Models and Their Applications

| MD Adams | Event / Maneuver | ADAMS/ Handling Tire | | | | | | | Specific Models | |
|-----------------|------------------------------------|----------------------|----------------------------|--------------------|---|--------------------|---------------------|----------------------|---------------------|-------|
| | | PAC2002 ¹ | PAC-TIME ¹ | PAC89 ¹ | PAC94 ¹ | FIALA ¹ | 5.2.1. ¹ | UA Tire ¹ | PAC-MC ¹ | FTire |
| Handling | Stand still and start | + | o/+ | o/+ | o/+ | o/+ | o/+ | o/+ | o/+ | + |
| | Parking (standing steering effort) | + | - | - | - | - | - | - | - | + |
| | Standing on tilt table | + | + | + | + | + | + | + | + | + |
| | Steady state cornering | + | + | o/+ | + | o | o | o/+ | + | o/+ |
| | Lane change | + | + | o/+ | + | o | o | o/+ | + | o/+ |
| | ABS braking distance | + | o/+ | o/+ | o/+ | o | o | o/+ | o/+ | + |
| | Braking/power-off in a turn | + | + | o | o | o | o | o | + | o/+ |
| | Vehicle Roll-over | + | o | o | o | o | o | o | o | + |
| | On-line scaling tire properties | + | - | - | - | - | - | - | - | o |
| | Cornering over uneven roads * | o/+ | o | o | o | o | o | o | o | o/+ |
| Ride | Braking on uneven road * | o/+ | o | o | o | o | o | o | o | + |
| | Crossing cleats / obstacles | - | - | - | - | - | - | - | - | + |
| | Driving over uneven road | - | - | - | - | - | - | - | - | + |
| | 4 post rig (A/Ride) | + | o/+ | o/+ | o/+ | o/+ | o/+ | o/+ | o/+ | o/+ |
| Chassis Control | ABS braking control | o/+ | o | o | o | o | o | o | o | + |
| | Shimmy ² | o/+ | o | o | o | o | o | o | o | + |
| | Steering system vibrations | o/+ | o | o | o | o | o | o | o | + |
| | Real-time | + | - | - | - | - | - | - | - | - |
| | Chassis control systems > 8 Hz | o/+ | - | - | - | - | - | - | - | + |
| Dura-bility | Chassis control with ride | - | - | - | - | - | - | - | - | + |
| | Driving over curb | - | - | - | - | - | o | o | - | o/+ |
| | Driving over curb with rim impact | o | - | - | - | - | o | o | - | o/+ |
| | Passing pothole | - | - | - | - | - | o | o | - | o/+ |
| | Load cases | - | - | - | - | - | o | o | - | o/+ |
| | | - | Not possible/Not realistic | | * wavelength road obstacles > tire diameter | | | | | |
| | | o | Possible | | ¹ use_mode on transient and combined slip | | | | | |
| | | o/+ | Better | | ² wheel yawing vibration due to suspension flexibility and tire dynamic response | | | | | |
| | | + | Best to use | | | | | | | |

The PAC2002 tire model is the best choice for the braking tests in this study simulation. But to get more realistic results from the simulation, the PAC2002 tire model parameters were extracted from a real tire measurement for steady-state pure longitudinal conditions, as shown in Table 3-2 through the PAC2002 Tire Data and Fitting Tool (TDFT).

The four-axle SUT model was mounted with a total of 14 tires. The drive and rear tandem axles were connected to dual tires, and a single tire was mounted on the steer axle. The tires' necessary parameters that were provided by the manufacturer individually

include section width, section height, aspect ratio, inflation pressure, rated pressure, and rim information. At the least, the tire deflection with different vertical load for the variety of inflation pressure is needed for the simulation to have better output results. Usually, only the vertical load which is exerted to the tire and the deflection of it are measured by the tire manufacturer.

Table 3-2: Tire 315/80 R 22.5 Specification

| PAC2002 | |
|--------------------------|-------------|
| Tire | 315/80R22.5 |
| Section Width (mm) | 315 |
| Aspect Ratio | 80 |
| Unloaded Radius (mm) | 548 |
| Inflation Pressure (kpa) | 800 |
| Rim Radius (mm) | 280 |
| Rim Width (mm) | 229 |
| Wheel Slip | +/- 1.5 |

As shown in Table 3-1, the tire data and the fitting tool in ADAMS were used to create the best real and experimental tire data to develop our PAC2002 Pacejka tire model. Some experimental test results as input for the Pacejka 2002 tire file for tire 315/80 R 22.5 and MATLAB Pacejka model are shown in Figure 3-11, and full information is in Appendix D.

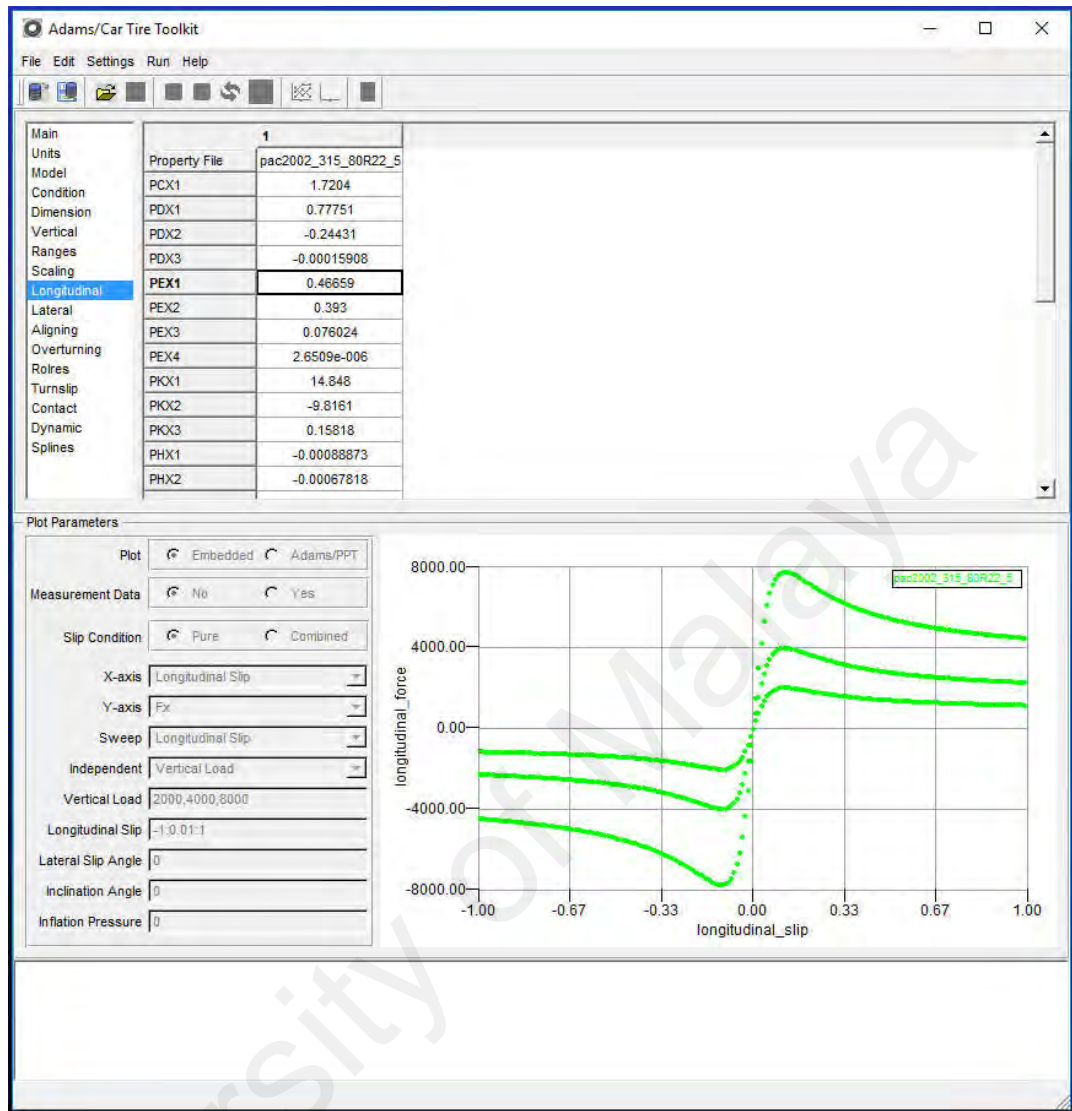


Figure 3-11: ADAMS/Truck Tire Data and Fitting Tool

3.1.6 Test Road for Simulation

The road builder is one of the features in ADAMS/Truck, and this is used for constructing the road for the simulation use of the study. The road layout can be used to construct the base of the coordinate user set, as shown in Figure 3-12.

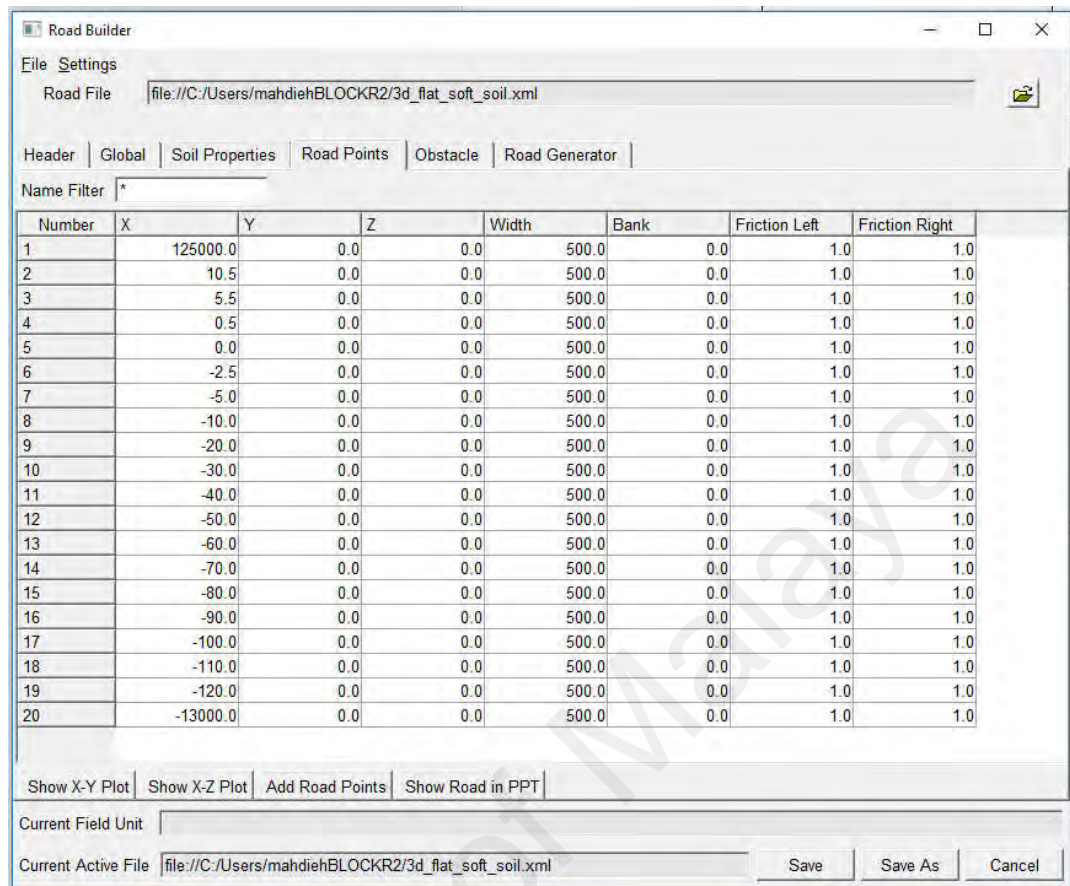


Figure 3-12: ADAMS/Truck Road Builder, Coordination Input

Furthermore, Furthermore, this road builder can be used to construct roads with different friction coefficient surfaces according to the length of the road, and it can be used to insert to the road builder table, as shown in Figure 3-13.

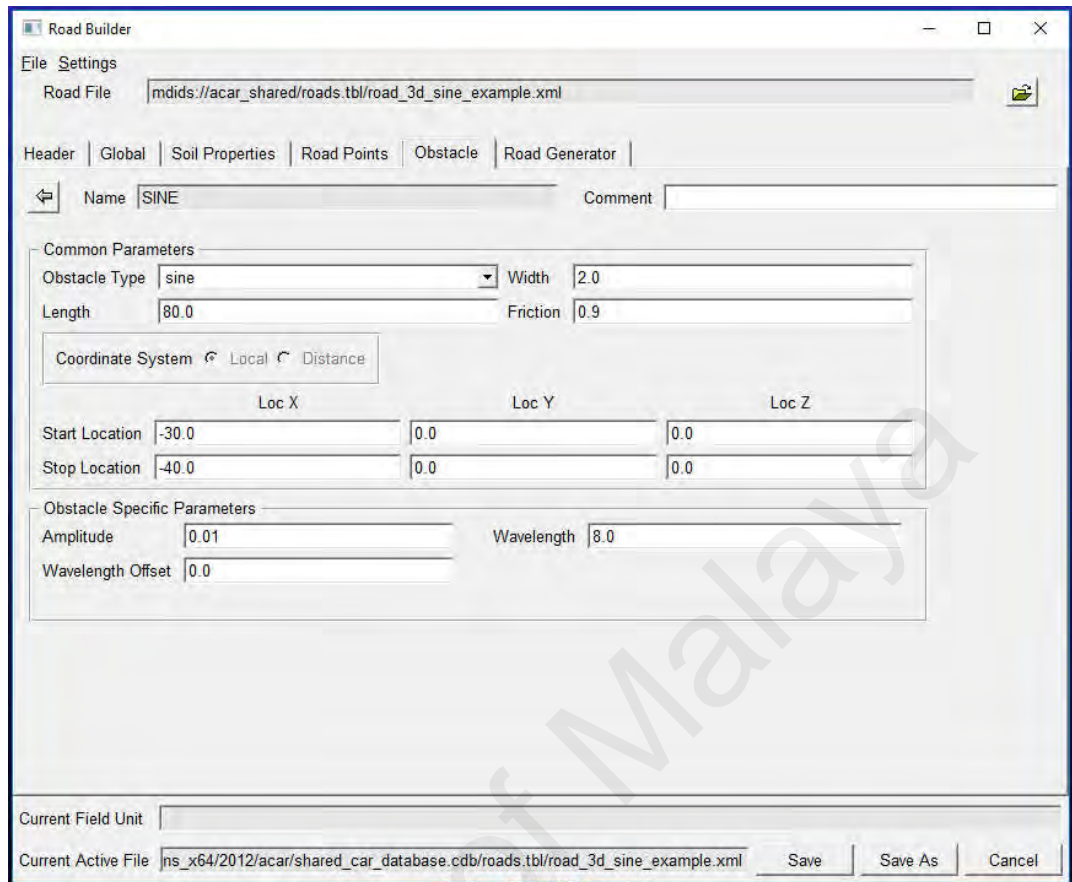


Figure 3-13: ADAMS/Truck Road Builder, the Coefficient of Friction Data

The next stage in tire validation was to compare the response of simulated tire with the experimental tire. Figure 3-14 shows the tire model and experimental tire load-deflection comparison with the measured data (Appendix D). The plot shows that the model replicates the experimental data very closely. The deviations observed in the model output and measured data are negligible with less than 5% error.

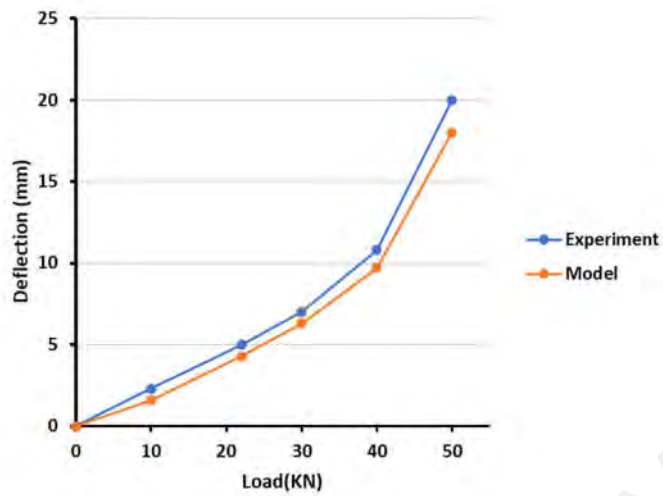


Figure 3-14: Tire Model and Experiment Comparison

3.1.7 Tire Model and Road Interaction

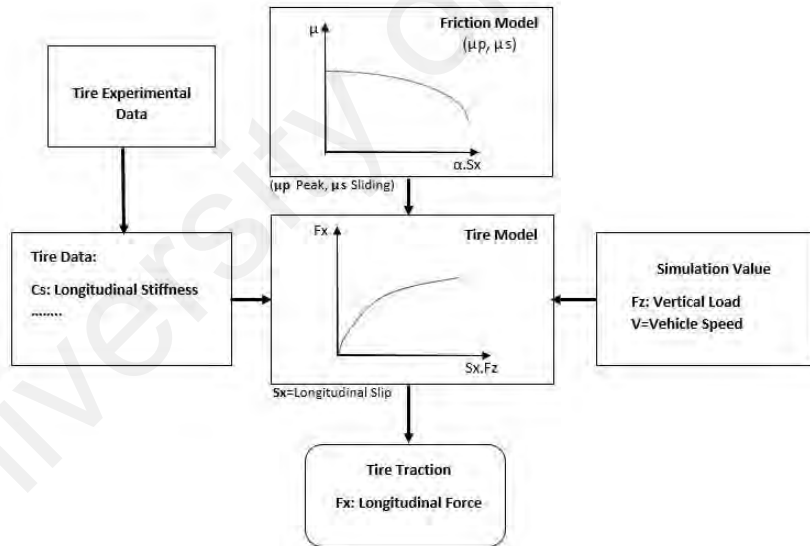


Figure 3-15: Tire-Road Interaction Model

In this study, the magic formula tire simulator model was implemented using a MATLAB- Simulink block diagram. The tire-road interaction is modeled using the Coulomb friction formulation due to our focus on mostly wheel lock-up and skidding

situations. As shown in our road–tire flow-chart in Figure 3-15, the transition between the static friction coefficient (μ_s) and the dynamic friction coefficient (μ_k) is considered based on the traction contact patch, which has sliding and adhesion zones.

Tire and friction models are important when vehicle braking is investigated. The validity of the tire model was established through a series of experimental tests done in Continental involving comparisons of coded tire results with the reported measure data considering nominal tire inflation pressure 800 kPa. It includes static load-deflection tests to verify the vertical tire stiffness and the contact patch size.

The study tire model calculated the vertical load and slip quantities based on the position and speed of the wheel concerning the road. The input for the magic formula consists of the wheel load (Fz), the longitudinal slip, and coefficient friction with the road. The output is the longitudinal force and moments in the contact point between the tire and the road. For calculating these forces, the MF equations use a set of MF parameters derived from tire-testing data. The forces and moments out of the magic formula are transferred to the wheel center and returned to ADAMS/Solver to transfer to the tire MATLAB code.

This tire traction model, for a slip ratio percentage from 0–20%, will consider the peak friction coefficient (μ_k) and calculate the longitudinal tire force by multiplying the vertical tire load by (μ_k). When the tire experiences a 100% slip and wheel lock-up happens, the model will indicate the sliding friction coefficient (μ_s). Furthermore, in the study simulations, a sustained road coefficient of friction from 0.2–0.7 was used to incorporate a wide range of road conditions. Table 3-3 shows the experimental friction coefficient results for a typical tractor on dry asphalt established through experimental tests. It can be seen that the vehicle loading condition has no significant effect on the average drag factor (if wheel lock-up, friction coefficient; Fricke, 1990).

**Table 3-3: Road Coefficient of Friction vs. Vehicle Loading Condition
(Experiment)**

| Loading Condition (lbs.) | 19,000 to 26,000 | 26,001 to 36,000 | 36,001 to 46,000 | 46,001 to 56,000 | Over 56,000 |
|---------------------------------|-------------------------|-------------------------|-------------------------|-------------------------|--------------------|
| Sample Size | 14 | 23 | 9 | NA | 12 |
| Friction Coefficient | 0.59 | 0.61 | 0.6 | | 0.58 |

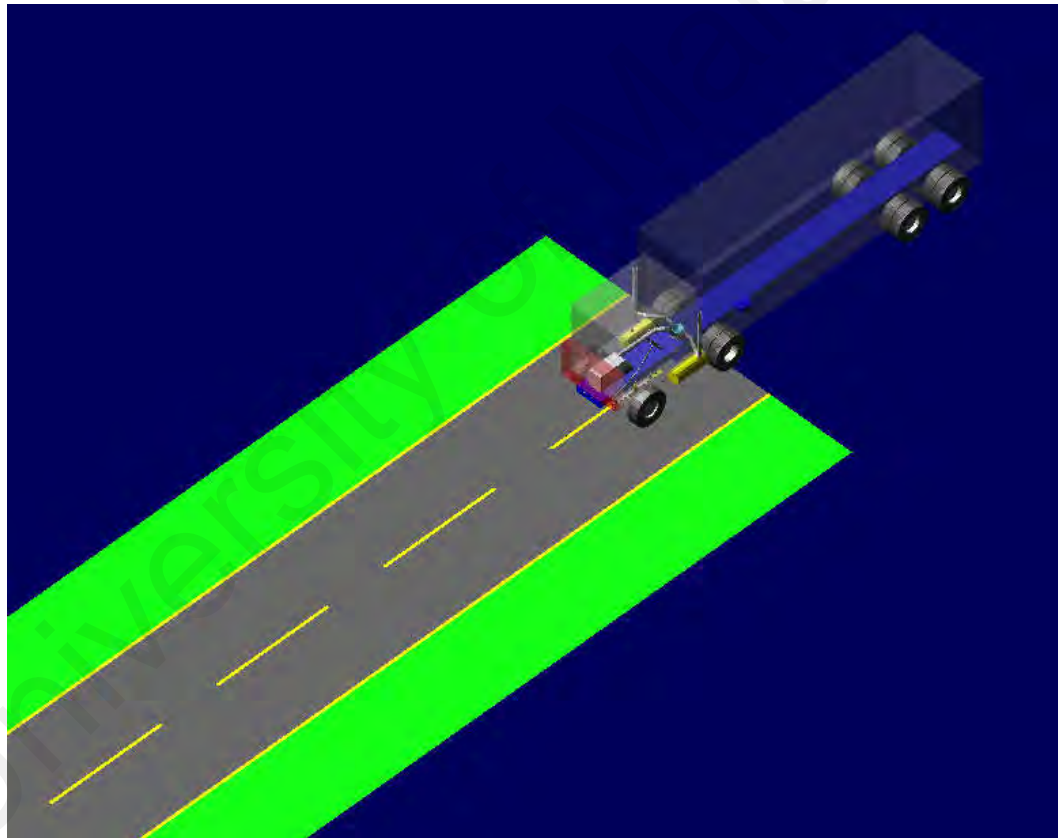


Figure 3-16: Research Model on the Road Profile in ADAMS/Truck

It is possible to define a variable friction coefficient for different vehicle tires. The friction expression could have an expression that can be set or preformatted with three

values: initial, intermediate, and final. If used as a preformatted expression, then it should be selected if the time to be used or the traveled distance is used as the independent variable for the expression. The friction will then pass from the initial to the intermediate value and from the intermediate to the final value via the STEP5 function, as shown in Figure 3-17.

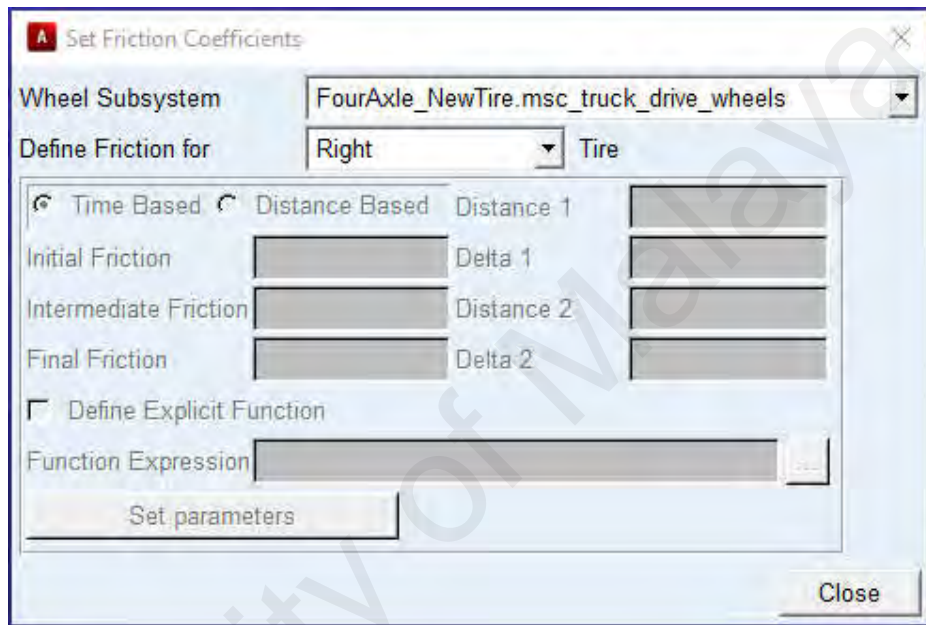


Figure 3-17: ADAMS/Truck road builder, Set Friction's data

3.1.8 Full Vehicle Assembly

The four-axle SUT heavy vehicle modeling is a highly complex process, as explained above. First, the process is supposed to model several components before they are assembled. The vehicle assembly file consists of different defined subsystems, and every subsystem by itself points to the related templates for the topology of the fully functional vehicle. In brief, it consists of the steering, suspension, chassis, braking system, and tires.

The vehicle steering is defined by the Pitman arm steering model. The suspensions include the steering and tandem axle, which are solid axle suspensions. The front one has

a parabolic leaf spring and a shock absorber, and the rear one has a multi-link suspension with a shock absorber. The chassis is a single rigid body that includes the frame and the cab. The braking system is controlled by working the driver's pedal force. Through the braking system, the model will be converted to the braking torque on the wheels. All the tires are modeled by using Pacejka's tire model.

Once all the subsystems are ready, then the full vehicle assembly model is created. This means that ADAMS/Truck can start analyzing the whole system. Table 3-4 shows the list of subsystems with their role as used in the study vehicle assembly.

Table 3-4: SUT Model Subsystems

| Subsystem Name | Major Role | Minor Roll |
|---------------------|----------------|------------|
| Steering | Steering | Front |
| Steer suspension | Suspension | Front |
| Steer wheels | wheel | Front |
| Rigid Cab | Cab | Any |
| Tractor | Body | Any |
| Powertrain | Powertrain | Any |
| Aux parts | Aux parts | Any |
| Beam leaf spring | leaf spring | Front |
| Air drum brakes | Braking system | Any |
| Drive axle | Suspension | Rear |
| Drive wheels | Wheels | Rear |
| Tandem drive axle | Suspension | Rear |
| Tandem drive wheels | Wheel | Rear |

3.2 Heavy Vehicle Multi-Body Model Validation

The heavy vehicle modeling has to be done so as to mimic the real behavior of the mechanical system. The dynamic behavior of the vehicle should not be affected by the approximations during vehicle modeling (Kutluay & Winner, 2014). To be able to

comment on the validity of the created vehicle model, verification is critical. To verify and validate the SUT model simulation results in MSc.ADAMS/Truck, the actual test results conducted with a real vehicle and the simulation results should be compared. During simulation and verification, if the simulation data do not match the experimental test data, then the model is changed for a better approximation.

The process is continued until the desired model results are matched with the empirical test results. In this study, the experimental data were presented according to the National Highway Traffic Safety Administration (NHTSA, 2011) field test results, which were then compared with the simulation results data.

3.2.1 Model Validation Experimental Test Plan (NHTSA)

In any model, the accuracy of simulation relies on the accuracy of the vehicle parameters and, finally, the created model. The objective of this part of the research is to compare data on stopping distance of the simulation model from a range of initial speeds with a real vehicle.

NHTSA's experiments were done to measure the stopping distance for different initial speeds, so we ran the model in the same conditions that experiments were done for two different loading conditions: a loaded and an unloaded vehicle. The experimental tests were carried out according to the Vehicle Safety Compliance Laboratory test standard of TP-121V-04 based on the FMVSS No. 121, Air Brake System. The experiment vehicle specifications used in the NHTSA test series are of a Volvo N12 6*4, as displayed in Figure 3-18. The detailed vehicle information was then included in Table 3-5, and the test loading conditions are illustrated in Table 3-6. The rest of the test vehicle information is fully explained in Appendix E.



Figure 3-18: Volvo 6x4, Experimental Vehicle

The experimental test series were carried out according to the standard SAE J1626. The test procedure was accepted by NHTSA for braking the maneuver of the air drum brake that is equipped in heavy vehicles.

**In this section, the units used for simulation and experiments are imperial, as it was used and reported by NHTSA.

Table 3-5: Test Vehicle Configuration

| | | |
|--|-----------------------|------------------------|
| Vehicle Model | Volvo N 12, Year 1991 | |
| Transmission | 18/manual | |
| Axle Configuration | 6x4 | |
| Wheelbase (mm) | 4814 | |
| Rear Axle Spread (mm) | 2439 | |
| Height of Fifth Wheel from Ground (mm) | 1143 | |
| Fifth Wheel center to rear centerline (mm) | 622 | |
| Suspension System | Front | Leaf Spring |
| | Rear | Leaf Spring |
| Braking System | Front | Disc |
| | Rear | ABS Rear Axle Disabled |

3.2.1.1 Loaded Vehicle Tests

Table 3-6: Test Vehicle Loading Conditions as Specified by NHTSA (Loaded)

| Axle | Corrected Weight (lb) | FMVSS (lb) |
|---------------|-----------------------|------------|
| Front axle | 10,990 | 11,120 |
| Rear axles | 27,360 | 33,680 |
| Trailer axles | 4,490 | 4,510 |
| Total Weight | 42,840 | 49,310 |

However, the vehicle was tested by NHTSA, could not achieve the FMVSS 121 stopping distance (Appendix H) for speed 60 mph in the experimental test, so for the test vehicle, loading was adjusted to a loading condition that brings the average braking distance to the standard target of 250 ft, as shown in Table: 3-7.

The heavy vehicle (loaded) braking test results for each desired initial speeds of 55, 50, 45, 40, 35, 30, 25, and 20 mph, in order, are shown in Table 3-7.

Table 3-7: Test Vehicle Stopping Distance (Loaded)

| Target Speed = 60 mph | | | |
|------------------------------|-----------------------------|-----------------------------------|------------------------------------|
| Stop Number | Actual Initial Speed | Measured Stopping Distance | Corrected Stopping Distance |
| | (mph) | (ft) | (ft) |
| 1 | 59.9 | 246.0 | 246.8 |
| 2 | 59.8 | 240.5 | 242.1 |
| 3 | 60.1 | 253.5 | 252.7 |
| 4 | 60.1 | 250.5 | 249.7 |
| 5 | 60.3 | 252.8 | 250.3 |
| 6 | 59.7 | 259.8 | 262.4 |
| Average Value | | | 250.7 |
| Standard Deviation | | | 6.8 |
| Target Speed = 55 mph | | | |
| Stop Number | Actual Initial Speed | Measured Stopping Distance | Corrected Stopping Distance |
| | (mph) | (ft) | (ft) |
| 1 | 54.9 | 197.1 | 197.8 |
| 2 | 55.2 | 207.2 | 205.7 |
| 3 | 55.2 | 201 | 199.5 |
| 4 | 55.3 | 211.8 | 209.5 |
| 5 | 55 | 190.9 | 190.9 |
| 6 | 55.2 | 201.2 | 199.7 |
| Average Value | | | 200.5 |
| Standard Deviation | | | 5.9 |
| Target Speed = 50 mph | | | |
| Stop Number | Actual Initial Speed | Measured Stopping Distance | Corrected Stopping Distance |
| | (mph) | (ft) | (ft) |
| 1 | 50.3 | 166.5 | 164.5 |
| 2 | 50.7 | 165 | 160.5 |
| 3 | 49.9 | 170.2 | 170.9 |
| 4 | 50.1 | 171 | 170.3 |
| 5 | 50.4 | 172.1 | 169.4 |
| 6 | 50.2 | 170.8 | 169.4 |
| Average Value | | | 167.5 |
| Standard Deviation | | | 4.1 |

| Target Speed = 45 mph | | | |
|------------------------------|-----------------------------|-----------------------------------|------------------------------------|
| Stop Number | Actual Initial Speed | Measured Stopping Distance | Corrected Stopping Distance |
| | (mph) | (ft) | (ft) |
| 1 | 44.9 | 136.6 | 137.2 |
| 2 | 45.1 | 139.0 | 138.4 |
| 3 | 45.5 | 137.0 | 134.0 |
| 4 | 44.9 | 133.3 | 133.9 |
| 5 | 45.1 | 136.8 | 136.2 |
| 6 | 45.6 | 139.1 | 135.5 |
| Average Value | | | 135.9 |
| Standard Deviation | | | 1.8 |
| Target Speed = 40 mph | | | |
| Stop Number | Actual Initial Speed | Measured Stopping Distance | Corrected Stopping Distance |
| | (mph) | (ft) | (ft) |
| 1 | 40.3 | 106.3 | 104.7 |
| 2 | 40.4 | 106.1 | 104.0 |
| 3 | 39.6 | 103.9 | 106.0 |
| 4 | 40.3 | 108.2 | 106.6 |
| 5 | 40.1 | 100.2 | 99.7 |
| 6 | 40.1 | 105.7 | 105.2 |
| Average Value | | | 104.4 |
| Standard Deviation | | | 2.5 |
| Target Speed = 35 mph | | | |
| Stop Number | Actual Initial Speed | Measured Stopping Distance | Corrected Stopping Distance |
| | (mph) | (ft) | (ft) |
| 1 | 35.3 | 80.2 | 78.8 |
| 2 | 35.8 | 81.0 | 77.4 |
| 3 | 35.4 | 81.7 | 79.9 |
| 4 | 35.2 | 79.6 | 78.7 |
| 5 | 35.3 | 81.0 | 79.6 |
| 6 | 35.2 | 79.2 | 78.3 |
| Average Value | | | 78.8 |
| Standard Deviation | | | 0.9 |

| Target Speed = 30 mph | | | |
|------------------------------|-----------------------------|-----------------------------------|------------------------------------|
| Stop Number | Actual Initial Speed | Measured Stopping Distance | Corrected Stopping Distance |
| | (mph) | (ft) | (ft) |
| 1 | 30.2 | 61.7 | 60.9 |
| 2 | 30.1 | 62.3 | 61.9 |
| 3 | 30.8 | 63.4 | 60.1 |
| 4 | 30.5 | 63.6 | 61.5 |
| 5 | 30.2 | 62.3 | 61.5 |
| 6 | 30.2 | 63.6 | 62.8 |
| Average Value | | | 61.4 |
| Standard Deviation | | | 0.9 |
| Target Speed = 25 mph | | | |
| Stop Number | Actual Initial Speed | Measured Stopping Distance | Corrected Stopping Distance |
| | (mph) | (ft) | (ft) |
| 1 | 24.8 | 43 | 43.7 |
| 2 | 25.6 | 45.3 | 43.2 |
| 3 | 24.7 | 42.8 | 43.8 |
| 4 | 24.6 | 45.3 | 46.8 |
| 5 | 25.2 | 44.7 | 44 |
| 6 | 25.4 | 44.9 | 43.5 |
| Average Value | | | 44.2 |
| Standard Deviation | | | 1.3 |
| Target Speed = 20 mph | | | |
| Stop Number | Actual Initial Speed | Measured Stopping Distance | Corrected Stopping Distance |
| | (mph) | (ft) | (ft) |
| 1 | 20.2 | 32.7 | 32.1 |
| 2 | 20.2 | 31.2 | 30.6 |
| 3 | 20.3 | 32.4 | 31.4 |
| 4 | 20 | 30.4 | 30.4 |
| 5 | 20.3 | 31.9 | 31 |
| 6 | 20.2 | 32.5 | 31.9 |
| Average Value | | | 31.2 |
| Standard Deviation | | | 0.7 |

The test data comparison for the braking distance between the NHTSA experimental results and simulation data using ADAMS/Truck is reported in Table 3-8 and graphically shown in Figure 3-19, with the comparison of experiment and simulation results for average BDs at various speeds. It shows the braking distance data for ADAMS/Truck and experimental data for different vehicle speeds as well as a percentage error.

Table 3-8: Braking Distance Analysis (Fully loaded)

| Testing Conditions | | FMVSS 121 (formula) | Experiment (NHTSA) | Simulation | Error Rate with Experiment |
|--------------------|------------------------|------------------------|-----------------------|---------------------|-------------------------------|
| Speed | a | Braking Distance | Braking Distance | Braking Distance | |
| (mph) | (ft/sec ²) | (ft) | (ft) | (ft) | (%) |
| 25 | 18.0 | 45 | 44.2 | 42.5 | 3.85 |
| 30 | 17.5 | 65 | 61.4 | 60.64 | 1.24 |
| 35 | 17.0 | 89 | 78.8 | 81.25 | -3.11 |
| 40 | 17.0 | 114 | 104.4 | 105.41 | -0.97 |
| 45 | 16.8 | 144 | 135.9 | 137.81 | -1.41 |
| 50 | 16.8 | 176 | 167.5 | 172.37 | -2.91 |
| 55 | 16.8 | 212 | 200.5 | 207.41 | -3.45 |
| 60 | 16.8 | 250 | 250.7 | 258.35 | -3.05 |

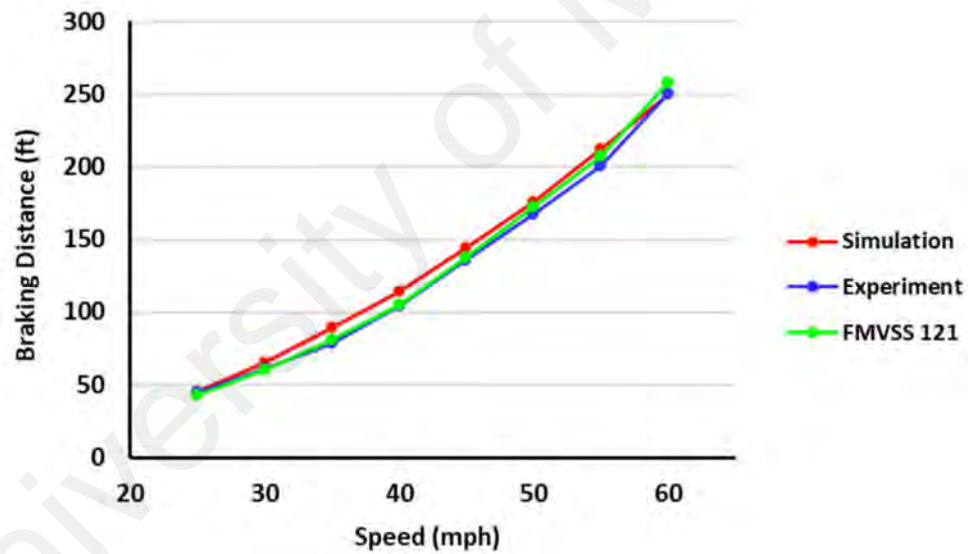


Figure 3-19: Comparison of Experiment and Simulation Results for Average BD's at Various Speeds (Fully-Loaded)

As Table 3-8 and Figure 3-19 show, the simulation braking distance results for different speeds ranging from 25–60 mph are very close to NHTSA's experiment tests, with an error rate of less than 4%.

3.2.1.2 Unloaded Vehicle Tests

The test data comparison for the braking distance between the NHTSA experimental results and simulation data using ADAMS/Truck is reported in this section. Table 3-9 shows the axles loading conditions.

Table 3-9: Test Vehicle Loading Conditions as Specified by NHTSA (Unloaded)

| Axle | (lb.) |
|---------------|--------|
| Front axle | 10,990 |
| Rear axles | 27,360 |
| Trailer axles | 4,490 |
| Total Weight | 42,840 |

Tables 3-10 and 3-11 graphically shown in Figure 3-20, with the comparison of experiment and simulation results for average BDs at various speeds. It shows the braking distance data for ADAMS/Truck and experimental data for different vehicle speeds as well as a percentage error.

Table 3-10: Test Vehicle Stopping Distance (Unloaded)

| Target Speed = 60 mph | | | |
|------------------------------|-----------------------------|-----------------------------------|------------------------------------|
| Stop Number | Actual Initial Speed | Measured Stopping Distance | Corrected Stopping Distance |
| | (mph) | (ft) | (ft) |
| 1 | 59.5 | 182.1 | 185.2 |
| 2 | 59.8 | 181.8 | 183.0 |
| 3 | 61.0 | 192.8 | 186.5 |
| 4 | 59.9 | 184.0 | 184.6 |
| 5 | 59.9 | 182.2 | 182.8 |
| 6 | 59.9 | 179.7 | 180.3 |
| Average Value | | | 183.7 |
| Standard Deviation | | | 2.2 |
| Target Speed = 55 mph | | | |
| Stop Number | Actual Initial Speed | Measured Stopping Distance | Corrected Stopping Distance |
| | (mph) | (ft) | (ft) |
| 1 | 55.5 | 159.2 | 156.3 |
| 2 | 55.7 | 155.6 | 151.7 |
| 3 | 54.3 | 148.8 | 152.7 |
| 4 | 55.6 | 160.4 | 157 |
| 5 | 54.7 | 154.8 | 156.5 |
| 6 | 54.6 | 155.4 | 157.7 |
| Average Value | | | 155.3 |
| Standard Deviation | | | |
| Target Speed = 50 mph | | | |
| Stop Number | Actual Initial Speed | Measured Stopping Distance | Corrected Stopping Distance |
| | (mph) | (ft) | (ft) |
| 1 | 49.4 | 121.5 | 124.5 |
| 2 | 50.8 | 129.7 | 125.6 |
| 3 | 50 | 124.8 | 124.8 |
| 4 | 50.3 | 120.9 | 119.5 |
| 5 | 50 | 128.6 | 128.6 |
| 6 | 50.1 | 127 | 126.6 |
| Average Value | | | 124.9 |
| Standard Deviation | | | 3.1 |

| Target Speed = 45 mph | | | |
|------------------------------|-----------------------------|-----------------------------------|------------------------------------|
| Stop Number | Actual Initial Speed | Measured Stopping Distance | Corrected Stopping Distance |
| | (mph) | (ft) | (ft) |
| 1 | 45.5 | 102.1 | 99.9 |
| 2 | 45.0 | 104.9 | 104.9 |
| 3 | 45.5 | 105.1 | 102.8 |
| 4 | 45.6 | 105.6 | 102.8 |
| 5 | 45.8 | 105.1 | 101.5 |
| 6 | 45.3 | 106.3 | 104.9 |
| Average Value | | | 102.8 |
| Standard Deviation | | | 2.0 |
| Target Speed = 40 mph | | | |
| Stop Number | Actual Initial Speed | Measured Stopping Distance | Corrected Stopping Distance |
| | (mph) | (ft) | (ft) |
| 1 | 40.5 | 84.2 | 82.1 |
| 2 | 41.4 | 87.7 | 81.9 |
| 3 | 40.9 | 84.6 | 80.9 |
| 4 | 40.3 | 84.7 | 83.4 |
| 5 | 40.4 | 84.4 | 82.7 |
| 6 | 41.0 | 84.1 | 80.0 |
| Average Value | | | 81.9 |
| Standard Deviation | | | 1.2 |
| Target Speed = 35 mph | | | |
| Stop Number | Actual Initial Speed | Measured Stopping Distance | Corrected Stopping Distance |
| | (mph) | (ft) | (ft) |
| 1 | 35.3 | 64.8 | 63.7 |
| 2 | 35.6 | 61.8 | 64.7 |
| 3 | 35.6 | 63.0 | 60.9 |
| 4 | 36.4 | 66.3 | 64.1 |
| 5 | 35.3 | 69.4 | 64.2 |
| 6 | | 64.8 | 63.7 |
| Average Value | | | 63.5 |
| Standard Deviation | | | 1.4 |

| Target Speed = 30 mph | | | |
|------------------------------|-----------------------------|-----------------------------------|------------------------------------|
| Stop Number | Actual Initial Speed | Measured Stopping Distance | Corrected Stopping Distance |
| | (mph) | (ft) | (ft) |
| 1 | 30.7 | 49.5 | 47.3 |
| 2 | 30.2 | 48.9 | 48.3 |
| 3 | 30.5 | 48.6 | 47 |
| 4 | 29.5 | 48.5 | 50.2 |
| 5 | 30.2 | 48 | 47.4 |
| 6 | 30 | 48.8 | 48.8 |
| Average Value | | | 48.1 |
| Standard Deviation | | | 1.2 |
| Target Speed = 25 mph | | | |
| Stop Number | Actual Initial Speed | Measured Stopping Distance | Corrected Stopping Distance |
| | (mph) | (ft) | (ft) |
| 1 | 25.1 | 36 | 35.7 |
| 2 | 25.1 | 36.7 | 36.4 |
| 3 | 25 | 37.4 | 37.4 |
| 4 | 24.8 | 36.5 | 37.1 |
| 5 | 25.2 | 36.1 | 35.5 |
| 6 | 25.3 | 34.7 | 33.9 |
| Average Value | | | 36.0 |
| Standard Deviation | | | 1.3 |
| Target Speed = 20 mph | | | |
| Stop Number | Actual Initial Speed | Measured Stopping Distance | Corrected Stopping Distance |
| | (mph) | (ft) | (ft) |
| 1 | 20.5 | 28.6 | 27.2 |
| 2 | 20 | 24.6 | 24.6 |
| 3 | 20 | 25.7 | 25.7 |
| 4 | 20.3 | 25.5 | 24.8 |
| 5 | 19.2 | 25.4 | 26 |
| 6 | 19.9 | 25.6 | 25.9 |
| Average Value | | | 25.7 |
| Standard Deviation | | | 1.0 |

Table 3-11: Braking Distance Analysis (Unloaded)

| NHTSA Testing Conditions | | FMVSS 121 (formula) | Experiment | Simulation | Error Rate with Experiment |
|-----------------------------|-----------------------------|-----------------------------|-----------------------------|-----------------------------|----------------------------------|
| Speed (mph) | a (ft/sec ²) | Braking Distance (ft) | Braking Distance (ft) | Braking Distance (ft) | |
| 25 | 18.0 | 43 | 36 | 39.11 | 8.64 |
| 30 | 17.5 | 61 | 48.1 | 51.92 | 7.94 |
| 35 | 17.0 | 84 | 63.5 | 69.3 | 9.13 |
| 40 | 17.0 | 108 | 81.9 | 90.22 | 10.16 |
| 45 | 16.8 | 136 | 102.8 | 112.47 | 9.41 |
| 50 | 16.8 | 166 | 124.9 | 136.29 | 9.12 |
| 55 | 16.8 | 199 | 155.3 | 167.14 | 7.62 |
| 60 | 16.8 | 235 | 183.7 | 199.7 | 8.71 |

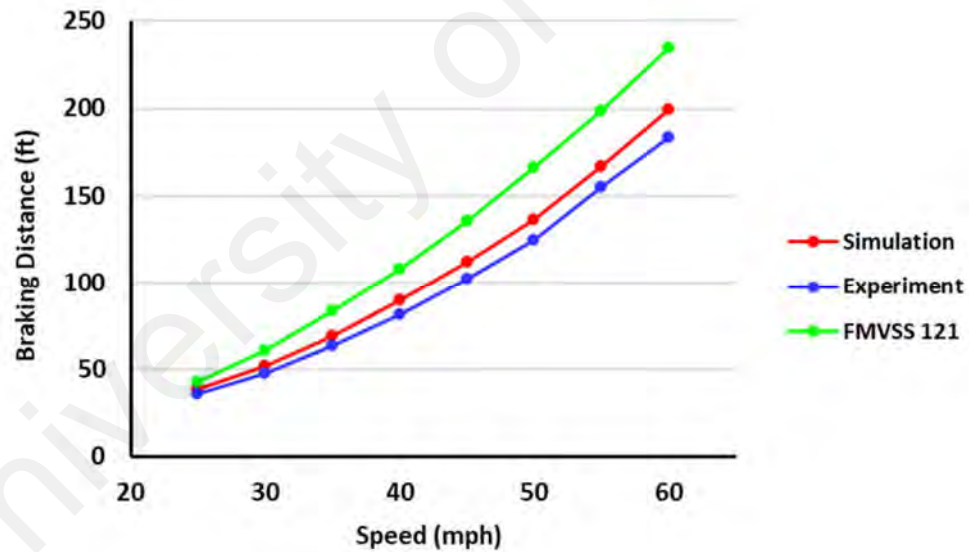


Figure 3-20: Comparison of Experiment and Simulation Results for Average BD's at Various Speeds (Unloaded)

From the figures plotted above and data reported in the tables, it's clear the error rate percentage lower than 10% was observed in all cases. The model generates reasonable

predictions for braking distance for the conditions in which the experimental tests were run. The NHTSA mentioned that the nearly constant acceleration in the experimental trials was challenging to achieve, whereas, in the simulation, there is a constant acceleration as described in the test procedure. Overall, the model meets the standard FMVSS requirements and hence is deemed satisfactory. It shows an acceptable representation of the vehicle's optimal behavior and can be used for vehicle braking test analysis.

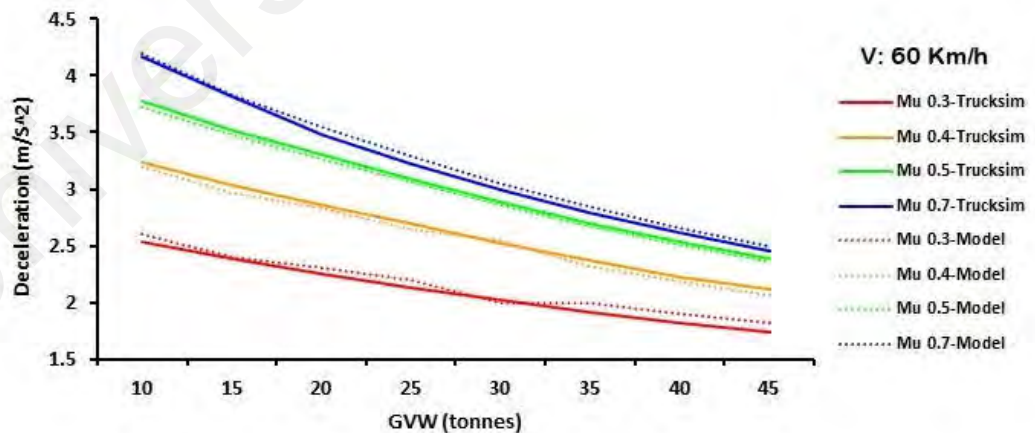
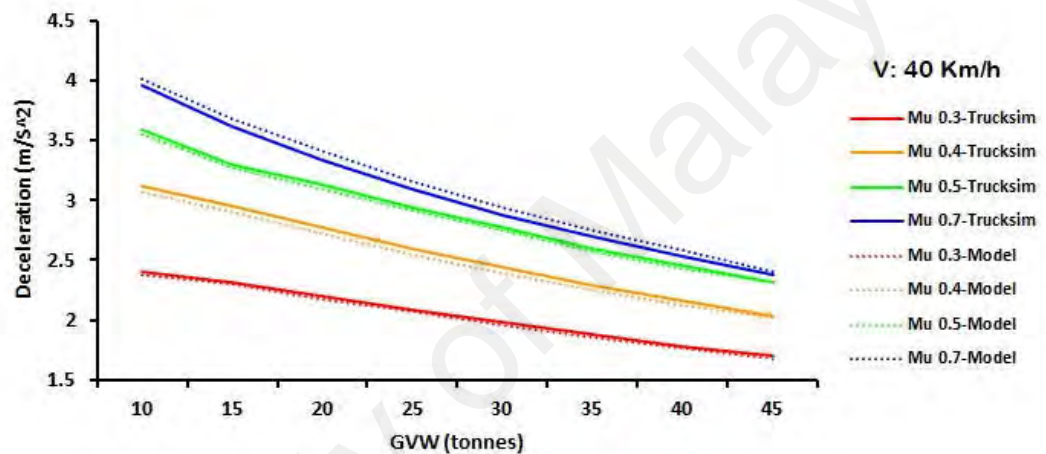
3.2.2 Model Validation with TruckMaker® (4-axle SUT)

Sharizli (2016) discussed a commercial multi-body dynamics simulation package from two-axle to four-axle single-unit trucks (SUTs) to estimate their braking distances under different loads, road surface conditions, and speed. Field data and experimental tests were used to validate his models. The four-axle vehicle model used in this thesis is the same vehicle used by Sharizli in his study. His study stated that the simulation results have the same trend as the test data. It was hence plausible that the longitudinal dynamics of the MSC.ADAMS model can be compared for accuracy to this relatively detailed model in IPG TruckMaker®, a software used to analyse multi-body dynamics (Appendix G).

The graphs plotted in Figure 3-21 are the results of the MSC.ADAMS model running in the same straight line braking test conditions with the Trucks model. It clearly shows the effect of GVW and road coefficient of friction with the deceleration under different speeds. The results confirm that the heavy vehicle loading, has a significant impact on deceleration; in other words as much as the loading condition increases, the deceleration will decrease. So it can be concluded that heavy vehicles with more load will cause a longer braking distance.

Furthermore, for the same GVW and speed, the road coefficient of friction also has a considerable effect on deceleration. As the road coefficient of friction decreases, the

deceleration will decrease as well. This means when the road coefficient of friction increases, the road surface will be rougher, and it causes better traction between the road and tire. In other words, the heavy vehicle moving on the road surfaces with a lower coefficient of friction in the emergency braking requires further braking distance before stopping. The simulation deceleration results for different speeds range from 20–80 mph and are close to the Trucksim validated model, with an error rate of less than 8%.



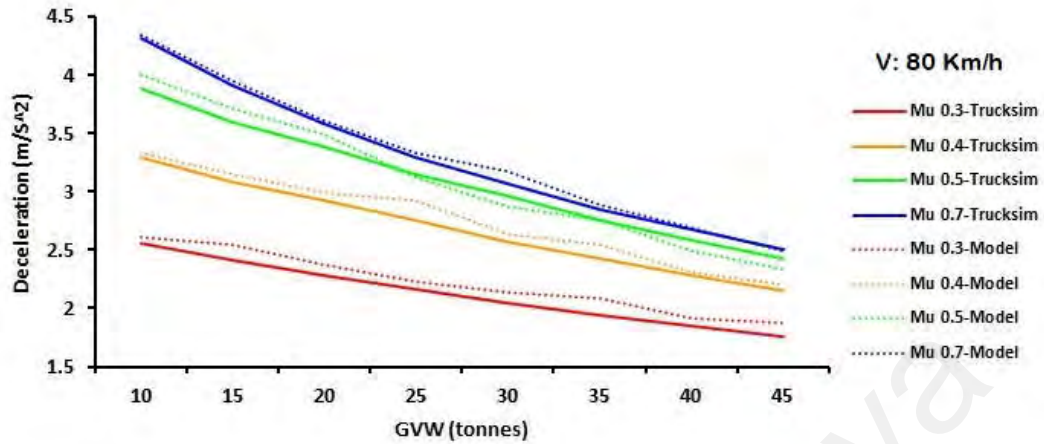


Figure 3-21: Comparison of Simulation Results for Deceleration vs. GVW for different speeds

3.3 Emergency Braking

At this stage, the model of a heavy vehicle had been constructed and verified for the emergency braking simulation. During this simulation stage, the model was run on a straight road with parameters that include the heavy vehicle's initial speed, GVW, and road surface friction coefficient. The initial speed and weight of the truck will change according to the interval set for each simulation. The emergency braking simulation will then be interpreted as a condition in which the driver observes an unwanted and sudden oncoming obstacle and how fast the driver applies the maximum pedal force to create brake pressure to stop the vehicle as soon as possible. The aerodynamic effects were neglected in this simulation.

This study mostly concerns the investigation of the heavy vehicle's wheel lock-up. When a vehicle is being driven in a straight line, and the driver applies brake pedal force sharply to slow down the vehicle, the massive braking torque is applied to the wheels to the point that one or more wheels will stop rotating. This makes the angular speed of the

locked wheel equal to zero, while the vehicle's longitudinal speed remains above zero. To obtain the wheel lock-up data from MSC.ADAMS/Truck, two key phases were included: (a) emergency braking simulation and (b) wheel lock-up data generation and interpretation.

This study requires making an identification of the wheel lock-up scenario because doing so allows the subsequent determination of PF_{crit} , which represents the critical state that triggered the wheel lock-up. In this study, the wheel lock-up scenario was identified by using a slip ratio as the criterion.

3.3.1 Emergency Braking Simulation

After the heavy vehicle model was verified to be of appropriate accuracy, particularly for the braking simulation, the model was then employed to simulate the emergency braking event. During the simulation, straight-line braking on the flat road was taken into account. The use of the flat road profile is consistent with other studies concerning vehicle handling (Tey, Soong, & Ramli, 2014) because braking can be classified as a type of handling maneuver. The emergency braking simulation begins with the heavy vehicle in its steady-state condition. Explicitly, the vehicle was allowed to remain at a constant speed for the first five seconds before any braking effort was initiated. Then a specific brake pedal force value was applied sharply to the vehicle in a 1.5-sec ramp. The pedal force was continuously exerted until the heavy vehicle came to a complete stop, at which point the braking simulation was considered to be finished.

3.3.2 Braking Maneuver Setting

To investigate the effect of the brake pedal force which is the fundamental factor for the wheel lock-up, the emergency braking simulation was performed repetitively at the range where the increasing pedal force values are as stated in Table 3-12. Apart from this, three external influential factors, GVW, road coefficient of friction (μ), and vehicle

speed, were also considered as the external conditions in this study. The ranges for these influential factors are stated in Table 3-12 as well.

In reality, GVW, Mu , and vehicle speed represent the vehicle load condition, the road surface condition, and the speed condition during an actual braking situation. For load condition, a GVW of 11 tons, 21 tons, 31 tons, and 41 tons represent empty, semi-loaded, fully-loaded, and overloaded conditions, respectively, for the heavy vehicle model used. Meanwhile, the range of Mu from 0.3–0.7 corresponds to a change evolving from slippery to high-traction surfaces such as from wet to dry road conditions.

Table 3-12: Simulation Input Parameters

| Influential Factors | Values |
|--------------------------------------|--|
| Gross Vehicle Weight, GVW (t=tonnes) | 11 (Empty), 21 (Semi-loaded), 31 (Fully-loaded), 41 (Overloaded) |
| Coefficient of friction, μ | 0.3, 0.4, 0.5, 0.6, 0.7 |
| Speed (km/h) | 40, 50, 60, 70, 80 |
| Pedal force (N) | 10 to 600 (in steps of 10) |

Finally, a vehicle speed oscillating from 40–80 km/h characterizes the common traveling speed for most heavy vehicles. From the combination of all these factors, a total of 6,000 vehicle response data sets were generated from the emergency braking simulations. The output generated incorporates the variation of pedal force and other influential factors that function as the external conditions. Coupled with the identification of the wheel lock-up simulations based on the slip ratio, as described previously, these repetitions of the braking simulation enabled the determination of the critical pedal force or PF_{crit} . In this study, a new parameter of interest was introduced, and this is defined as the minimum pedal force that initiates the wheel lock-up.

3.3.3 Wheel Lock-up and PF_{crit}

After the emergency braking simulation was completed for all combinations of the conditions the vehicle responses especially the slip ratio, the wheel's angular speed, and the longitudinal vehicle speed were evaluated to identify the wheel lock-up occurrence and to investigate the direct effect of the brake pedal force on the wheel lock-up occurrence. To demonstrate, the slip ratios for the different pedal forces corresponding to $GVW = 31$ ton, $Mu = 0.3$, and speed = 40 km/h are presented in Figure 3-22 and Figure 3-23. From the slip ratios, it can be seen that for straight-line braking under a set of external conditions, and there is a minimum value of pedal force that results in the slip ratio's being -100% (sample Point A in Figure 3-23). Because a slip ratio of -100% represents a wheel lock-up occurrence, this critical value (70 N for the case shown in Figure 3-23) is therefore identified and named as the critical pedal force that triggered the wheel lock-up, PF_{crit} .

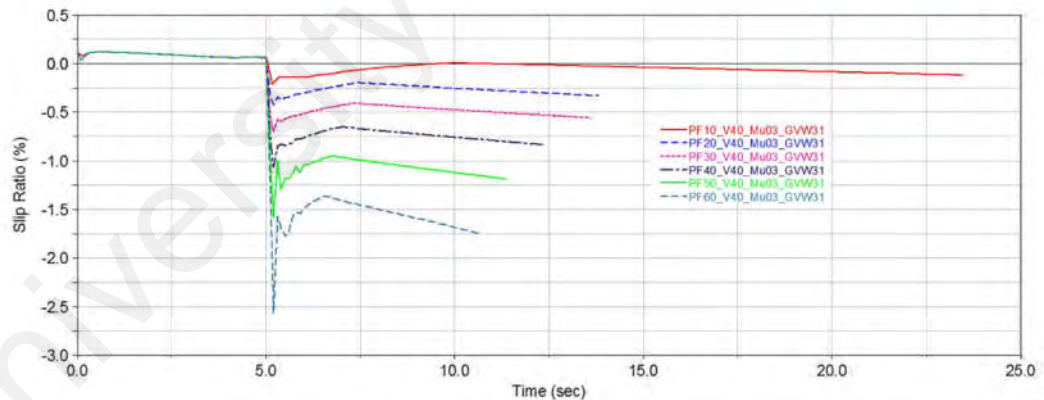


Figure 3-22: Slip Ratios for Straight-line Braking under Various Pedal Forces (Non-wheel Lock-up)

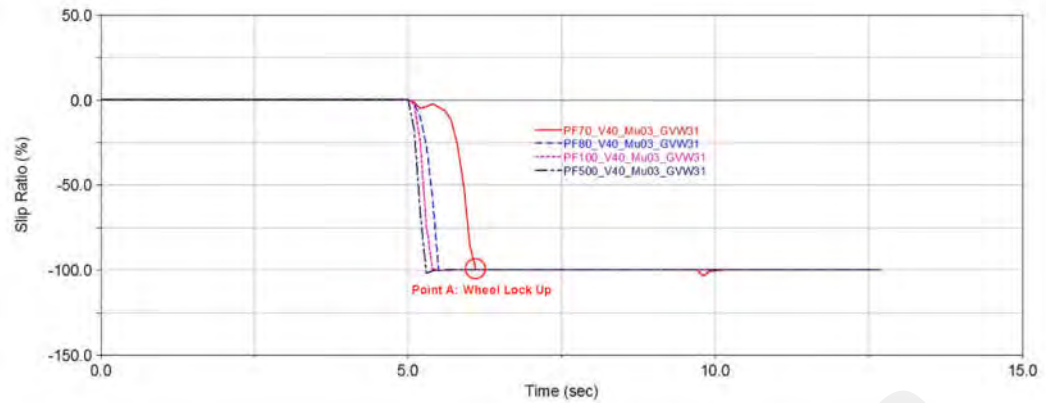


Figure 3-23: Slip Ratios for Straight-line Braking under Various Pedal Forces (Wheel Lock-up)

The slip ratio plots clearly show that the heavy vehicle responses can be distinctively divided into two regions: the non-wheel lock-up region (Figure 3-22, pedal force $< PF_{crit}$), and wheel lock-up region (Figure 3-23 pedal force $\geq PF_{crit}$). In the non-wheel lock-up region, an increase in pedal force will increase the slip ratio generated during braking, but the values remain relatively small (e.g., slip ratio magnitude $< 3\%$ in this case). In contrast, when the pedal force reaches or exceeds the identified PF_{crit} , the slip ratio changes to -100% . In this wheel lock-up region, an increase in pedal force has little effect on the -100% slip ratio value. This implies that wheel lock-up always occurs once the critical state is exceeded. It is also worth noting that the transition from the non-wheel lock-up state to the wheel lock-up state Changes greatly with pedal force. This justifies the importance of the parameter of interest in emergency braking situations.

By its definition, the slip ratio is mathematically related to the wheel's angular speed, and longitudinal vehicle speed. Therefore, it is also relevant to study the effect of pedal force on these result components to evaluate the relationship between pedal force and the braking behavior of the heavy vehicle. Figure 3-24 and Figure 3-25 show the wheel's angular speed results for the same simulation. In the same non-wheel lock-up region

(Figure 3-24, pedal force $< PF_{crit}$, where $PF_{crit} = 70$ N), it can be observed that an increase in pedal force gives a faster rate of reduction for the wheel's angular speed. However, once the pedal force reaches 70 N, there is an evident and immediate reduction of the wheel's angular speed to zero, as shown in the Point B. This is an indirect indication of a wheel lock-up. It can also be noted that once the wheel reaches a lock-up state, it remains locked with zero angular speed for the rest of the braking maneuver. Meanwhile, in the wheel lock-up region (Figure 3-25), the variation of the pedal force makes only insignificant changes to the rate of the wheel's angular speed reduction even though the angular speed reaches zero sooner with a greater pedal force. This shows that wheel lock-up and skidding occur earlier (Zamzamzadeh, Saifizul, & Ramli, 2015).

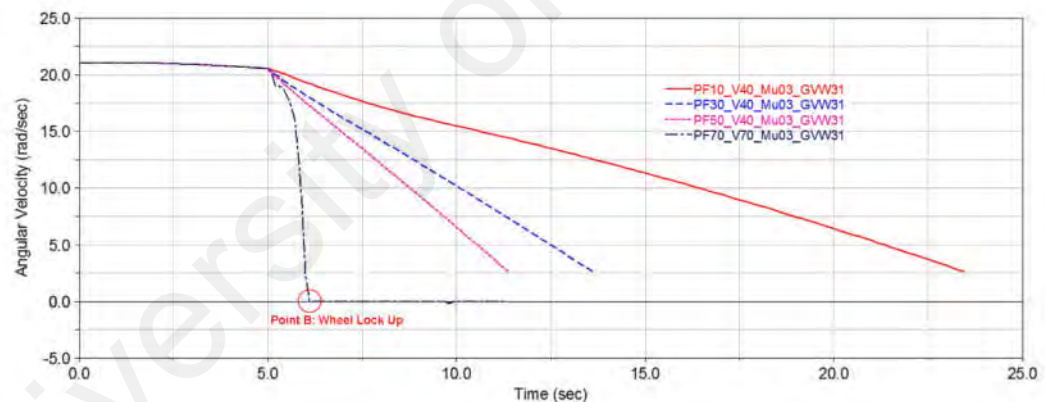


Figure 3-24: Wheel's Angular Speeds for Straight-line Braking under Various Pedal Forces (Non-wheel lock-up)

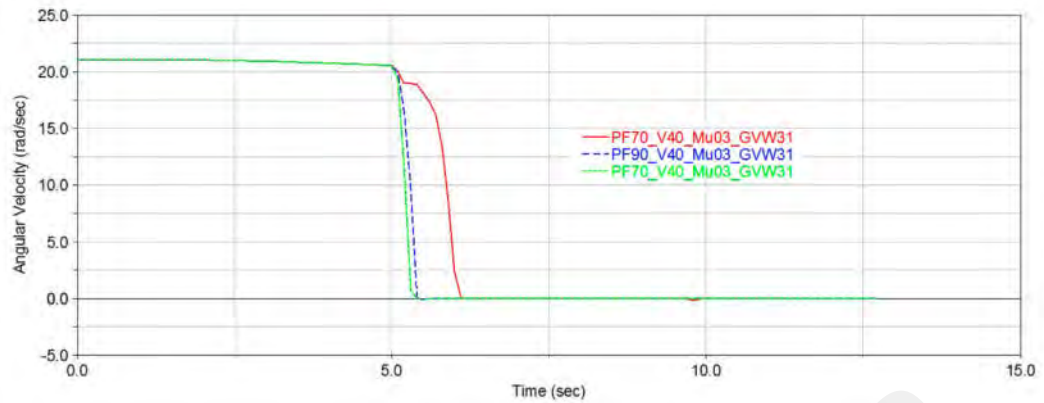


Figure 3-25: Wheel's Angular Speeds for Straight-line Braking under Various Pedal Forces (Wheel lock-up)

Apart from the wheel's angular speed, the other contributing component in the slip ratio's definition, namely the longitudinal vehicle speed, provided very similar observations. The results also confirm a noticeable difference between the non-wheel lock-up state and the wheel lock-up state. Prior to the wheel lock-up (Figure 3-26), it was observed that the greater the pedal force, the faster the longitudinal vehicle speed's reduction rate. Conversely, after wheel lock-up occurs (Figure 3-27, pedal force $\geq PF_{crit}$), a higher pedal force will undesirably give a slower rate of vehicle speed reduction due to wheel lock-up. Consequently, skidding occurs sooner, as described previously.

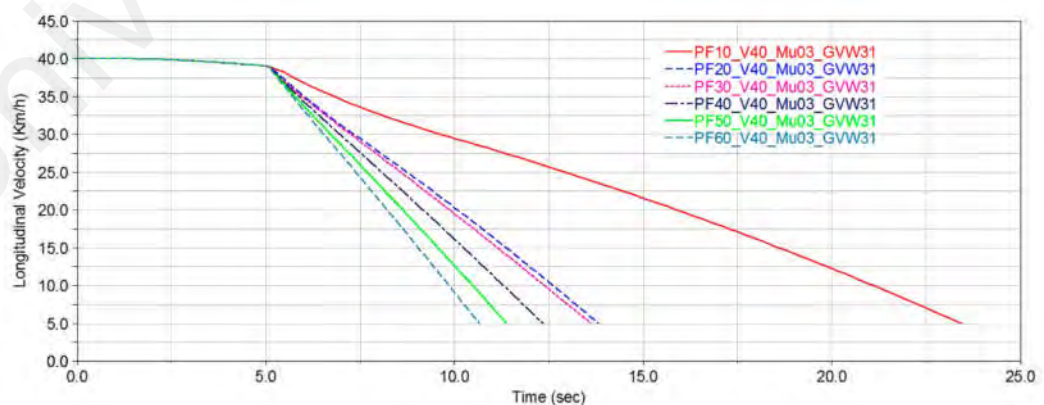


Figure 3-26: Longitudinal Vehicle Speeds for Straight-line Braking under Various Pedal Forces (Non-wheel lock-up)

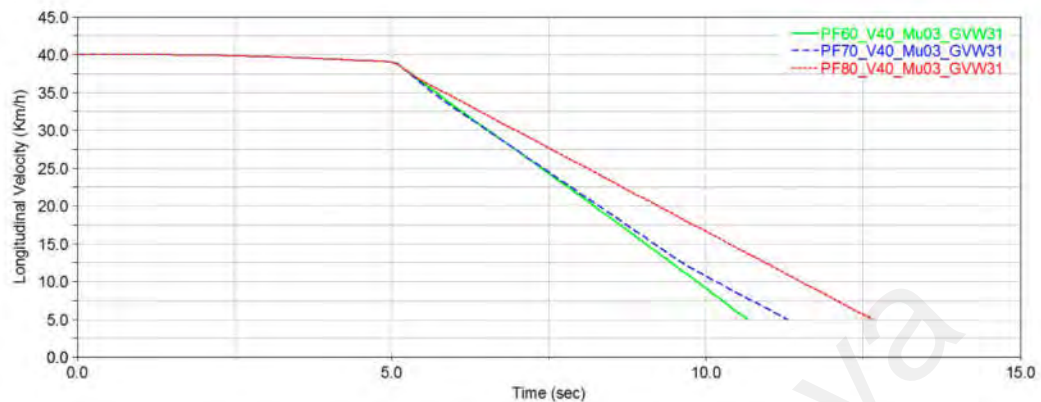


Figure 3-27: Longitudinal Vehicle Speeds for Straight-line Braking under Various Pedal Forces (Wheel lock-up)

The results appeared in the form of slip ratio, wheel angular speed, and longitudinal vehicle speed, and these show that PF_{crit} can serve as a separation between the non-wheel lock-up and the wheel lock-up states during braking. From all the available vehicle response data sets generated by the 6,000 combinations of factors in the braking simulation, 100 PF_{crit} values were detected. These were subsequently analyzed to determine the external factors that had significantly influenced PF_{crit} .

3.3.4 Tire Normal Force versus Longitudinal Force (F_x) at Pure Slip Condition

Figure 3-28 shows the longitudinal tire forces produced when braking the model versus the slip ratio for one tire at three different loading conditions. The graph indicates that the tire longitudinal force is dependent principally on the longitudinal wheel slip or slip ratio and the tire's normal loading condition.

The graph shows that the maximum longitudinal tire force reached a very low slip ratio and then decreased to a limiting value at full slip. In other words, the wheel lock-up had

zero angular velocity. According to Figure 3-28, the peak value of F_x increased. This limiting value depends on the friction caused at the tire-road interface.

Based on the graph, it is reasonable to say that according to the traditional formula, $F_x = \mu \cdot F_z$. F_z is just for the linear part of the graph. It should be noted that the relation after peak point is not linear and needs to be considered nonlinear. As the graph shows, the peak increases with increasing tire normal force. Thus, this proves the tire's load sensitivity with the longitudinal slip.

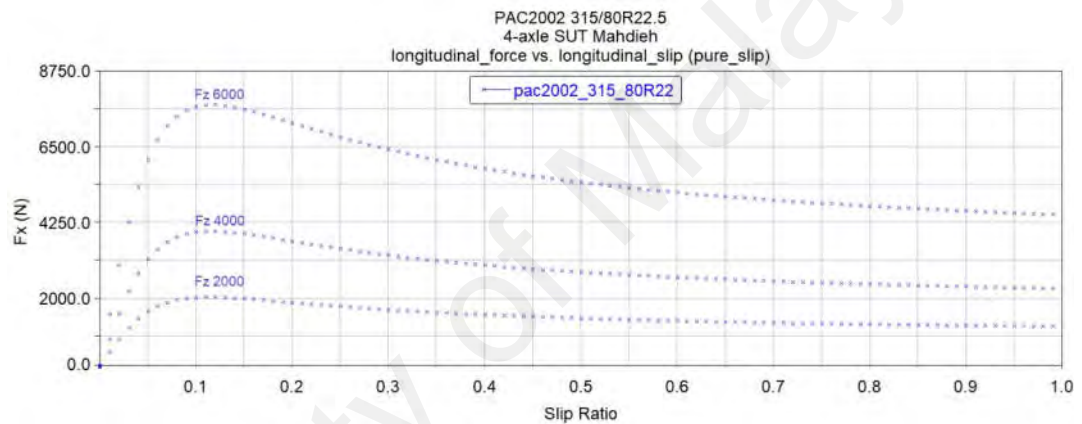


Figure 3-28: Tire Longitudinal Force with Slip Ratio Due to Different Tire Normal Force

As explained in the literature review, the relation between longitudinal force (F_x) or braking force can be assumed linear in the pure longitudinal slip for vehicle loading conditions and small slip ratios. However, this assumption is restricted with a high slip ratio and the tire's high-loading condition.

The research simulation proves that for high tire loading condition, the relation between F_x and F_y is not more linear. In contrast, for low tire loading conditions, the linear relationship can be accepted, but as the tire loading increases, the curve starts to be further away from the straight line, bending away from its initial linear slope. This is

indicated as the limit for the tire traction during a wheel lock-up where the slip ratio is 100%.

Therefore, in practice, the longitudinal force relation with the tire's normal load is not entirely linear as used in the formula, as indicated in Figure 3-29.

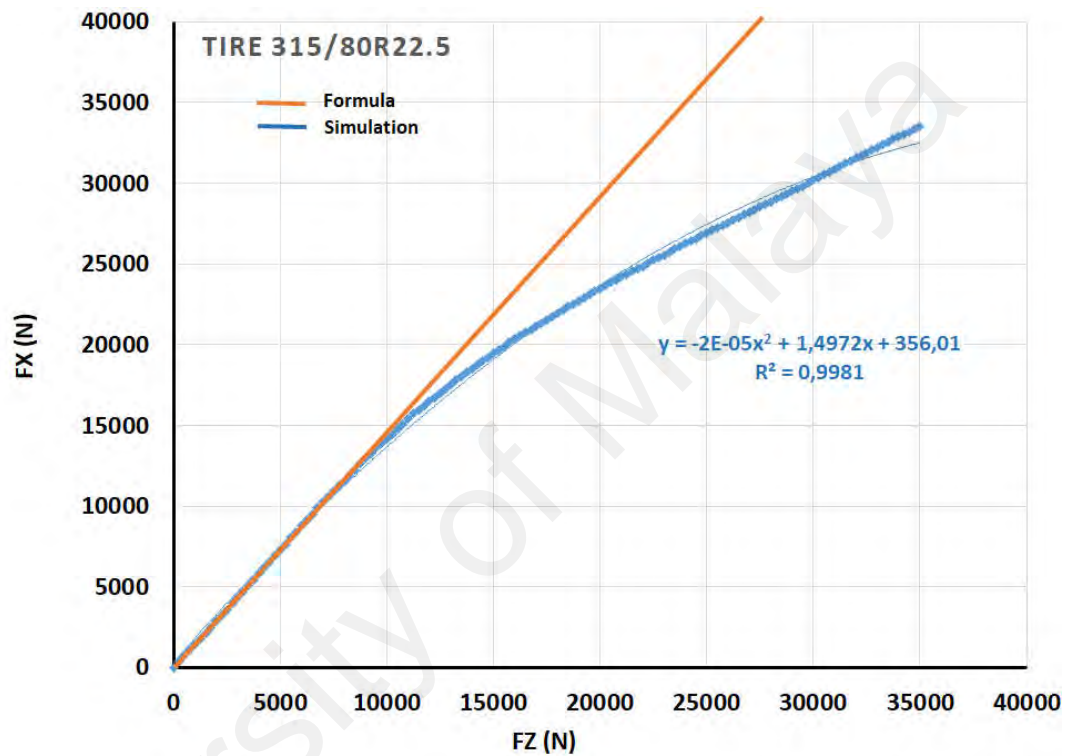


Figure 3-29: Plot Tire Normal Force versus Longitudinal Force at Pure Slip Condition

3.3.5 Braking Distance

Throughout this study, the initial focus had been on the development of a straight-ahead heavy vehicle braking simulation at different speeds and loading conditions on different road surface conditions with varying pedal force applied. For the braking simulations alone, the full-brake condition was applied because it only occurs when the

driver desires the maximum deceleration to stop the vehicle due to an unwanted situation. In other words, the emergency braking situation in an emergency stop was implemented.

In this regard, the braking behavior of a heavy vehicle in emergency stops for different pedal forces was simulated. The simulation results were then grouped according to the heavy vehicle GVW and speed.

3.3.5.1 Braking Simulation

In this section, the braking simulation was run on the ADAMS/Truck, full vehicle analysis, braking analysis. The braking performance of the tractor was tested in this simulation. To start the simulation, the user is required to understand all the options and settings in the braking simulation window, as shown in Figure 3-30.

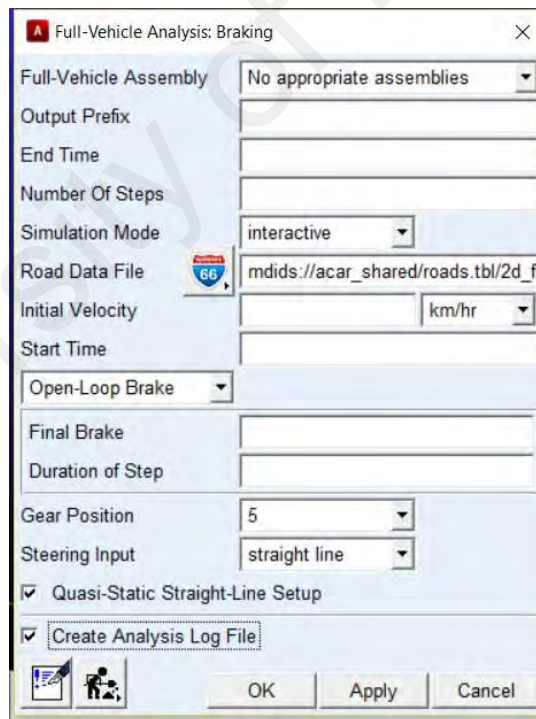
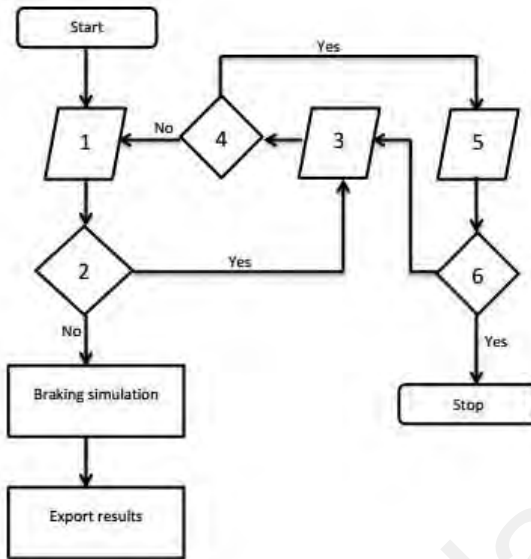


Figure 3-30: Braking Simulation Window in ADAMS/Truck

The parameters change for each single pedal force is shown in Figure 3-31.



1. Constant GVW and speed, surface roughness from 0.3 to 0.7 with 0.1 interval
2. If surface roughness > 0.7
3. Constant GVW, speed from 40 km/h to 80 km/h with 10km/h interval.
4. If speed > 80 km/h
5. GVW from 10 to 45 tons with 5 tons interval
6. If GVW > 45 tons

Figure 3-31: Braking Simulation Flowchart

3.3.5.2 Data Collection and Interpretation

After the simulation, all the results were shown in graph form and exported as a spreadsheet for Microsoft Excel in ADAMS/Post-Processor MD. Then the results were summarized in tables and plotted in a graph by using Microsoft Excel.

3.3.6 Braking Marks and Skidding Distance Through Braking Distance

This is the final stage of the methodology involved in determining the braking distance and finally skidding distance. From the 6,000 simulated tests run for the full brake simulations, excluding cases where wheel lock-up did not occur, a total of 1,800 tests that had all wheels locked-up were chosen to generate the data sets for the braking mark estimation.

From the data sets compiled, several relevant variables were analyzed, including the longitudinal velocity, wheel's angular velocity, slip ratio, time, and braking distance (BD). Usually, these were used to identify the wheel lock-up occurrences and to determine the braking mark or skidding distance (SD). The results were extracted based on the theory that at a higher slip ratio, the tire's longitudinal force decreases. When the wheel lock-up occurs due to low tire traction, the vehicle starts to skid. It was further assumed that SD begins as soon as the wheel lock-up takes place and is continuous until the vehicle comes to a full stop.

Figure 3-32 and Figure 3-33 display the typical vehicle speed, angular velocity, and braking distance for the vehicle model based on the emergency braking simulation with a wheel lock-up situation. The lock-up is apparent in Figure 3-33; it shows that the tire angular velocity is equal to zero. This means a 100% slip ratio and wheel lock-up.

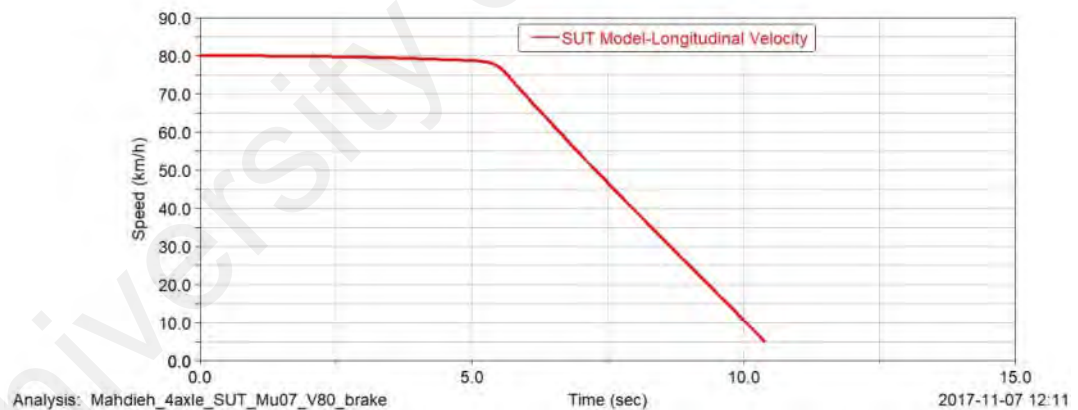


Figure 3-32: Emergency Braking: Vehicle speed profile

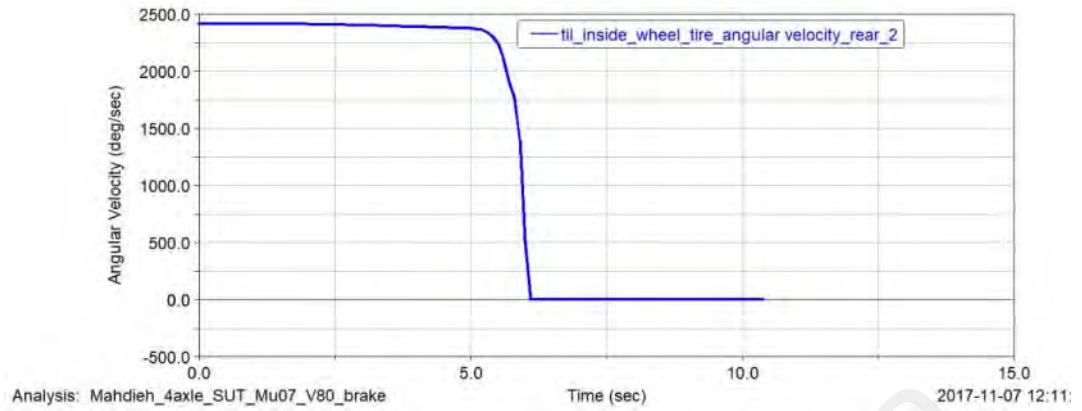


Figure 3-33: Emergency Braking Angular Velocity Profile during Wheel Lock-Up

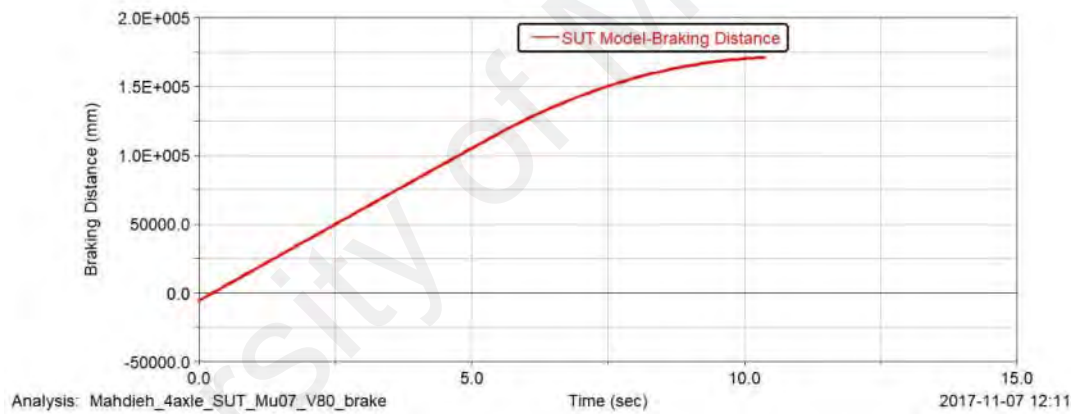


Figure 3-34: Braking Distance

To examine the skidding distance in the MSC.ADAMS postprocessor, the data cursor was used to determine the exact wheel lock-up data along with the created graphs. This means that for every braking simulation, angular velocity and slip ratio was plotted for different tires, and the wheel lock-up cases were specified. Thus, by creating the braking distance graph Figure 3-34, the skidding distance was estimated.

To obtain the skidding distance, the distance at which the vehicle traveling with a locked wheel(s) to be stopped was noted as just sliding along the road. First, the total braking distance for every emergency braking simulation was estimated through the graph braking distance versus time. Then the time the wheel lock-up happened was taken by the ADAMS cursor. The total braking distance was then determined at this particular time and finally considered for the total braking distance.

The wheel lock-up detection was conducted for every simulation and every tire separately. Next, all the data were transferred and then tabulated to be used as input for the analysis of the results in the next chapter. The list of the skidding distance for the simulations with wheel lock-up scenarios that caused the skidding is tabulated.

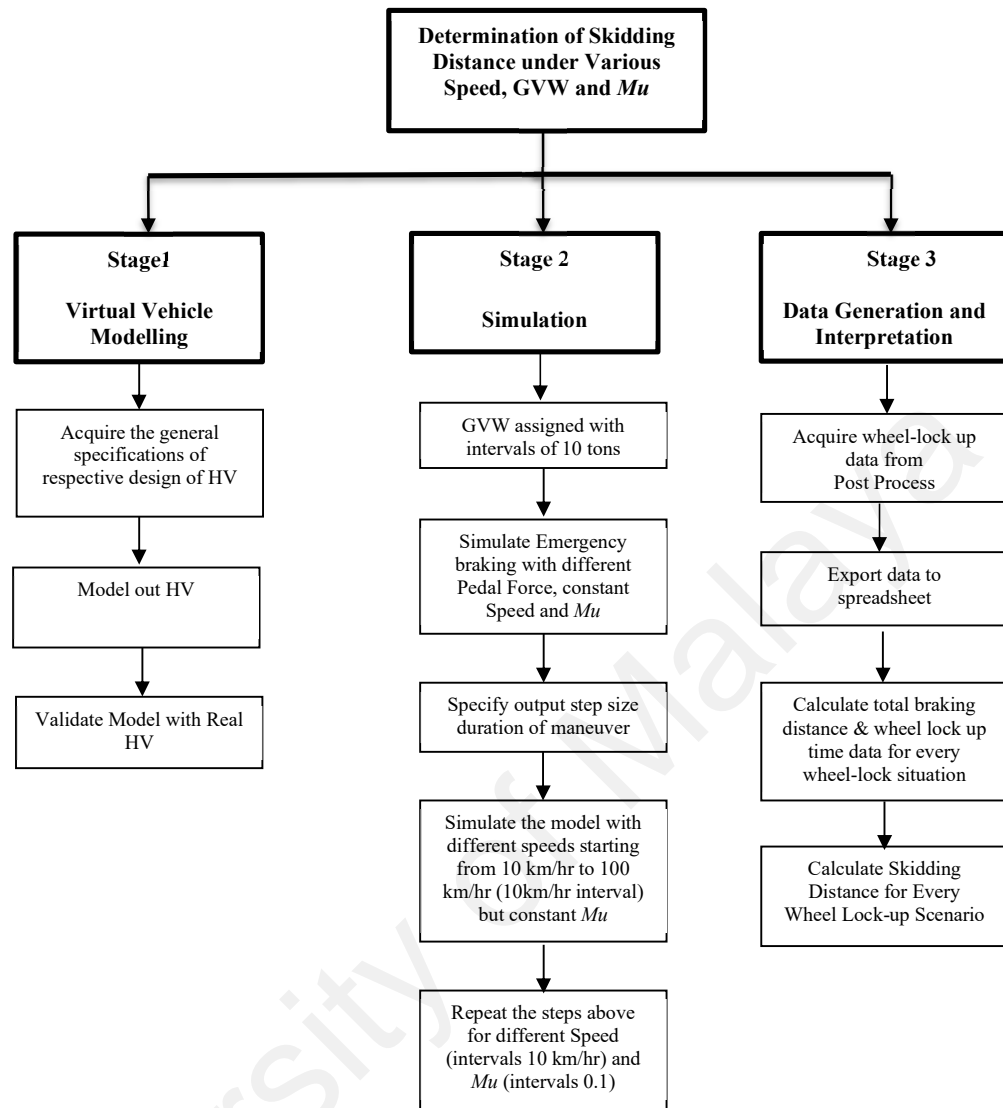


Figure 3-35: Workflow to Calculate Skidding Distance

3.4 Simulation Data Analysis

The Statistical Package for the Social Science (SPSS) V17.1 was used for data analysis because it is an adequate tool for entering data, for creating new variables, and for performing further formal statistical analysis. Statistical models are ideal, mathematical representations of experimental or simulation characteristics. An analysis of the research data using SPSS starts with an exploratory data analysis to detect mistakes, check

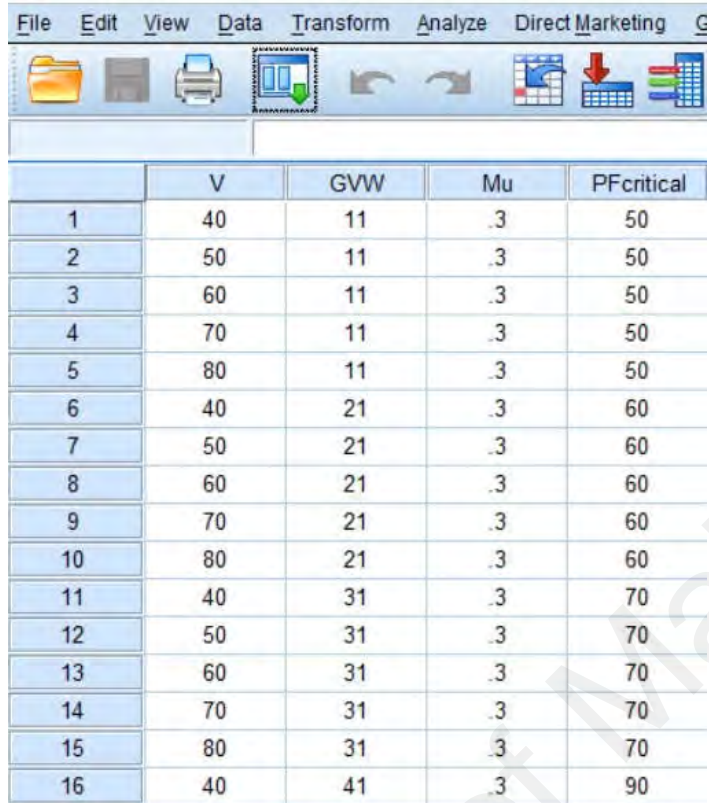
assumptions, determine relationships among the variables, assess relationships between variables, and select appropriate models of the relationship between the variables.

3.4.1 Steps to Create Data Plots

- Export data from spreadsheets to SPSS,
- Define variable list,
- Perform exploratory data analysis,
- Perform confirmatory analysis,
- Create graphs to highlight variables dependency or independence and
- Create a model, perform model checking, and make comparisons.

3.4.2 Data Setup and Scaled Data

A total of 1,200 data sets were generated from these steps. The first step, prior to analysis, was to set up the collected data properly. The process began by selecting and filtering out the missing data and the outlier data. Next, the data were split according to the GVW, Mu , and speed. This made it easier to analyze the data, as shown in Figure 3-36. Then the graph between the PF_{crit} , GVW, speed, and Mu was plotted to study the relationship between the variables.



| | V | GWV | Mu | PFcritical |
|----|----|-----|----|------------|
| 1 | 40 | 11 | .3 | 50 |
| 2 | 50 | 11 | .3 | 50 |
| 3 | 60 | 11 | .3 | 50 |
| 4 | 70 | 11 | .3 | 50 |
| 5 | 80 | 11 | .3 | 50 |
| 6 | 40 | 21 | .3 | 60 |
| 7 | 50 | 21 | .3 | 60 |
| 8 | 60 | 21 | .3 | 60 |
| 9 | 70 | 21 | .3 | 60 |
| 10 | 80 | 21 | .3 | 60 |
| 11 | 40 | 31 | .3 | 70 |
| 12 | 50 | 31 | .3 | 70 |
| 13 | 60 | 31 | .3 | 70 |
| 14 | 70 | 31 | .3 | 70 |
| 15 | 80 | 31 | .3 | 70 |
| 16 | 40 | 41 | .3 | 90 |

Figure 3-36: Sample Data Set in SPSS

CHAPTER 4:

RESULTS AND DISCUSSIONS

Based on the braking maneuver line charts shown in Figure 4-1, it is clear that the braking pedal force applied by the driver can be performed, and it also affected the braking distance in three different phases such as:

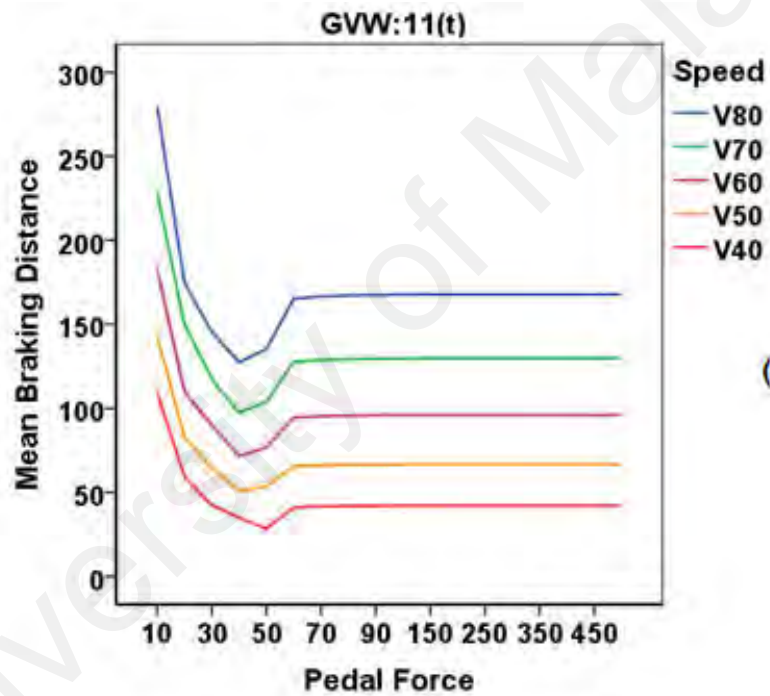
- i) When the pedal force was increased, the braking distance decreased accordingly.
- ii) When the pedal force was increased, the braking distance increased subsequently.
- iii) When the pedal force was increased, the braking distance's change was not significant.

Phase 1 occurs when the pedal force is too small to lock up any wheel. Thus, as the driver increases the pedal force, the braking performance efficiently stops the heavy vehicle, thereby producing a shorter braking distance. In Phase 2, the brake grips the wheel tightly to prevent it from rotating. Under this condition, the heavy vehicle starts to skid along the road. When the driver increases the pedal force, a lock-up occurs sooner. As more wheels begin to lock up, the braking distance also increases. This phenomenon usually happens during emergency braking situations, resulting in a longer braking distance. Phase 3 indicates that dependence between pedal force and braking distance is very weak and that the pedal force has a minimum effect on the braking distance (Dunn, Guenther, & Radlinski, 2012; Gangopadhyay & Wilson, 1995).

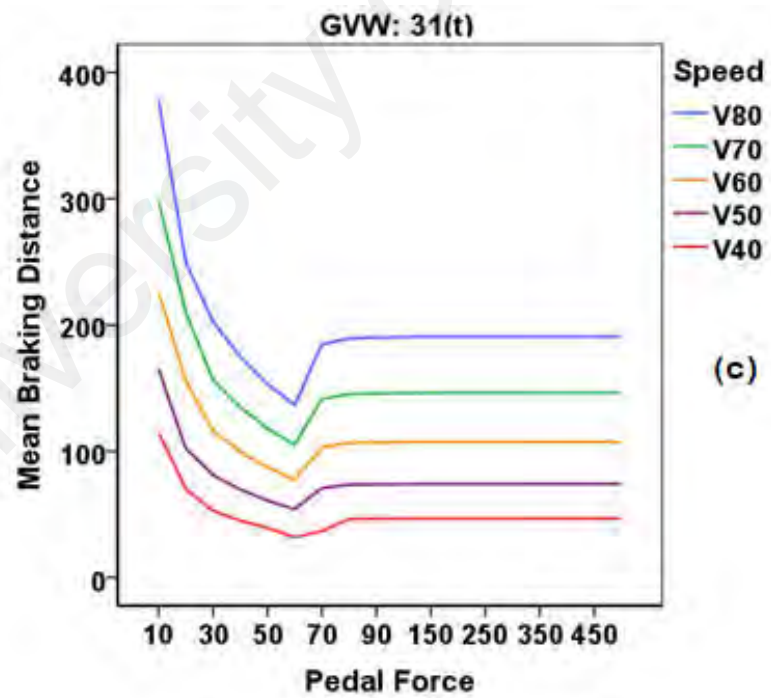
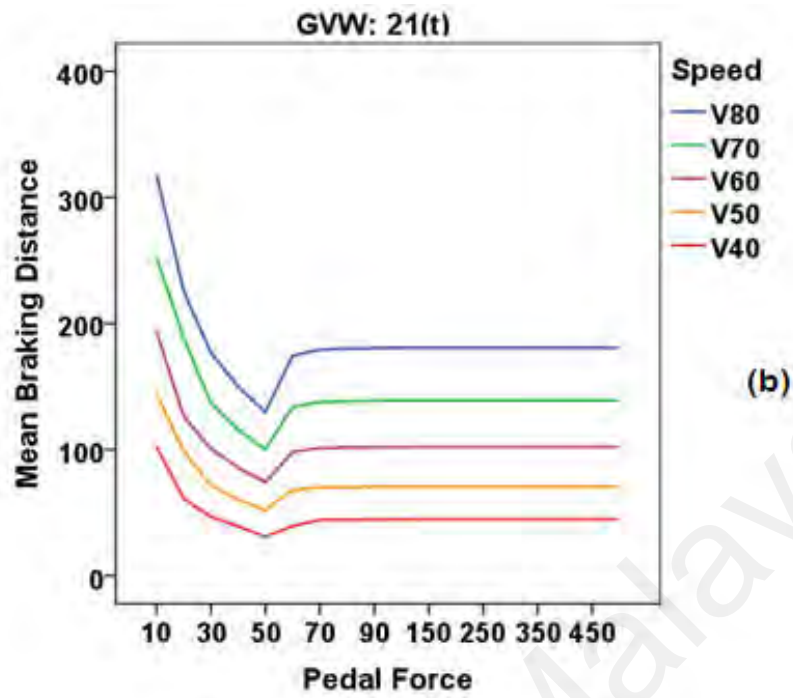
Braking distance simulation results for different vehicles, speed, loading conditions, and pedal forces on the various road surfaces are tabulated and shown in Appendix F.

From the plots for different GVWs, as shown in Figure 4-1, it can be observed that the braking distances for various heavy vehicle speeds are compared when the GVW is

constant and when the pedal force is increased. From the plots, it can be implied that for all vehicle loading and speed conditions, the three phases of the pedal force are observed. The safety implication of speed for heavy vehicles is that the higher the forward velocity, the longer the stopping distance. This increases the likelihood of a rear-end collision, especially in a close-following situation. The result of the vehicle speed alone is not enough to explain the pedal force effect on the braking distance, particularly for those involving heavy vehicles. The GVW is also an essential factor in the braking distance calculations with varying pedal force (Gobbi et al., 2014).



(a)



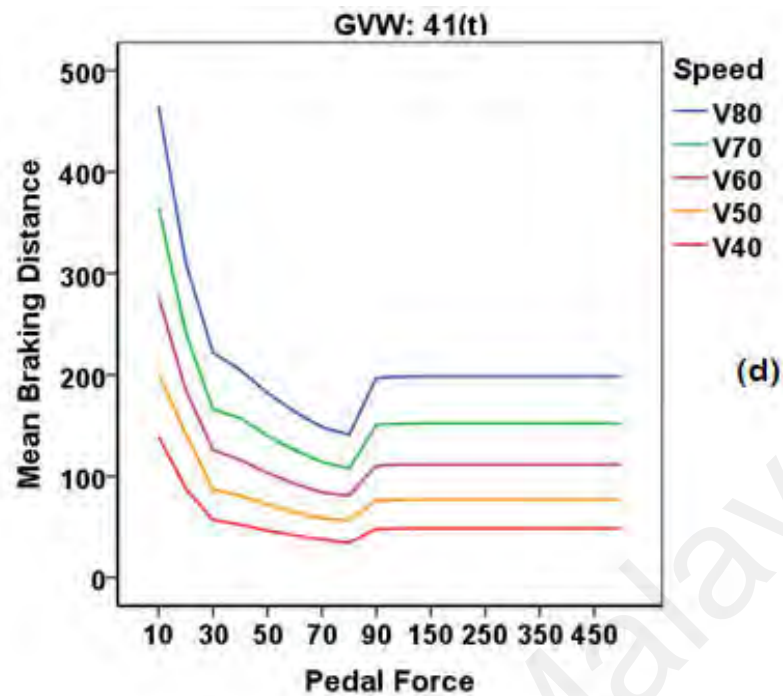
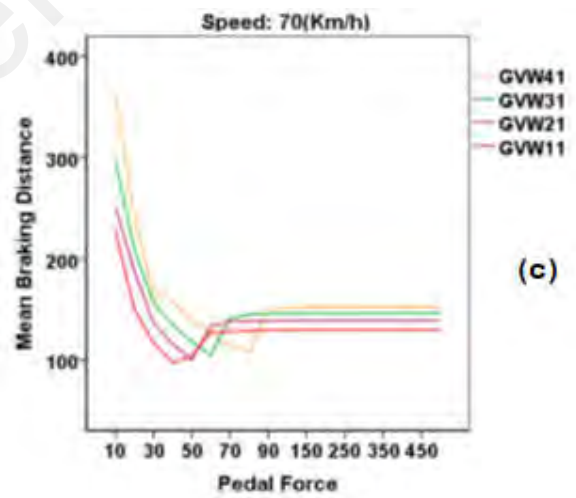
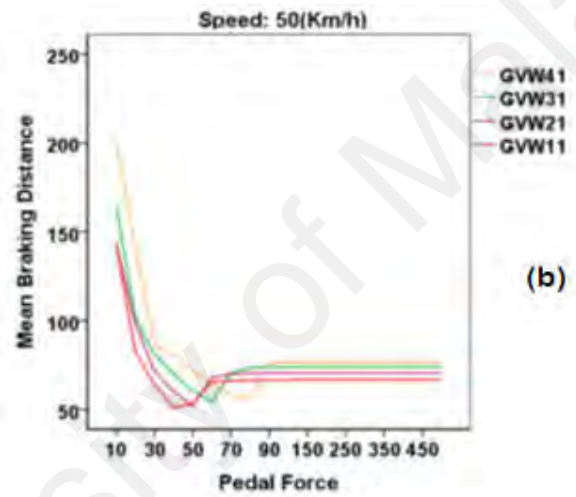
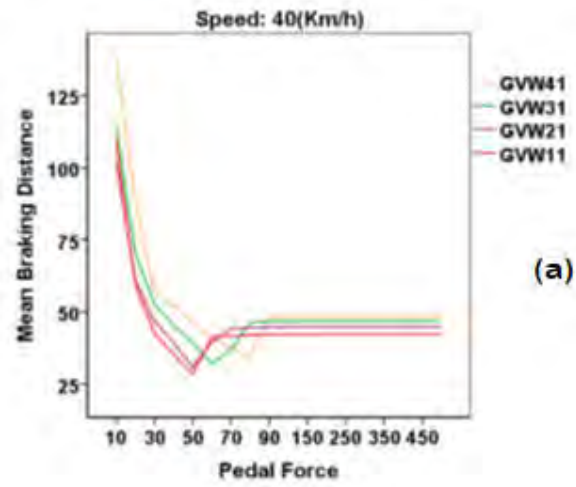


Figure 4-1: Pedal Force Effect on Braking Distance under Different Conditions (a. GVW:11t, b. GVW:21t, c:GVW:31t, d. GVW:41t)

The overall simulation output of this study recommends that the variation in brake pedal force for massive forces has a minimal effect on the BD because brake pedal forces of more than 100 N tend to lead to skidding during an emergency braking situation. In such occurrences, the brake mechanism is fully engaged, and the wheel becomes locked (Seiler, Song & Hedrick, 1998; Karim, Saifizul, et al., 2013).

For lower brake pedal forces for heavy vehicles, the brake mechanism was not fully engaged, resulting in a longer braking distance. The braking distance for different heavy vehicle loading conditions at a certain speed is shown in Figure 4-2.



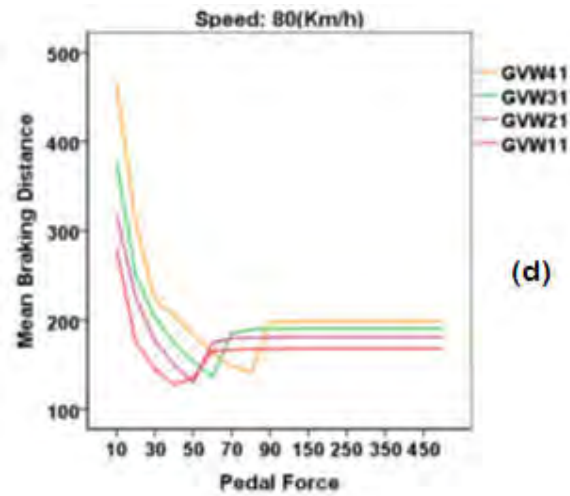


Figure 4-2: Brake Pedal Force Effect on Braking Distance
 (a. V:40 km/h, b. V:50 km/h, c. V:70 km/h, d. 80 km/h)

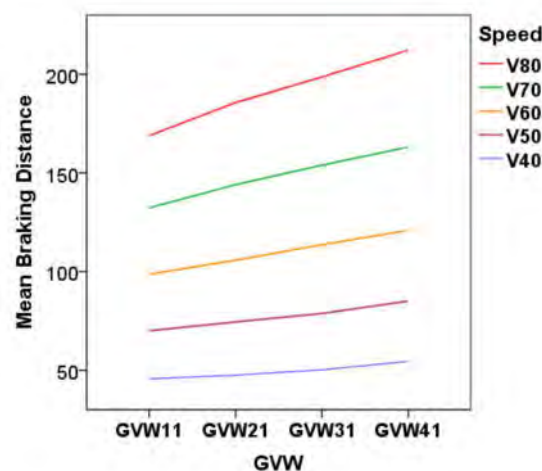
For the different pedal forces, heavy vehicles with a higher GVW have a longer braking distance. In an emergency braking situation for an overloaded heavy vehicle, no matter how hard the driver applies the brake pedal, the vehicle is unable to stop with the same braking distance as those from semi-loaded or unladen heavy vehicles. Moreover, based on the results summarized in the graph, the vehicle loading condition has a definite impact on the characterization of the vehicle braking process. The simulation results seem to be in line with the trend observed in LuTy (2018) and Zagorski (2013). Because overloaded vehicles increase the braking distance, this elongation in the braking distance significantly influences road traffic safety due to its effect on the vehicle dynamics, tire behavior, and braking performance, especially the pedal force (Yang, Liu & Cheng, 2008). The results from all the simulations suggest that the variation in pedal force shows different effects on braking distance based on changes in speed and GVW.

The effect of the GVW and speed on the pedal force properties of the heavy vehicle plays an essential role in accident reconstruction. This effect has a strong influence on heavy vehicle speeds. As the speed increases, the braking distance increases accordingly.

The focus of the analysis presented in this study is the estimation of the effects of pedal force on the braking distance of heavy vehicles. This information can be used for accident reconstruction purposes. From the results presented above, it is clear that with a higher running speed for the heavy vehicle, under the same brake pedal force, accordingly, the braking distance increase. This confirms that the braking distance is affected by vehicle speed. This implies that there are scientific reasons for reducing speed, to lessen the chance of a crash, and to reduce the impact of the crash. Speeding or excessive speed is one of the leading causes of accidents. Excessive speed causes more serious crashes because heavy vehicles require longer distances to stop.

After discussing the effect of the different pedal forces on braking distance, because the primary objective of this thesis is to analyze the emergency braking of a vehicle with wheel lock-up, and establishing the braking mark under different conditions, it is proposed this section only consider the simulations that including all wheels locked up, nor simulations making partial lock-up.

The graphs plot in Figure 4-3 clearly shows the relationship between the mean braking distance and GVW when the speed increases from 40-80 km/h.



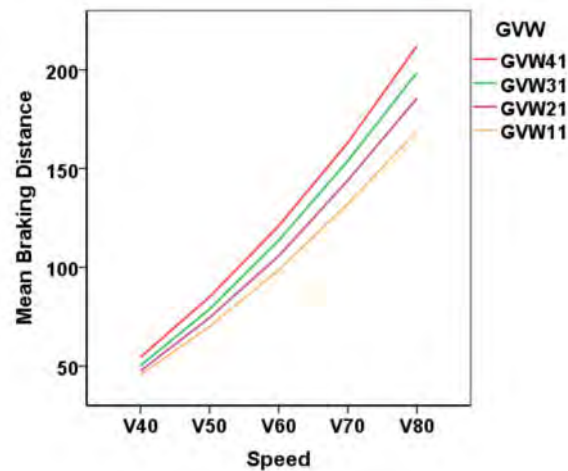


Figure 4-3: Simulation of the Effect of Speed and GVW on Braking Distance

Reviewing the plots, we can see that an increase in vehicle loading will increase the braking distance in emergency braking. Based on the tire's nonlinear behavior presented above, a statement may be made that an increase in the vehicle loading conditions or mass is directly causing the tire normal force F_z growth, that during emergency braking wheel lock-up increases the braking distance. This increase comes from:

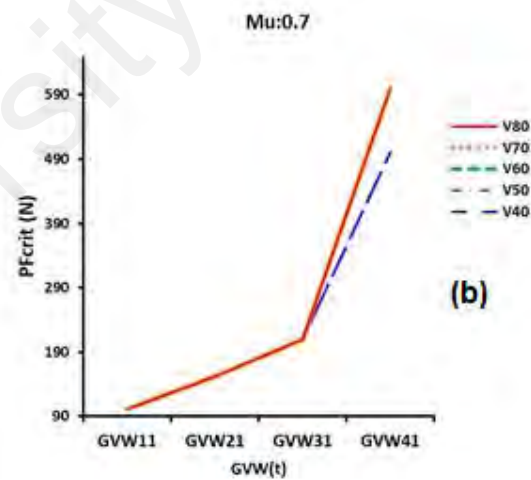
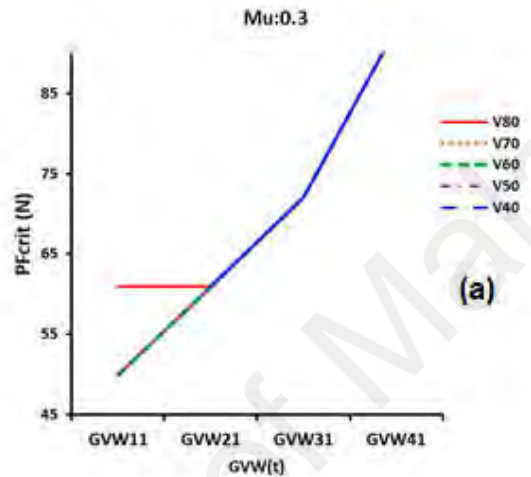
- the time the tires need to drop the angular velocity until the wheel lock-up increases; and
- the rise in time for the tire longitudinal force F_x to reach the tire-road coefficient of friction needed for wheel lock-up.

From a safety perspective, these results are essential to analyze regarding vehicle motion for road events with emergency braking and related accident reconstruction (Gobbi, Mastinu & Previati, 2014; LuTy, 2018; Shah, Sharma, Mathew, Kateshiya & Parmar, 2016; Vrabel, Skrucany, Bartuska & Koprna, 2019).

4.1 Critical Braking Pedal Force (PF_{crit})

4.1.1 *PFcrit* Influential Factors and Their Significance

In the current study, several external conditions were considered as influential factors, and they encompass the GVW (vehicle loading condition), μ (road surface condition), and vehicle speed. To explore the primary influence of these factors on *PFcrit*, the correlation charts depicting these variables are plotted and shown in Figure 4-3.



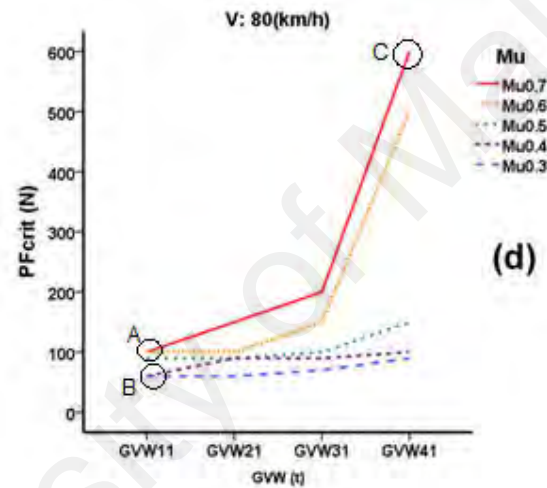
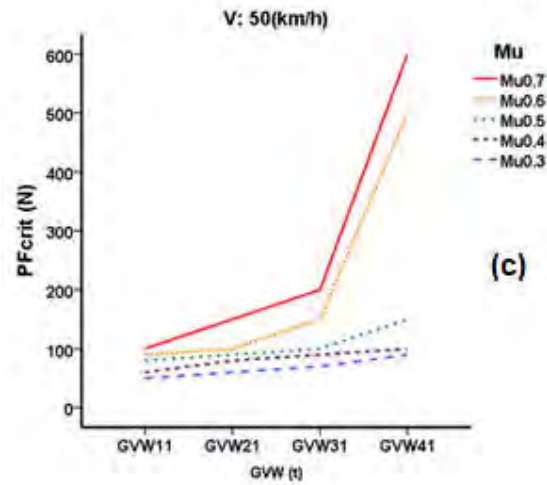


Figure 4-4: Correlation Charts Relating Influential Factors to PF_{crit}
(a. $Mu:0.3$, b. $Mu:0.7$, c. $V50$ km/h, d: 80 km/h)

Figure 4-4 shows an apparent variation of the PF_{crit} concerning the GVW and Mu . As a general trend, an increase in the GVW would cause an increase in the PF_{crit} . This is especially true for cases with high Mu values. From another perspective, there was a similar positive relationship between the Mu and the PF_{crit} , mostly for cases with high GVW values.

The graphs showed that the wheel lock-up risk was the highest (lower PF_{crit}) when overloaded vehicles were driving on road surfaces with lower Mu . A wet or snow-covered

road seemed to impose the highest risk of accidents, specially when the heavy vehicle was overloaded. This shows that the GVW plays an important role.

To investigate whether the stated effects are statistically significant or not, a one-way ANOVA was conducted. The ANOVA model uses GVW, Mu , and speed as the independent variables and PF_{crit} as the dependent measure. By breaking the data down according to each influential factor as a condition, it was possible to allow the three factors to be presented separately, thereby providing a more detailed analysis of uncovering the factor as a condition.

The results indicate that when the vehicle speed is ignored, the mean PF_{crit} increases dramatically across the range of the GVW values. For instance, at $Mu = 0.3$, the value of $F (df = 3, 16, p < 0.05) = 269.33, \eta^2 = 0.97$ shows that GVW has a significant influence on PF_{crit} . Thus, differences in PF_{crit} can be attributed to the vehicle's loading conditions (empty, semi-loaded, fully-loaded, or overloaded heavy vehicle).

Analysis from another result set shows that Mu has a similar significant influence on PF_{crit} . For example, the results: (i) $Mu = 0.3$ and $v = 40$ km/h gives the mean of $M = 67.5$ and standard deviation of $SD = 17.08$, (ii) $Mu = 0.6$ and $v = 40$ km/h gives the mean of $M = 210$ and $SD = 195.07$; (iii) $Mu = 0.3$ and $v = 80$ km/h gives the mean of $M = 70$ and $SD = 14.142$, (iv) $Mu = 0.6$ and $v = 80$ km/h gives the mean of $M = 212.5$ and $SD = 193.111$, These results clearly indicate that a change in Mu causes a significant variation to the mean PF_{crit} regardless of speed. In fact, from the individual PF_{crit} values noted (Figure 4-4), the PF_{crit} for GVW = 41 ton, $Mu = 0.7$, speed = 80 km/h (Point C) is about six times the PF_{crit} for both GVW = 11 ton (Point A) and $Mu = 0.3$ (Point B). These outcomes suggest that GVW and Mu are the major factors that affect PF_{crit} . Consistently, additional post hoc tests using the Tukey HSD correction also point to the same findings.

While a heavy vehicle's traveling speed is commonly regarded as a crucial factor that determines the braking distance, this factor is surprisingly insignificant to PF_{crit} . Based on the results noted in Figure 4-5, the mean PF_{crit} is very similar when speed is increased from 40 km/h to 80 km/h regardless of the Mu value. Any difference in PF_{crit} cannot be determined based on whether the heavy vehicle is driven slowly or fast.

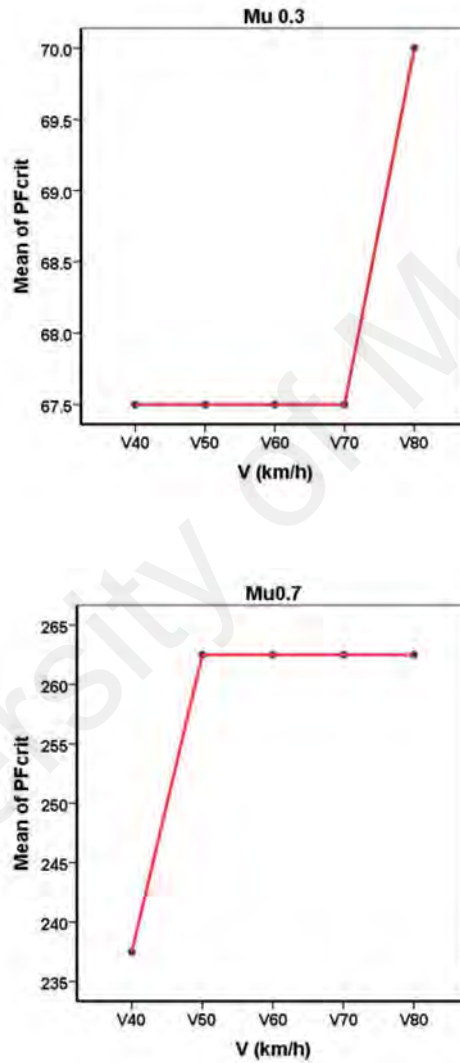


Figure 4-5: Effect of Speed on Mean of PF_{crit}

4.1.2 Assessment of Interactions among PF_{crit} Influential Factors

To verify whether or not the effect of Mu and GVW as well as their interaction on PF_{crit} are statistically significant, the two-way ANOVA was conducted. The results are presented in Table 4-1. In particular, Table 4-1 shows that there is significant effect of both GVW and Mu on PF_{crit} , as $F(3, 80) = 2148.138, p < 0.05$ and $F(4, 80) = 1359.601, p < 0.05$. More importantly, the results indicate that there is significant interaction between GVW and Mu on PF_{crit} , as $F(12, 80) = 512.152, p < 0.05$.

Table 4-1: Two-way ANOVA Test Results

| Source | Type III Sum of Squares | <i>df</i> | Mean Square | <i>F</i> | Sig. | Partial Eta Squared |
|-----------------|-------------------------|-----------|-------------|-----------|-------|---------------------|
| Corrected Model | 1874979.0a | 19 | 98683.105 | 948.876 | 0.000 | 0.996 |
| Intercept | 2099601.0 | 1 | 2099601.00 | 20188.471 | 0.000 | 0.996 |
| <i>Mu</i> | 565594.0 | 4 | 141398.500 | 1359.601 | 0.000 | 0.986 |
| GVW | 670219.0 | 3 | 223406.333 | 2148.138 | 0.000 | 0.988 |
| <i>Mu</i> *GVW | 639166.0 | 12 | 53263.833 | 512.152 | 0.000 | 0.987 |
| Error | 8320.0 | 80 | 104.000 | | | |
| Total | 3982900.0 | 100 | | | | |
| Corrected Total | 1883299.0 | 99 | | | | |

a. *R* Squared = 0.996 (Adjusted *R* Squared = 0.995)

4.1.3 Modeling of PF_{crit}

Based on the available PF_{crit} data, a mathematical model relating PF_{crit} to the two dominant factors, GVW and Mu , can be derived from the regression analysis. The proposed model has the form expressed in Equation 4.1.

$$PF_{crit} = aw + b \quad \text{Eq. 4.1}$$

$$a = C_1\mu + C_2 \quad \text{Eq. 4.2}$$

$$b = C_3\mu + C_4 \quad \text{Eq. 4.3}$$

where w represents GVW, μ represents Mu , while C_1, C_2, C_3, C_4 are the relevant regression coefficients of the model. A first regression was done to determine the coefficients of regression lines, a and b for various μ . The values of coefficients and the respective coefficients of determination, R^2 for all cases are stated in Table 4-2. The following points summarize the outcome of the first regression:

(i) The analysis of standard residuals that were performed indicates that the data contained no outliers (Standard Residual Min = -0.981, Standard Residual Max = 2.747).

(ii) Tests conducted to verify whether the data met the assumption of collinearity indicated that multi-collinearity was not a concern (for Mu : Tolerance = 1.00, VIF = 1.00; for GVW: Tolerance = 1.00, VIF = 1.00).

(iii) Using the ENTER method, it was found that GVW and Mu levels explain a significant amount of the variance in the value of PF_{crit} ($F(2, 97) = 59.14, p < 0.01, R^2 = 0.741, R^2 \text{ Adjusted} = 0.549$).

(iv) The analysis shows that both GVW and Mu managed to significantly estimate the value of PF_{crit} (GVW Beta = 0.526, $t(99) = 7.722, p < 0.001$) (Mu Beta = 0.522, $t(99) = 7.658, p < 0.001$).

Following the first regression, a second regression was conducted to determine the individual coefficients, C_i , where $i = 1, 2, 3, 4$, as well as the respective coefficients of determination R^2 . These are shown in Table 4-3. using the coefficient values noted in Equation 4.3 and simplifying these, the mathematical model for PF_{crit} can be determined (Equation 4.4).

$$PF_{crit} = 38.78w\mu - 12.93w - 501.78\mu + 227.83 \quad \text{Eq. 4.4}$$

Thus, Equation 4.4 can be used to predict the critical value of pedal force during braking when the vehicle loading condition and road condition are known.

Table 4-2: Regression Coefficients with a p -value for a and b

| μ | a | p -value (a) | b (constant) | p -value (b) | R^2 | N |
|-------|--------|-----------------------|-------------------|-----------------------|-------|-----|
| 0.3 | 1.24 | < 0.001 | 35.76 | < 0.001 | 0.933 | 20 |
| 0.4 | 1.28 | < 0.001 | 49.72 | < 0.001 | 0.927 | 20 |
| 0.5 | 2.14 | < 0.001 | 49.86 | < 0.001 | 0.812 | 20 |
| 0.6 | 12.740 | < 0.001 | -120.74 | < 0.001 | 0.714 | 20 |
| 0.7 | 14.9 | < 0.001 | -129.9 | < 0.001 | 0.910 | 20 |

Table 4-3: Regression coefficients with a p -value for C_i

| C_i | C_1 | C_2 | C_3 | C_4 | $R^2(a)$ | $R^2(b)$ | $N(a)$ | $N(b)$ |
|------------|--------|--------|---------|--------|----------|----------|--------|--------|
| | 38.78 | -12.93 | -501.78 | 227.83 | 0.820 | 0.719 | 5 | 5 |
| p -value | < 0.05 | < 0.05 | < 0.05 | < 0.05 | | | | |

4.2 Braking Distance, Braking Mark, and Skidding Distance

4.2.1 Impact of GVW, Speed and Road Surface Condition on SD

Following the emergency braking simulation, the heavy vehicle's braking marks and SD data during the phase wheel lock-up was compiled. The results were then plotted to investigate the effects of the GVW, speed, and road coefficient of friction on the braking mark of the tested heavy vehicle. This is illustrated in Figure 4-6.

To quantify the impact at different levels of vehicle load, on the braking mark length during skidding, a sequence of different GVW values was analyzed. Figure 4-6 illustrates the variation of the SD as a function of the heavy vehicle's GVW for various speed and road

coefficients of friction. It can be seen that there is an increase in SD with an increase in GVW. This is especially significant at high vehicle speeds. Meanwhile, plots for heavy vehicle's SD at low vehicle speed only indicate a slight growth with an increase in the GVW. This means that when the heavy vehicle is traveling at its minimum speed, the GVW factor does not significantly influence the SD on both wet and dry road surfaces (different road coefficients of friction).

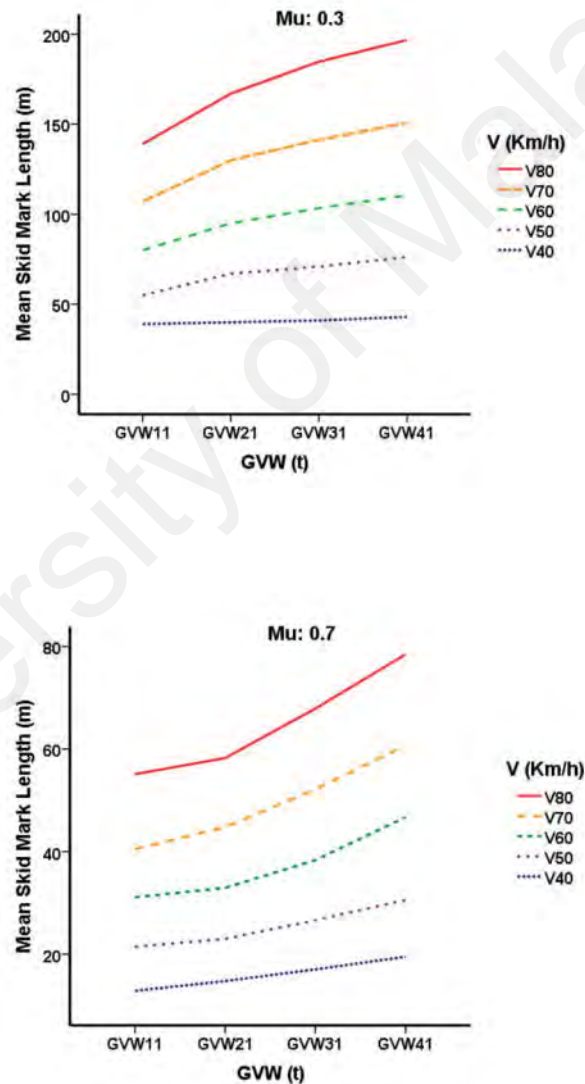
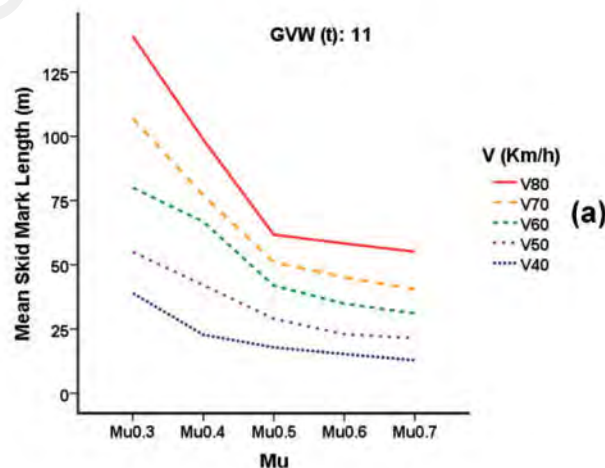


Figure 4-6: Effect of Heavy Vehicle's GVW on SD under Different Speed and μ Condition

Based on the result shown, it is important to note that the higher the heavy vehicle's load is, the longer the SD will be for the truck to stop. Thus, in an emergency situation, an overloaded truck will not be able to stop at the same distance as a properly loaded truck, regardless of the condition of the road surface. The overloading of a truck represents a safety risk. From another perspective, Figure 4-7 (a)-(d) compares the variation of the SD under different road surface conditions (road coefficient of friction, Mu), ranging from a wet road surface ($Mu = 0.3$) to a dry road condition (a maximum of $Mu = 0.7$). This was performed for several speeds and GVW. From the plots, it is observed that the SD is affected not only by the GVW, as discussed previously, but also by the road surface condition. In this context, the SD decreases for an increase in the road coefficient of friction. For example, the tested heavy vehicle with a GVW of 41 tons, traveling by a speed of 80 km/h on a wet road ($Mu = 0.3$) needs around 200 m to stop (Point A in Figure 4-7 d). As for the truck with the same conditions except that it is traveling on a dry road ($Mu = 0.7$), it only needs around 100 m to stop (Point B in Figure 4-7 d). Based on this, it can be deduced that wet road conditions with a lower coefficient of friction can result in a longer SD due to a higher chance of wheel lock-up during the braking of a heavy vehicle.



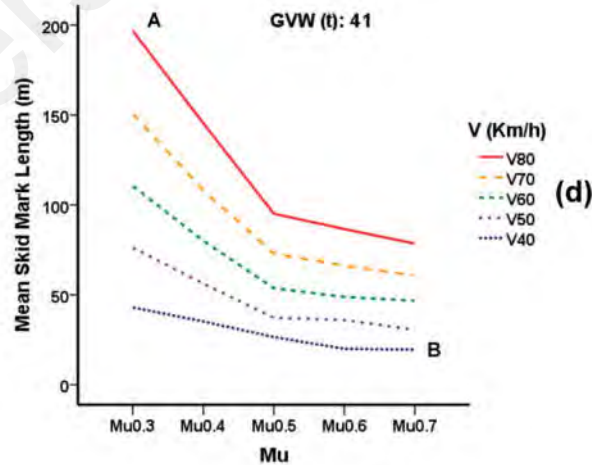
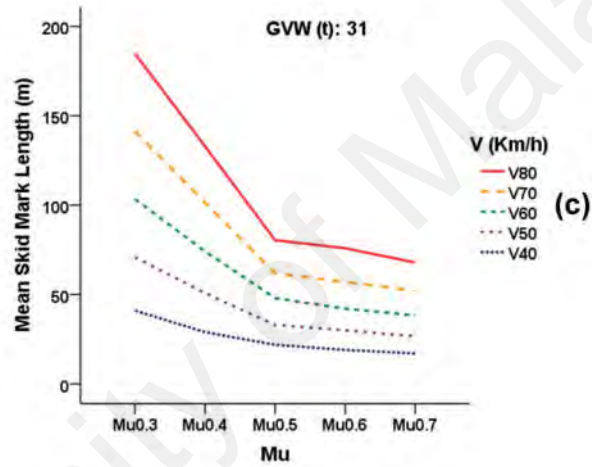
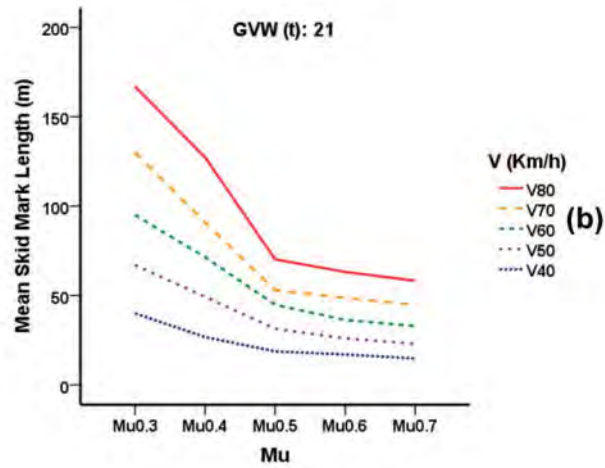
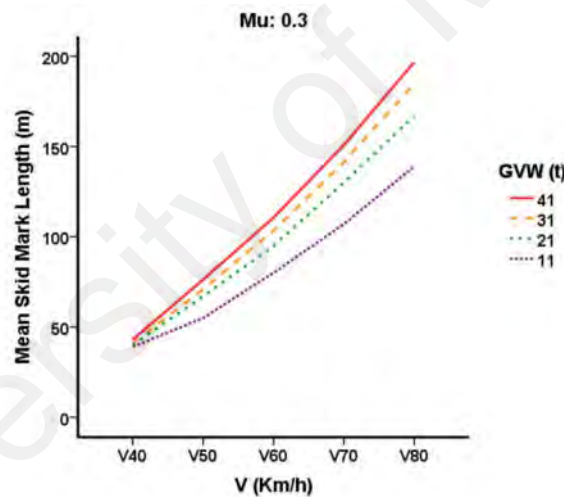


Figure 4-7: Effect of Road Surface Coefficient of Friction on SD under Different Vehicle's GVW and Speed Condition

Finally, the relation between the SD and vehicle speed, regarding several GVW and road coefficients of friction, is presented in Figure 4-8. Here, it is observed that the SD tends to rise proportionally with an increase in vehicle speed, regardless of the other factors. From the plots, it is clear the SD for the tested heavy vehicle at high speed is approximately four times the SD at low speed, which is quite significant when the vehicle speed is higher only by a factor of two. Therefore, it can be deduced that vehicle speed condition also has a significant effect on heavy vehicle safety. A heavy truck traveling at high speed has a greater chance of not being able to stop safely, especially in close-following situations.



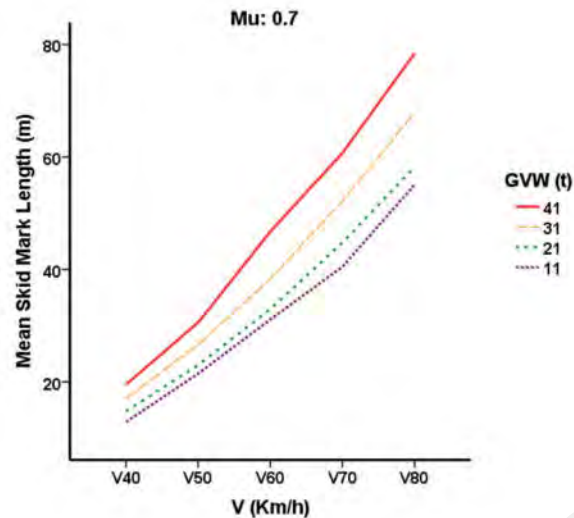


Figure 4-8: Effect of Heavy Vehicle’s Traveling Speed on SD for Different μ and GVW

Overall, the analysis shows that a heavy vehicle’s SD is noticeably influenced by all three factors: the GVW, speed, and road coefficient of friction. These factors respectively represent vehicle load, speed, and road conditions. For example, a relatively larger truck’s GVW shows a higher SD during emergency braking in all situations. Although this means that the empty truck contributes to the shortest SD, other factors such as truck speed and road surface conditions can also cause the situation to become critical. Therefore, all three factors adopted for this study have to be considered simultaneously in the modeling of braking marks.

4.2.2 Assessment of Correlation between the SD and Influential Factors

Further bivariate correlation analysis of the data reported in Table 4-4 was conducted to verify the strength of the correlation between all influential factors and SD.

Table 4-4: Pearson Correlations between SD and Influential Factors

| Correlations | | | | | |
|-------------------------|---------------------|--|----------|---------|---------|
| | | Braking Mark Length (m) | V (km/h) | μ | GVW (t) |
| Braking Mark Length (m) | Pearson Correlation | 1 | .694** | -.572** | .491* |
| | Sig. (2-tailed) | | .000 | .000 | .035 |
| | N | 100 | 100 | 100 | 100 |
| **. | | Correlation is significant at the 0.01 level (2-tailed). | | | |
| *. | | Correlation is significant at the 0.05 level (2-tailed). | | | |

The analysis of the data using Pearson's r indicates that the coefficient of friction was significantly negatively correlated with the mean ratings of the SD , $r(98) = -0.572$, $p = .00$. This means that an increase in the road coefficient of friction (μ) can be associated with a decrease in the rating of the skidding distance. For slippery roads, heavy vehicle skidding distances will be greater as the condition becomes more dangerous.

Also, the significant and positive correlation between the skidding distance with speed ($r = .694$, $p < .01$) as well as GVW ($r = .491$, $p < .05$) with small effect sizes indicates that an increase in vehicle speed or GVW causes more skidding distance in emergency braking situations.

4.2.3 Heavy Vehicle SD Prediction Model for Accident Reconstruction

At this point, it has already been noted that vehicle load, speed, and road conditions need to be considered in SD modeling because they have effects that cannot be ignored. Consequently, a new mathematical model for the SD was derived so as to provide a reliable SD estimation. The proposed model not only incorporates the vehicle speed and road coefficient of friction, as is usual in the skid to stop formula, it also takes into account the GVW. The model was developed based on nonlinear multiple regression, as expressed in Equation 4.5:

$$SD|\mu_j = aw + b \quad \text{Eq. 4.5}$$

Where:

$$\begin{cases} a = C_1V + C_2 \\ b = C_3V + C_4 \end{cases} \quad \text{Eq. 4.6}$$

SD: Skidding distance (m), μ_j : Road surface coefficient of friction ($j = 0.3$ to 0.7), W: Truck's GVW (t), V: Truck's traveling speed (km/h), a, b: Regression parameters.

In the multiple regression analysis, the first regression calculation involves estimating the coefficients of the regression lines, a and b , as noted in Equation 4.3 for various speeds. The values of these coefficients as well as the p -values and the coefficients of the determination, R^2 values for all cases, are stated in Table 4-5. An additional regression calculation was then performed to determine the coefficients, C_i in Eq 4.6 where $i = 1, 2, 3,$ and 4 . These coefficient values and the corresponding R^2 values for all cases are also described in Table 4-6.

By replacing C_i 's in equation Equation 4.5 with the values as in Table 4-5 and Table 4-6, the value for skidding distance can be determined as shown in Equation 4.7.

$$SD|\mu = C_1VW + C_2W + C_3V + C_4 \quad \text{Eq. 4.7}$$

Table 4-5: Regression Coefficients a and b

| μ | V (km/h) | a | p - value (a) | b (constant) | p - value (b) | R^2 | N |
|-------|---------------|-------|------------------------|-------------------|------------------------|-------|---|
| 0.3 | 40 | 0.130 | 0.017 | 37.370 | 0.049 | 0.966 | 4 |
| | 50 | 0.677 | 0.032 | 49.698 | 0.005 | 0.936 | |
| | 60 | 1.000 | 0.016 | 71.235 | 0.003 | 0.967 | |
| | 70 | 1.426 | 0.024 | 95.194 | 0.004 | 0.952 | |
| | 80 | 1.911 | 0.017 | 122.194 | 0.003 | 0.966 | |

| | | | | | | | |
|-----|----|-------|-------|--------|-------|-------|---|
| 0.4 | 40 | 0.396 | 0.019 | 18.114 | 0.007 | 0.962 | 4 |
| | 50 | 0.438 | 0.028 | 38.237 | 0.003 | 0.945 | |
| | 60 | 0.425 | 0.010 | 62.050 | 0.000 | 0.979 | |
| | 70 | 1.040 | 0.012 | 67.365 | 0.002 | 0.975 | |
| | 80 | 1.456 | 0.048 | 88.234 | 0.011 | 0.906 | |
| 0.5 | 40 | 0.289 | 0.041 | 13.726 | 0.015 | 0.920 | 4 |
| | 50 | 0.266 | 0.021 | 25.759 | 0.002 | 0.958 | |
| | 60 | 0.386 | 0.014 | 37.059 | 0.001 | 0.971 | |
| | 70 | 0.749 | 0.037 | 40.216 | 0.011 | 0.927 | |
| | 80 | 1.104 | 0.008 | 48.141 | 0.003 | 0.984 | |
| 0.6 | 40 | 0.161 | 0.008 | 13.629 | 0.001 | 0.984 | 4 |
| | 50 | 0.429 | 0.012 | 17.581 | 0.006 | 0.976 | |
| | 60 | 0.476 | 0.033 | 28.155 | 0.008 | 0.935 | |
| | 70 | 0.717 | 0.018 | 35.653 | 0.006 | 0.965 | |
| | 80 | 0.975 | 0.014 | 45.635 | 0.005 | 0.973 | |
| 0.7 | 40 | 0.222 | 0.002 | 10.268 | 0.001 | 0.997 | 4 |
| | 50 | 0.310 | 0.004 | 17.366 | 0.016 | 0.968 | |
| | 60 | 0.523 | 0.037 | 23.687 | 0.015 | 0.988 | |
| | 70 | 0.681 | 0.010 | 31.839 | 0.004 | 0.980 | |
| | 80 | 0.797 | 0.023 | 44.193 | 0.006 | 0.950 | |

Table 4-6: Regression Coefficients C_1 to C_4

| μ | C_1 | C_2 | C_3 | C_4 | $R^2(a)$ | $R^2(b)$ | N(a) | N(b) |
|-------|-------|-------|-------|--------|----------|----------|------|------|
| 0.3 | 0.043 | - | 2.151 | - | 0.995 | 0.984 | 5 | 5 |
| | 0.000 | 1.558 | 0.001 | 53.948 | | | | |
| 0.4 | 0.027 | - | 1.694 | - | 0.813 | 0.973 | 5 | 5 |
| | 0.036 | 0.822 | 0.019 | 46.821 | | | | |
| 0.5 | 0.021 | - | 0.833 | - | 0.856 | 0.961 | 5 | 5 |
| | 0.024 | 0.709 | 0.003 | 16.992 | | | | |
| 0.6 | 0.019 | - | 0.821 | - | 0.966 | 0.979 | 5 | 5 |
| | 0.003 | 0.598 | 0.001 | 21.120 | | | | |
| 0.7 | 0.015 | - | 0.823 | - | 0.986 | 0.981 | 5 | 5 |
| | 0.001 | 0.406 | 0.001 | 23.923 | | | | |

Based on the coefficient values presented in Tables 4-5 and 4-6, an efficient model for the SD estimation that incorporates the GVW, speed, and road coefficient of friction as factors can be obtained. For the regression model validation, the SD was determined from the model by comparing it with those obtained from the multi-body dynamic simulation. It was found that the two means of determining the SD are in good agreement with each other, and it was

predicted with less than 4% error. In general, the regression model matches the simulation and experimental results very well. Therefore, it can be used as a typical means of estimating the SD without the need of a detailed simulation.

The findings strongly support the road safety and accident reconstruction reports on crash injury (Raftery, Grigo, & Woolley, 2008) high crash rates have been reported for overloaded trucks due to the inefficiency of brake performance (Aliakbari & Moridpoure, 2016).

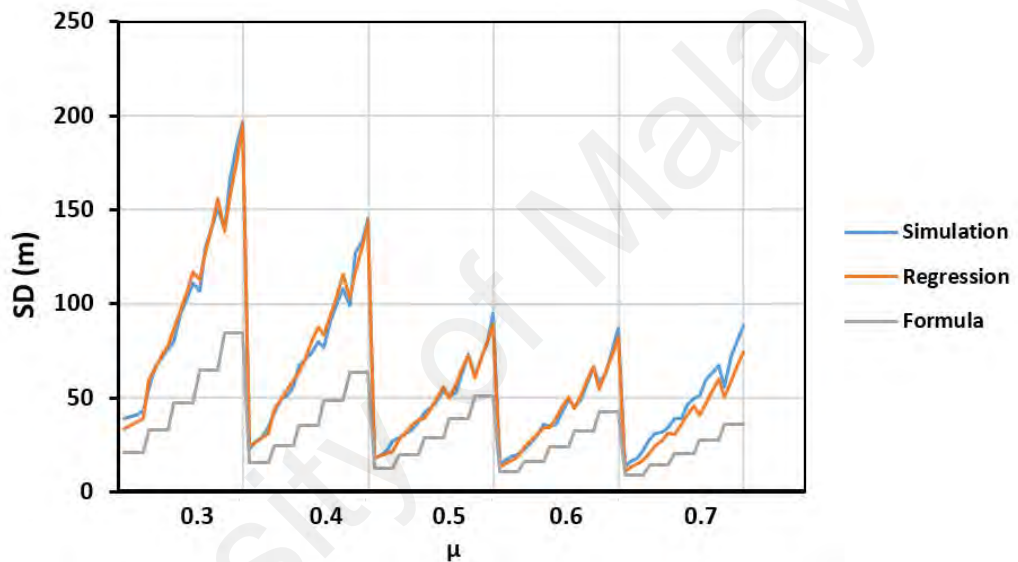


Figure 4-9: Comparison of Model, Simulation, and Traditional Formula average SD (V: 40-80 Km/h GVW: 11-41 tonnes)

Figure 4-9 shows a comparison of average skidding distances results with GVW and speed merged effect on skidding distance. For every constant road coefficient of friction area, the average skidding distances have increments, the formula increase SD is originating just from changing the speed, while the simulation and regression model has a greater increment in the skidding distance considering the vehicle loading condition impact on skidding distance.

The lengthening of the vehicle skidding distance, due to overloading was estimated through simulation and modeling in this research according to the assumptions adopted. This conclusion is important from the point of safety of heavy vehicle motion, where loading is excessive and reconstruction of the road event during which emergency braking took place. It is worth elaborating on the applicability of the obtained SD estimation model. With the emergency braking situation considered for straight and even road sections, this model is logically applicable for skidding distance estimation in straight-line braking events. It is naturally expected that the skidding distance will be different for braking situations involving other types of road sections, such as curved road sections and gradient road sections. For the former, it is expected that the skidding distance will be longer due to the lower longitudinal tire traction in the presence of lateral components due to the cornering maneuver. This needs to be incorporated into the estimation model.

This study has presented an approach to determine the skidding distance through vehicle dynamics by consideration of vehicle loading conditions. This is an improvement over the traditional approach. The study's critical skidding distance analysis clearly illustrates that if the vehicle loading changes from unloaded to overloaded along with different road coefficient of friction and speed, the wheel lock-up condition will be different. This represents a refinement of the severity loading condition with its importance to the road safety of heavy vehicles. For this study, the SD as a function of the vehicle loading condition is to be inferred in the form of the simulation output through a verified model. However, the regression model should be used in limited conditions and cannot be expanded for all heavy vehicles, in the way the traditional formula can be used.

CHAPTER 5:

CONCLUSIONS AND RECOMMENDATIONS

5.1 Summary

The escalation of heavy vehicles on the roads has created a remarkable increase in road accidents, particularly skidding accidents in accident-prone areas. To develop effective skidding accident countermeasures, it is important to understand the characteristics of heavy vehicles and road environment features.

Driving with an excessive GVW is believed to be a dominant accident contributory factor, especially when it involves high-speed driving on different road surface conditions. While most prior work looking at heavy vehicle accident reconstruction focused on using tire braking marks derived from accident scenes to estimate vehicle speed only (without considering the vehicle's GVW and road surface conditions), the current study had investigated the overall characteristics of heavy vehicles so as to determine the skidding accident factors. This was achieved by focusing on the GVW's relationships with different speeds and various ranges of road conditions. To do this, a new skidding distance derived from the logistic regression method was introduced.

The research data that were collected through a multi-body dynamic model were successfully implemented into the MSC.ADAMS/Truck. After the model was validated, and numerous simulations were conducted for the emergency braking situations, the following conclusion was obtained.

5.2 Conclusions

5.2.1 Pedal Force Effect on Wheel Lock-up, PF_{crit}

The relation between the brake pedal force and wheel lock-up was explored under the various vehicle dynamic conditions: loading condition, speed on the different road surface, and vehicle specifications. The amount of brake pedal force applied during

emergency braking was unknown, so this new approach could provide an insight into how the pedal force affects the braking performance of heavy vehicles.

Simulation results indicated that heavy vehicle wheel lock-up clearly occurs with respect to pedal force, highlighting the importance of this parameter. However, as far as pedal force is concerned, the critical values appear to be influenced by different conditions. For instance, both vehicle load and road conditions have a significant effect on PF_{crit} . Surprisingly, vehicle speed does not affect PF_{crit} significantly, even though it is known to be an important contributor to braking or skidding distance. Overall, this study has led to the introduction of the PF_{crit} , which serves as an important representation of the limit of braking that a heavy vehicle driver can initiate without causing wheel lock-up. The information on brake pedal force, as found in this study, provides a greater understanding of the braking characteristics of a typical heavy vehicle, and this can help in improving accident reconstruction.

Lastly, the results of this part of the study suggest that the braking pedal force is a vital factor to consider in the safety issues of heavy vehicles. Furthermore, heavy vehicle drivers should be aware of their vehicle's braking performance during emergency braking, especially when their vehicle is overloaded and running at high speed.

5.2.2 Wheel Lock-up, Braking Marks and Skidding Distance

This study has confirmed that the braking marks and skidding distance of a heavy vehicle is not dominated by a single factor, but rather depends on various conditions, including vehicle load, vehicle speed, and road surface condition.

As expected, through using a multi-body dynamics simulation, results have shown that an increase in the GVW and speed and a decrease in the road coefficient of friction lead

to a notably greater skidding distance, which poses a safety risk. Therefore, all three factors are significant and have to be incorporated in the estimation of the skidding distance due to emergency braking situations.

5.2.3 Influential Factors on Braking Distance or Braking Mark Model

Finally, the outcome derived from this study can help improve accident reconstruction. From the findings noted, the regression model for skidding distance or braking mark length has been proposed. This may help to have a typical model originating from vehicle dynamics that considers more vehicle parameters (GVW) in the calculation.

5.2.4 New model

The derivation of the relation between skidding distance and vehicle GVW has been formally presented in this study through the application of vehicle dynamic behavior. The skidding distance regression model introduced in this study had considered parameters such as GVW with a relevant effect on the computed dynamics. This is a step forward to use and assess the vehicle loading conditions in accidents.

The model offers a practical way of estimating the skidding distance of heavy vehicles because it has been shown to be as accurate as a detailed multi-body simulation. The model is particularly useful for accident reconstruction as it allows an estimation of braking mark length based on vehicle condition and road parameters. Also, it provides a general understanding of the heavy vehicle's behavior during the braking situation.

Finally, it is well-known that by considering the vehicle dynamics, the factors affecting heavy vehicle skidding are numerous and complicated. It is a difficult task to estimate the extent and direction of their overall contribution. However, the analyses shown in this study pertain to identifying the significant factors and comparing relative accident involvement with skidding. The skidding propensity analyses noted in this study provide

a better understanding of the heavy vehicle's overloading and its high speed on different road conditions in affecting road accidents. These factors may be used to seek effective accident countermeasures. In this regard, the current study has shown that there is a relationship among the unique independent variables, as noted in the precise regression model. The present research has also shown that the most important aspect of this model is its ability to consider the vehicle's loading condition.

The overall goal of this study was to increase the knowledge of overloading effects in heavy vehicle single accidents with emergency braking and to improve the methods and tables used in accident reconstruction. Several results of interest to accident investigators and reconstructionist were developed. This is a starting point for vehicle loading condition consideration in heavy vehicle accident reconstruction. For accident reconstructionist, it is necessary to know how vehicle loadings influence single-vehicle accidents. An accurate model can be obtained by considering tires and masses. In this way, the expansion of the model can be pursued, improve future heavy vehicle accident reconstruction and analysis.

5.3 Contributions of Research

For a four-axle single unit truck model without ABS, emergency braking maneuvers were conducted through a multi-body dynamics model with nonlinear tire behavior. The main contributions provided by this research are the proposal of formulating the brake pedal force during wheel lock up as a function of vehicle and road condition. Another outcome of this research was the development of a typical skidding distance model incorporating vehicle dynamics. These results showed some significant understanding of how the vehicle loading conditions affect skidding distance in emergency braking, which will be useful for vehicle safety and accident reconstruction.

5.4 Recommendations for Future Work

The primary recommendation to further improve this study is to develop a new general braking mark model with extra data that can be collected through simulation for other vehicle types such as two-axle, two-axle, and commercial vehicles with a trailer. The current four-axle SUT ADAMS model provides satisfactory results for the needs of this study. However, there is still a major challenge due to the absence of different heavy vehicle types. Given the favorable results derived from the simulations performed in this study regarding heavy vehicles, it is clear that the addition of heavier vehicle models would be useful.

Moreover, an analysis with the complete parameterization of the SUT model, such as different braking systems, especially ABS braking, suspensions, steering compliances, and chassis behavior along with the detailed wheel-tire kinematics could be included, because implementing these parameters would result in more accurate simulations and final characterizations of what influences the skidding distance.

Another important recommendation is to resolve the problem for different road structures such as curved road sections and the gradient road sections. It is also worthwhile to focus on heavy vehicle turning because the interaction of longitudinal and lateral tire forces is an important criterion that would strongly affect the heavy vehicle's performance during turning. Finally, the tire model may be revised to introduce more parameters, such as the influence of the inclination angle in the longitudinal force.

REFERENCES

- Aarts, L., & Van Schagen, I. (2006). Driving speed and the risk of road crashes: A review. *Accident Analysis & Prevention*, 38(2), 215-224.
- ADAMS, M. (2005). r2: Automatic Dynamic Analysis of Mechanical Systems. *MSC Software Corporation*.
- Al-Mansour, A. I. (2006). Effects of pavement skid resistance on traffic accidents. *The Journal of Engineering Research [TJER]*, 3(1), 75-78.
- Albinsson, A., Bruzelius, F., Jonasson, M., & Jacobson, B. (2014). *Tire force estimation utilizing wheel torque measurements and validation in simulations and experiments*. Paper presented at the 12th International Symposium on Advanced Vehicle Control (AVEC'14), Tokyo Japan.
- Aliakbari, M., & Moridpoure, S. (2016). *Management of truck loading weight: A critical review of the literature and recommended remedies*. Paper presented at the MATEC Web of Conferences.
- Amoroso, D., Arricale, V. M., Brancati, R., Cuomo, R., D'Agostino, M., Di Mare, G., ... & Farroni, F. (2019, September). A Preliminary Study for the Comparison of Different Pacejka Formulations Towards Vehicle Dynamics Behaviour. In Conference of the Italian Association of Theoretical and Applied Mechanics (pp. 1136-1144). Springer, Cham.
- Andrey, J., Mills, B., & Vandermolen, J. (2001). Weather information and road safety. *Institute for Catastrophic Loss Reduction, Toronto, Ontario, Canada*.
- Baffet, G., Charara, A., & Lechner, D. (2009). Estimation of vehicle sideslip, tire force and wheel cornering stiffness. *Control Engineering Practice*, 17(11), 1255-1264.
- Baker, C. (1991). Ground vehicles in high cross winds part III: The interaction of aerodynamic forces and the vehicle system. *Journal of fluids and structures*, 5(2), 221-241.
- Bao, W. N. (2014). Study and Simulation on Truck Front Suspension Using ADAMS. *Applied Mechanics and Materials*, 433, 2235-2238.
- Bartlett, W., Wright, W., Masory, O., Brach, R., Baxter, A., Schmidt, B., & Navin, F. (2002). Evaluating the uncertainty in various measurement tasks common to accident reconstruction. *SAE Transactions*, 657-668.
- Batista, M. (2011). Some methods of estimating uncertainty in accident reconstruction. arXiv preprint arXiv:1107.3742.
- Bedsworth, K., Butler, R., Rogers, G., Breen, K., & Fischer, W. (2013). Commercial Vehicle skid Distance Testing and Analysis: SAE Technical Paper.
- Berjoza, d., Dukulis, i., Pirs, v., & Jurgena, i. *Testing Automobile Braking Parameters by Varying the Load Weight*. Paper presented at the 7th International Conference on Trends in Agricultural Engineering (TAE, 2019), Prague, Czech Republic.

- BITRE, Bureau of Infrastructure, Transport and Regional Economics (2017). Fatal heavy vehicle crashes Australia quarterly bulletin, Jan-Mar 2017. (Jan-Mar 2017 ed.). Australia. Retrieved from www.bitre.gov.au/publications/ongoing/fatal_heavy_vehicle_crashes_quarterly
- BITRE, Bureau of Infrastructure, Transport and Regional Economics (2019). Fatal Heavy Vehicle Crashes Australia-Quarterly Bulletin, Jan-Mar 2019. Australia. Retrieved from: https://www.bitre.gov.au/publications/ongoing/fatal_heavy_vehicle_crashes_quarterly
- Brach, R. M. (1994). Uncertainty in accident reconstruction calculations: SAE Technical Paper.
- Brach, R. M., & Brach, R. M. (2009). Tire models for vehicle dynamic simulation and accident reconstruction: SAE Technical Paper.
- Brodie, L., Lyndal, B., & Elias, I. J. (2009). Heavy vehicle driver fatalities: Learning's from fatal road crash investigations in Victoria. *Accident Analysis & Prevention*, 41(3), 557-564.
- Captain, K., Boghani, A., & Wormley, D. (1979). Analytical tire models for dynamic vehicle simulation. *Vehicle System Dynamics*, 8(1), 1-32.
- Carlson, C. R., & Gerdes, J. C. (2003). *Nonlinear estimation of longitudinal tire slip under several driving conditions*. Paper presented at the American Control Conference, 2003. Proceedings of the 2003.
- Carter, N., Beauchamp, G., & Rose, N. (2012). Comparison of Calculated Speeds for a Yawing and Braking Vehicle to Full-Scale Vehicle Tests: SAE Technical Paper.
- Cebon, D. (1993). Interaction between heavy vehicles and roads: SAE Technical Paper.
- Chao, W. (2017). Study on Uncertainty of Traffic Accident Reconstruction Parameters. *DEStech Transactions on Engineering and Technology Research*(tmcm).
- Chen, C., Zhang, G., Huang, H., Wang, J., & Tarefder, R. A. (2016). Examining driver injury severity outcomes in rural non-interstate roadway crashes using a hierarchical ordered logit model. *Accident Analysis & Prevention*, 96, 79-87.
- Chen, T., & Wei, L. (2011). *Study on computer aided analysis and reconstruction system for traffic accidents*. Paper presented at the Electric Information and Control Engineering (ICEICE), 2011 International Conference on.
- Clark, S. K. (1981). *Mechanics of pneumatic tires*: US Government Printing Office.
- Clarke, S., & Robertson, I. (2005). A meta-analytic review of the Big Five personality factors and accident involvement in occupational and non-occupational settings. *Journal of Occupational and Organizational Psychology*, 78(3), 355-376.

- Colli, V., Tomassi, G., & Scarano, M. (2006). "Single Wheel" longitudinal traction control for electric vehicles. *IEEE Transactions on Power Electronics*, 21(3), 799-808.
- Datentechnik, D. S. (1999). PC-Crash, A Simulation Program for Vehicle Accidents. *Technical Manual, Version, 5*.
- Day, T. D. (1999). An overview of the EDSMAC4 collision simulation model: SAE Technical Paper.
- Delaigne, P., & Eskandarian, A. (2004). A comprehensive vehicle braking model for predictions of stopping distances. *Proceedings of the Institution of Mechanical Engineers, Part D: Journal of Automobile Engineering*, 218(12), 1409-1417.
- Dorsch, V., Becker, A., & Vossen, L. (2002). Enhanced rubber friction model for finite element simulations of rolling tyres. *Plastics, rubber and composites*, 31(10), 458-464.
- Doumiati, M., Victorino, A., Charara, A., & Lechner, D. (2010). *A method to estimate the lateral tire force and the sideslip angle of a vehicle: Experimental validation*. Paper presented at the American Control Conference (ACC), 2010.
- Doumiati, M., Victorino, A., Charara, A., & Lechner, D. (2011). *Estimation of road profile for vehicle dynamics motion: experimental validation*. Paper presented at the American Control Conference (ACC), 2011.
- Driscoll, O., & Australia, B. Q. (2013). Major accident investigation report. *National Transport Insurance*.
- Dugoff, H., Fancher, P., & Segel, L. (1970). An analysis of tire traction properties and their influence on vehicle dynamic performance. *SAE transactions*, 1219-1243.
- Dunn, A. L., Guenther, D. A., & Radlinski, R. (2012). Application of Air Brake Performance Relationships in Accident Reconstruction and Their Correlation to Real Vehicle Performance. *SAE International Journal of Commercial Vehicles*, 5(2012-01-0609), 251-270.
- El-Basyouny, K., Barua, S., & Islam, M. T. (2014). Investigation of time and weather effects on crash types using full Bayesian multivariate Poisson lognormal models. *Accident Analysis & Prevention*, 73, 91-99.
- Every, J. L. (2015). *Development of a driver behavior based active collision avoidance system*: The Ohio State University.
- Evtiukov, S., Kurakina, E., Lukinskiy, V., & Ushakov, A. (2017). Methods of Accident Reconstruction and Investigation Given the Parameters of Vehicle Condition and Road Environment. *Transportation Research Procedia*, 20, 185-192.
- Ewing, R., & Dumbaugh, E. (2009). The built environment and traffic safety: a review of empirical evidence. *CPL bibliography*, 23(4), 347-367.

- Fancher, P. S. (1986). A factbook of the mechanical properties of the components for single-unit and articulated heavy trucks. Phase I. Final report.
- Fancher, P. S., & Mathew, A. (1987). *Vehicle Dynamics Handbook for Single-Unit and Articulated Heavy Truck*.
- Fittanto, D. A., Ruhl, R. A., Southcombe, E. J., Burg, H., & Burg, J. (2002). Overview of CARAT-4, a multi-body simulation and collision modeling Program: SAE Technical Paper.
- FMCS, Federal Motor Carrier Safety (2015). Large Truck and Bus Crash Facts. <https://www.fmcsa.dot.gov/safety/data-and-statistics/large-truck-and-bus-crash-facts>
- Fricke, L. B. (1990). *Traffic accident reconstruction (The Traffic accident investigation manual, Vol. 2)*.
- Fricke, L. B. (2010). *Traffic crash reconstruction*: Northwestern University Center for Public Safety.
- Gangopadhyay, S., & Wilson, F. (1995). Analysis of the braking performance of a tractor-trailer unit. *Canadian Journal of Civil Engineering*, 22(6), 1178-1184.
- Garrott, W. R., Heitz, M., & Bean, B. (2012). Experimental measurement of the stopping performance of a tractor-semitrailer from multiple speeds. *Accident reconstruction journal*, 22(3), 45-57.
- Gillespie, T. D. (1992). *Fundamentals of Vehicle Dynamics*. SAE International.
- Gillespie, T. D. (1992). *Fundamentals of Vehicle Dynamics*. Warrendale, PA: Society of Automotive Engineers: Inc.
- Gobbi, M., Mastinu, G., & Previati, G. (2014). The effect of mass properties on road accident reconstruction. *International Journal of Crashworthiness*, 19(1), 71-88.
- Goudie, D. W., Bowler, J. J., Brown, C. A., Heinrichs, B. E., & Siegmund, G. (2000). Tire friction during locked wheel braking: SAE Technical Paper.
- Greibe, P., Braking distance, friction and behavior, Technical report, Trafitec, Scion-DTU (Jul. 2007).
- Grzebieta, R., Rechnitzer, G., & Simmons, K. (2015). Static Stability Test Results. *Quad Bike Performance Project TARS Research Report(1)*.
- Gunaratne, M., Bandara, N., Medzorian, J., Chawla, M., & Ulrich, P. (2000). Correlation of tire wear and friction to texture of concrete pavements. *Journal of materials in civil engineering*, 12(1), 46-54.
- Guo, K., & Sui, J. (1996). A theoretical observation on empirical expression of tire shear forces. *Vehicle System Dynamics*, 25(S1), 263-274.

- Gustafsson, F. (1998). Estimation and change detection of tire-road friction using the wheel slip. *IEEE Control System Magazine*, 18(4), 42-49.
- Guzek, M. (2016). Uncertainty in calculations at the reconstruction of road accidents. *Proceedings of the Institute of Vehicles/Warsaw University of Technology*, 109(5), 117-139.
- Habtemichael, F. G., & de Picado Santos, L. (2014). Crash risk evaluation of aggressive driving on motorways: microscopic traffic simulation approach. *Transportation Research Part F: Traffic Psychology and Behaviour*, 23, 101-112.
- Häkkinen, H., & Summala, H. (2001). Fatal traffic accidents among trailer truck drivers and accident causes as viewed by other truck drivers. *Accident Analysis & Prevention*, 33(2), 187-196.
- Hall, J., Smith, K., Titus-Glover, L., Wambold, J., Yager, T., & Rado, Z. (2009). Guide for pavement friction. NCHRP. Web-only document 108. Contractor's Final Report NCHRP Project 01-43. *Transportation Research Board of the National Academies*.
- Han, I. (2017). Modelling the tyre forces for a simulation analysis of a vehicle accident reconstruction. *Proceedings of the Institution of Mechanical Engineers, Part D: Journal of Automobile Engineering*, 231(1), 16-26.
- Han, I. H., & Park, S. B. (2010). Uncertainty of Measurements in the Analysis of Vehicle Accidents. *Journal of Korean Society of Transportation*, 28(3), 119-130.
- Hartman, J., & Alam, F. (2014). The Effects of Velocity on the Friction Coefficient of Motor Vehicle Tyres and Paired Road Surfaces. *Nonlinear Engineering Nonlinear Engineering*, 3(2), 71-79.
- Hegazy, S., & Sandu, C. (2010). Evaluation of Heavy Truck Ride Comfort and Stability: SAE Technical Paper.
- Heinrichs, B. E., Allin, B. D., Bowler, J. J., & Siegmund, G. P. (2004). Vehicle speed affects both pre-skid braking kinematics and average tire/roadway friction. *Accident Analysis & Prevention*, 36(5), 829-840.
- Henry, J. J. (2000). *Evaluation of pavement friction characteristics* (Vol. 291): Transportation Research Board.
- Hernandez, J. A., & Al-Qadi, I. L. (2017). Tire-pavement interaction modelling: hyperelastic tire and elastic pavement. *Road materials and pavement design*, 18(5), 1067-1083.
- Ho, J., & Manan, M. A. (2019). A Study on Commercial Vehicle Speeds and Its Operational Characteristics. *Journal of the Society of Automotive Engineers Malaysia*, 3(4).
- Huzafah, M. M., & Wong, S. V. (2010). Rear End Crash Compatibility between Cars and Trucks in Malaysia: A Preliminary Study. In *Proceedings of the 8~(th) International Forum of Automotive Traffic Safety*.

- Ishikawa, H. (1993). Impact model for accident reconstruction-normal and tangential restitution coefficients: SAE Technical Paper.
- Ismael, K. S., & Razzaq, N. A. (2017). Traffic Accidents Analysis on Dry and Wet Road Bends Surfaces in Greater Manchester-UK. *Kurdistan Journal of Applied Research*, 2(3), 284-291
- Jaroszweski, D., Chapman, L., & Petts, J. (2013). Climate change and road freight safety: a multidisciplinary exploration. *Climatic change*, 120(4), 785-799.
- Johansen, T. A., Petersen, I., Kalkkuhl, J., & Ludemann, J. (2003). Gain-scheduled wheel slip control in automotive brake systems. *Control Systems Technology, IEEE Transactions on*, 11(6), 799-811.
- Karim, M. R., Abdullah, A. S., Yamanaka, H., Abdullah, A. S., & Ramli, R. (2013). Degree of vehicle overloading and its implication on road safety in developing countries.
- Karim, M. R., Saifizul, A., Yamanaka, H., Sharizli, A., & Ramli, R. (2013). Minimum safe time gap (mstg) as a new safety indicator incorporating vehicle and driver factors. *Journal of the Eastern Asia Society for Transportation Studies*, 10, 2069-2079.
- Karim, M. R., Saifizul, A., Yamanaka, H., Sharizli, A., & Ramli, R. (2014). An Investigation on Safety Performance Assessment of Close-Following Behavior of Heavy Vehicle Using Empirical-Simulation Technique. *Journal of Transportation Technologies*, 2014.
- Khekare, A. D. (2009). *Straight Line Braking Performance of a Road Vehicle with Non Linear Tire Stiffness Formulation*, Master of Science Thesis, Clemson University. https://tigerprints.clemson.edu/all_theses/748
- Klein, P., & Anfosso-Ledee, F. (2004). *An envelopment procedure for tire-road contact*. Paper presented at the Symposium on Pavement Surface Characteristics [of Roads and Airports], 5th, 2004, Toronto, Ontario, Canada.
- Krishnan, S., Hizam, S. M., Firdhaus, A., Sarah, S., & Taufiq, A. (2017). Analysis of Exhaustion Related Psychological Risk Factors among Oil and Gas Tanker Drivers in Malaysia. *International Journal of Advanced and Multidisciplinary Social Science*, 3(1), 22-27.
- Lang, W., Tao, C., & Qiang, Y. (2003). Three-dimensional vehicle dynamics model for road traffic accident simulation and reconstruction [J]. *Journal of Traffic and Transportation Engineering*, 3(3), 88-92.
- Lee, C., & Li, X. (2014). Analysis of injury severity of drivers involved in single-and two-vehicle crashes on highways in Ontario. *Accident Analysis & Prevention*, 71, 286-295.
- Lee, H., & Tomizuka, M. (2003). Adaptive vehicle traction force control for intelligent vehicle highway systems (IVHSs). *IEEE Transactions on Industrial Electronics*, 50(1), 37-47.

- Leiss, P. J., Becker, S., & Derian, G. (2013). Tire Friction Comparison of Three Tire Types: SAE Technical Paper.
- Li, B., Yang, X., & Yang, J. (2014). Tire model application and parameter identification-A literature review. *SAE International Journal of Passenger Cars-Mechanical Systems*, 7(2014-01-0872), 231-243.
- Li, L., Wang, F.-Y., & Zhou, Q. (2006). Integrated longitudinal and lateral tire/road friction modeling and monitoring for vehicle motion control. *IEEE TRANSACTIONS ON INTELLIGENT TRANSPORTATION SYSTEMS*, 7(1), 1-19.
- Li, Y. B., Yuan, Q., & Chen, L. (2004). Study of uncertain factors in traffic accidents of vehicle impaction pedestrian. *China Journal of Highway and Transport*, 17(1), 82-85.
- Li, Z., & Kota, S. (2001). Virtual prototyping and motion simulation with ADAMS. *Journal of Computing and Information Science in Engineering*, 1(3), 276-279.
- Lian, Y., Zhao, Y., Hu, L., & Tian, Y. (2015). Cornering stiffness and sideslip angle estimation based on simplified lateral dynamic models for four-in-wheel-motor-driven electric vehicles with lateral tire force information. *International Journal of Automotive Technology*, 16(4), 669-683.
- Lian, Y., Zhao, Y., Hu, L., & Tian, Y. (2016). Longitudinal collision avoidance control of electric vehicles based on a new safety distance model and constrained-regenerative-braking-strength-continuity braking force distribution strategy. *IEEE Transactions on Vehicular Technology*, 65(6), 4079-4094.
- Limpert, R. (1992). *Brake design and safety* (Vol. 120).
- Liu, J and Ramnath, V. (2016), Accelerated Road Load Simulation Road Load Data for Fatigue Analysis in Concept Phase, Department of Applied Mechanics, Chalmers University of Technology, Gothenburg.
- Ludwig, C., & Kim, C. (2017). *Influence of testing surface on tire lateral force characteristics—Einfluss der Prüfoberfläche auf die Reifenseitenkraft-Eigenschaften*. Paper presented at the 8th International Munich Chassis Symposium 2017.
- MAA, Malaysian Automotive Association (2019). Market Review for 2018. Retrieved from http://www.maa.org.my/pdf/Market_Review_2018.pdf
- Mayora, J. M. P., & Piña, R. J. (2009). An assessment of the skid resistance effect on traffic safety under wet-pavement conditions. *Accident Analysis & Prevention*, 41(4), 881-886.
- McKnight, A. J. (2004). Investigative Analysis of Large truck Accident Causation: White Paper. Washington, DC: Transportation Research Board. <http://docs.trb.org/01030753.pdf>.
- McKnight, A. J., & Bahouth, G. T. (2009). Analysis of large truck rollover crashes. *Traffic Inj Prev*, 10(5), 421-426.

- Melnikov, G. I., Dudarenko, N. A., Melnikov, V. G., & Alyshev, A. S. (2015). Parametric identification of inertial parameters. *Applied Mathematical Sciences*, 9(136), 6757-6765.
- Miller, S. L., Youngberg, B., Millie, A., Schweizer, P., & Gerdes, J. C. (2001). *Calculating longitudinal wheel slip and tire parameters using GPS velocity*. Paper presented at the American Control Conference, 2001. Proceedings of the 2001.
- MIROS, Malaysian Institute of Road Safety Research (2017). A Study on Commercial Vehicle Speed and its Operational Characteristics. (MRR No. 243), Malaysia.
- Mokhiamar, O., & Abe, M. (2004). Simultaneous optimal distribution of lateral and longitudinal tire forces for the model following control. *Journal of dynamic systems, measurement, and control*, 126(4), 753-763.
- Mooren, L., Grzebieta, R., Williamson, A., Olivier, J., & Friswell, R. (2014). Safety management for heavy vehicle transport: A review of the literature. *Safety science*, 62, 79-89.
- Morrison, G., & Cebon, D. (2017). Combined emergency braking and turning of articulated heavy vehicles. *Vehicle system dynamics*, 55(5), 725-749.
- Mortimer, R., Segel, L., Dugoff, H., Campbell, J., Jorgeson, C., & Murphy, R. (1970). Brake force requirement study: driver-vehicle braking performance as a function of brake system design variables.
- Mousseau, C., & Hulbert, G. (1996). An efficient tire model for the analysis of spindle forces produced by a tire impacting large obstacles. *Computer Methods in Applied Mechanics and Engineering*, 135(1-2), 15-34.
- Mustafa, M. N. (2005). Overview of current road safety situation in Malaysia. *Highway planning Unit, Road Safety Section, Ministry of Works*, 5-9.
- Nagurnas, S., Mitunevičius, V., Unarski, J., & Wach, W. (2007). Evaluation of veracity of car braking parameters used for the analysis of road accidents. *Transport*, 22(4), 307-311.
- Nair, S. M., & Shankar, C. S. (2017). Impact of Road Safety Initiatives on Road Accidents in India.
- Nantais, N. C. (2006). Active brake proportioning and its effects on safety and performance. *University of Windsor: Faculty of Mechanical Engineering Graduate Studies and Research*.
- NHTSA, National Highway Traffic Safety Administration (2011). Experimental Measurement of The Stopping Performance of A Tractor-Semitrailer From Multiple Speeds. (Report No. DOT HS 811 488). Retrieved from <https://one.nhtsa.gov/DOT/NHTSA/NVS/VRTC/ca/811488.pdf>
- NHTSA, National Highway Traffic Safety Administration (2015). Traffic Safety Facts, 2012 Data: Pedestrians. *Annals of Emergency Medicine*, 65(4), 452.

- Nogowczyk P., Pałka A., Szczeńniak G. The influence of mass parameters of the body on active safety of a fire engine in terms of the selection of chassis. *The Archives of Automotive Engineering – Archiwum Motoryzacji*. 2018;82(4):87-98. doi:10.14669/AM.VOL82.ART7
- Noon, R. K. (1992). *Introduction to forensic engineering*: CRC Press.
- Noor Syukri, A. Z. A., Abdul Rahim, M. M., Shaw Voon, W., & Radin Sohadi, R. U. (2009). Single-Vehicle Accidents Involving in Malaysia – a Preliminary Study.
- Nunney, M. J. (2007). *Light and heavy vehicle technology* (4th ed.). USA: Routledge.
- Oh, Y., & Lee, H. (2014). Characteristics of a Tire Friction and Performances of a Braking in a High Speed Driving. *Advances in Mechanical Engineering*, 6, 260428.
- Ong, G., & Fwa, T. (2008). Modeling and analysis of truck hydroplaning on highways. *Transportation Research Record: Journal of the Transportation Research Board*(2068), 99-108.
- Ong, G., & Fwa, T. (2009). Modeling skid resistance of commercial trucks on highways. *Journal of Transportation Engineering*, 136(6), 510-517.
- Pacejka, H. (2006). *Tyre and Vehicle Dynamics*. Elsevier.
- Pacejka, H. B., & Bakker, E. (1992). The magic formula tyre model. *Vehicle System Dynamics*, 21(S1), 1-18.
- Pacejka, H. B., & Sharp, R. S. (1991). Shear force development by pneumatic tyres in steady state conditions: a review of modelling aspects. *Vehicle System Dynamics*, 20(3-4), 121-175.
- Park, S. (2005). EFFECT OF BRAKE PEDAL IMPEDANCE ON BRAKING. *International Journal of Automotive Technology*, 6(4), 391-402.
- Paultan.org. (2016). Adoption rate of ABS in Malaysia. from <https://paultan.org/2016/04/06/adoption-rate-of-abs-in-msia-behind-thailand-indonesia-and-china-only-11-of-new-vehicles-have-esp/>
- Petersen, I., Johansen, T. A., Kalkkuhl, J., & Lüdemann, J. (2001). *Wheel slip control in ABS brakes using gain scheduled constrained LQR*. Paper presented at the European Control Conference.
- Popov, V. L. (2010). *Contact mechanics and friction*: Springer.
- Prato, C. G., Kaplan, S., Patrier, A., & Rasmussen, T. K. (2017). Considering Built Environment and Spatial Correlation in Modeling Injury Severity for Pedestrian Crashes.
- Priddy, J. D., Jones, R. A., & Sandu, C. (2013). Experimental Determination of the Effect of Cargo Variations on Steering Stability. *SAE International Journal of Commercial Vehicles*, 6(2013-01-2359), 308-314.

- Prynne, K., & Martin, P. (1995). Braking behaviour in emergencies: SAE Technical paper.
- Qian, R., Shi, Q., Wang, Z., & Lv, J. (2007). *Predicting the truck speed based on four factors of transportation engineering: A curvilinear regression model*. Paper presented at the International Conference on Transportation Engineering 2007.
- Qin, X., Ivan, J. N., & Ravishanker, N. (2004). Selecting exposure measures in crash rate prediction for two-lane highway segments. *Accident Analysis & Prevention*, 36(2), 183-191.
- Raftery, S., Grigo, J., & Woolley, J. (2008). Heavy vehicle road safety: Research scan. *Prevention*, 43, 565-572.
- Randles, B., Jones, B., Welcher, J., Szabo, T., Elliott, D., & MacAdams, C. (2010). *The accuracy of photogrammetry vs. hands-on measurement techniques used in accident reconstruction* (No. 2010-01-0065). SAE Technical Paper.
- Ray, L. R. (1995). Nonlinear state and tire force estimation for advanced vehicle control. *IEEE Transactions on Control Systems Technology*, 3(1), 117-124.
- Raymond Brach, M. (1998). A review of Impact Models for Vehicle Collision. *SAE*, 870048, 430-435.
- Rill, G. (2006). *First order tire dynamics*. Paper presented at the Proceedings of the III European Conference on Computational Mechanics Solids, Structures and Coupled Problems in Engineering, Lisbon, Portugal.
- Rittmann, B. E., & Manem, J. A. (1992). Development and experimental evaluation of a steady-state, multispecies biofilm model. *Biotechnology and bioengineering*, 39(9), 914-922.
- Rogers, M., & Gargett, T. (1991). A skidding resistance standard for the national road network. *HIGHWAYS & TRANSPORTATION*, 38(4).
- Ruhl, L. L. (2006). *Truck Accident Litigation* (3rd ed.). American Bar Association
- Ryu, T., Lee, S., Jung, W., & Cheon, J. (2010). *A Study on Correlation Between Skid Distance and Pre-braking Speed*. Paper presented at the 17th ITS World Congress.
- Saifizul, A. A., Yamanaka, H., & Karim, M. R. (2011). Empirical analysis of gross vehicle weight and free flow speed and consideration on its relation with differential speed limit. *Accident Analysis & Prevention*, 43(3), 1068-1073.
- Sapietová, A., Gajdoš, L., Dekýš, V., & Sapieta, M. (2016). Analysis of the influence of input function contact parameters of the impact force process in the MSC.ADAMS. In *Advanced mechatronics solutions* (pp. 243-253). Springer, Cham.
- Sarani, R., Allyana, S., Mohd Marjan, J., & Shaw Voon, W. (2012). Predicting Malaysian Road Fatalities for Year 2020.

- Sarip, S., (2018). A Study of Road Accidents of Heavy Vehicles in Malaysia. Retrieved from: https://people.utm.my/shamsul/wp-content/blogs.dir/949/files/2018/10/Case-study-2_MRSE2573_A-Study-of-Road-Accidents-of-Heavy-Vehicles-in-Malaysia.pdf
- Savkoor, A. (1986). Mechanics of sliding friction of elastomers. *Wear*, 113(1), 37-60.
- Sayers, M. W. (1990). Symbolic computer methods to automatically formulate vehicle simulation codes. *PhD, University of Michigan Transportation Research Institute*.
- Schiehlen, W., Guse, N., & Seifried, R. (2006). Multibody dynamics in computational mechanics and engineering applications. *Computer Methods in Applied Mechanics and Engineering*, 195(41), 5509-5522.
- Schmeitz, A. J. C. (2004). A semi-empirical three-dimensional model of the pneumatic tyre rolling over arbitrarily uneven road surfaces.
- Shrestha, S., Spiryagin, M., & Wu, Q. (2019). Friction condition characterization for rail vehicle advanced braking system. *Mechanical Systems and Signal Processing*, 134, 106324.
- Shvets, A. O. (2018). Influence of the longitudinal and transverse displacement of the cargo gravity center in gondola cars on their dynamic indicators. *Science and Transport Progress. Bulletin of Dnipropetrovsk National University of Railway Transport*, (5 (77)), 115-128.
- Seiler, P., Song, B., & Hedrick, J. K. (1998). Development of a collision avoidance system. *SAE transactions*, 1334-1340.
- Seipel, G., & Winner, H. (2013a). Development and Intensity of Tire Marks-Analysis of Influencing Parameters.
- Seipel, G., Winner, H., Baumann, F., & Hermanutz, R. (2013b). Approach to determine slip values based on the intensity of tire marks with respect to tire and road properties: SAE Technical Paper.
- Sharizli, A. (2016). *Development of Collision Avoidance Warning System Featuring Adaptive Critical Safe Distance Method*, Doctoral dissertation, University Malaya.
- Sharizli, A., Ramli, R., Karim, M. R., & Abdullah, A. S. (2014). *Simulation and analysis on the effect of gross vehicle weight on braking distance of heavy vehicle*. Paper presented at the Applied Mechanics and Materials.
- Skrúčaný, T., Vrábel, J., & Kazimir, P. (2020). The influence of the cargo weight and its position on the braking characteristics of light commercial vehicles. *Open Engineering*, 10(1), 154-165.
- Skrúčaný, T., Vrábel, J., Kendra, M., & Kažimír, P. (2017). Impact of cargo distribution on the vehicle flatback on braking distance in road freight transport. In *MATEC Web of Conferences* (Vol. 134, p. 00054). EDP Sciences.

- Smith, R. (1990). Skidding to a stop. *Impact*, 1(1), 11-12.
- Smith, R. (1998). The formula commonly used to calculate velocity change in vehicle collisions. *Proceedings of the Institution of Mechanical Engineers, Part D: Journal of Automobile Engineering*, 212(1), 73-78.
- Solomon, P. L. (1974). *The Simulation Model of Automobile Collisions (SMAC): Operator's Manual*.
- Soole, D. W., Watson, B. C., & Fleiter, J. J. (2013). Effects of average speed enforcement on speed compliance and crashes: A review of the literature. *Accident Analysis & Prevention*, 54, 46-56.
- Steffan, H. (2009). Accident reconstruction methods. *Vehicle System Dynamics*, 47(8), 1049-1073.
- Steffan, H., & Moser, A. (1996). The collision and trajectory models of PC-CRASH: SAE Technical Paper.
- Stronge, W. J. (2018). *Impact mechanics*. Cambridge university press. 2nd Edition.
- Surblys, V., & Sokolovskij, E. (2016). Research of the vehicle brake testing efficiency. *Procedia Engineering*, 134, 452-458.
- Svendenius, J. (2003). *Tire models for use in braking applications*. Department of Automatic Control, Lund Institute of Technology Masters, Lund, Sweden.
- Seyedi, M., Jung, S., & Wekezer, J. (2020). A comprehensive assessment of bus rollover crashes: integration of multibody dynamic and finite element simulation methods. *International Journal of Crashworthiness*, 1-16.
- Tanelli, M., Ferrara, A., & Giani, P. (2012). *Combined vehicle velocity and tire-road friction estimation via sliding mode observers*. Paper presented at the Control Applications (CCA), 2012 IEEE International Conference.
- Tang, T., Anupam, K., Kasbergen, C., & Scarpas, A. (2017). Study of Influence of Operating Parameters on Braking Distance. *Transportation Research Record*, 2641(1), 139-148.
- Tass, B. (2010). MADYMO Reference Manual. *TNO Automotive*.
- Taylor, M. C., Lynam, D., & Baruya, A. (2000). *The effects of drivers' speed on the frequency of road accidents*: Transport Research Laboratory Crowthorne.
- Tey, J. Y., Soong, M. F., & Ramli, R. (2014). Optimized suspension kinematic profiles for handling performance using 10-degree-of-freedom vehicle model. *Proceedings of the Institution of Mechanical Engineers, Part K: Journal of Multi-body Dynamics*, 228(1), 82-99.
- The Star (2019, 26 January). Ban on heavy vehicles during CNY. Retrieved from: <https://www.thestar.com.my/news/nation/2019/01/26/ban-on-heavy-vehicles-during-cny/>

- Tseng, W. K., & Liao, S. (2012). *Estimation of Vehicle Pre-Braking Speed*. Paper presented at the Applied Mechanics and Materials.
- Vadeby, A., & Forsman, Å. (2014). *Speed distribution and traffic safety measures*. Paper presented at the Transport Research Arena (TRA).
- Van Oosten, J. (2007). TMPT tire modeling in ADAMS. *Vehicle System Dynamics*, 45(S1), 191-198.
- Varunjikar, T. (2011). Design of horizontal curves with downgrades using low-order vehicle dynamics models.
- Velenis, E., Tsiotras, P., & Canudas-de-Wit, C. (2002). *Extension of the LuGre dynamic tire friction model to 2D motion*. Paper presented at the Proceedings of the 10th IEEE Mediterranean Conference on Control and Automation-MED.
- Villagra, J., D'Andréa-Novel, B., Fliess, M., & Mounier, H. (2011). A diagnosis-based approach for tire-road forces and maximum friction estimation. *Control Engineering Practice*, 19(2), 174-184.
- Viner, H., Sinhal, R., & Parry, A. (2005). Linking road traffic accidents with skid resistance—recent UK developments. *TRL Paper reference PA/INF4520/05*.
- Vrábel, J., Jagelcak J, Zamecnik J, Caban J. Influence of Emergency Braking on Changes of the Axle Load of Vehicles Transporting Solid Bulk Substrates. *Procedia Engineering*. 2017;187:89-99.
- Vrábel, J. et al. Influence of Emergency Braking on Changes of the Axle Load of Vehicles Transporting Solid Bulk Substrates. In: *Transbaltica 2017: Transportation and technology*, Vol: 187, pp: 89 – 99, 2017, DOI: 10.1016/j.proeng.2017.04.354.
- Wach, W. (2016). Calculation reliability in vehicle accident reconstruction. *Forensic science international*, 263, 27-38.
- Wach, W., & Unarski, J. (2007). Uncertainty of calculation results in vehicle collision analysis. *Forensic Sci Int*, 167(2), 181-188.
- Wang, H., Al-Qadi, I. L., & Stanciulescu, I. (2010). *Effect of Friction on Rolling Tire-pavement Interaction*: Purdue University Discovery Park.
- Wang, Y. (2007). A tire mark localization method for forensic image analysis. *Journal of the Eastern Asia Society for Transportation Studies*, 7, 2881-2890.
- Windhoff-Héritier, A., Kerwer, D., & Knill, C. (2001). *Differential Europe: the European Union impact on national policymaking*: Rowman & Littlefield.
- Wong, J. Y. (2008). *Theory of ground vehicles*: John Wiley & Sons.
- Woolley, R. L. (1985). The “IMPAC” Computer Program for Accident Reconstruction: SAE Technical Paper.

- Woolley, R. L., Warner, C. Y., & Perl, T. R. (1986). An Overview of Selected Computer Programs for Automotive Accident Reconstruction. *Transportation Research Record, 1068*, 85-100.
- Wu, Y., Boyle, L. N., McGehee, D., Roe, C. A., Ebe, K., & Foley, J. (2015). Modeling types of pedal applications using a driving simulator. *Human factors, 57*(7), 1276-1288.
- Wu, Y., Boyle, L. N., McGehee, D., Roe, C. A., Ebe, K., & Foley, J. (2017). Foot placement during error and pedal applications in naturalistic driving. *Accident Analysis & Prevention, 99*, 102-109.
- Xia, K., & Yang, Y. (2012). Three-dimensional finite element modeling of tire/ground interaction. *International journal for numerical and analytical methods in geomechanics, 36*(4), 498-516.
- Xiaoyun, Z., Xianlong, J., Wenguo, Q., Yizhi, G., & Genguo, L. (2007). Parallel computing with domain decomposition for the vehicle crashworthiness simulation. *Vehicle System Dynamics, 45*(11), 1051-1064.
- Xu, J., Li, Y., Lu, G., & Zhou, W. (2009). Reconstruction model of vehicle impact speed in pedestrian-vehicle accident. *International Journal of Impact Engineering, 36*(6), 783-788.
- Yao, G. N., Huang, H. Y., Wei, J. H., & Sun, G. J. (2010). Research on Dynamics Modeling and Simulation for Transportation Truck Based on ADAMS. *Applied Mechanics and Materials, 26*, 32-35.
- Yilmaz, A. C., & Aydin, K. (2016). *Impact Velocity Prediction in a Traffic Accident*. Paper presented at the MATEC Web of Conferences.
- Zamzamzadeh, M., Abdullah, A. S., & Ramli, R. (2015). *Analysis of Wheel Lock up Effects on Skidding Distance for Heavy Vehicles*. Paper presented at the 17th International Conference on Traffic and Transportation Engineering, Istanbul, Turkey.
- Zamzamzadeh, M., Saifizul, A., Ramli, R., & Soong, M. (2016). Dynamic simulation of brake pedal force effect on heavy vehicle braking distance under wet road conditions. *International Journal of Automotive & Mechanical Engineering, 13*(3).
- Zamzamzadeh, M., Saifizul, A. A., Ramli, R., & Soong, M. F. (2018). Heavy vehicle multi-body dynamic simulations to estimate skidding distance. *Baltic Journal of Road and Bridge Engineering, 13*(1), 23-33.
- Zebala, J., Wach, W., Cięпка, P., & Janczur, R. (2016). Determination of critical speed, slip angle and longitudinal wheel slip based on yaw marks left by a wheel with zero tire pressure (No. 2016-01-1480). SAE Technical Paper.
- Zhang, M., Meuleners, L., Chow, C., & Govorko, M. (2014). The Epidemiology of Heavy Vehicle Crashes in Western Australia: 2001-2013. *Accident Analysis & Prevention, 36*(5), 851-860.

- Zhang, X.-y., Jin, X.-l., Qi, W.-g., & Guo, Y.-z. (2008). Vehicle crash accident reconstruction based on the analysis 3D deformation of the auto-body. *Advances in Engineering Software*, 39(6), 459-465.
- Zheng, B., Huang, X., Zhang, W., Zhao, R., & Zhu, S. (2018). Adhesion Characteristics of Tire-Asphalt Pavement Interface Based on a Proposed Tire Hydroplaning Model. *Advances in Materials Science and Engineering*.
- Zhu, X., & Srinivasan, S. (2011). A comprehensive analysis of factors influencing the injury severity of large-truck crashes. *Accident Analysis & Prevention*, 43(1), 49-57.
- Žuraulis, V., & Sokolovskij, E. (2018). Vehicle velocity relation to slipping trajectory change: an option for traffic accident reconstruction. *Promet-Traffic&Transportation*, 30(4), 395-406.

University of Malaysia